# Incorporation of Historical Disturbance Identified With LandTrendr Algorithm For Land Cover Mapping In Malaysia

Supervisors:

Dr Alex Lechner (UNM)

Dr Ahimsa Campos-Arceiz (UNM)

Dr Simon Jones (RMIT)


Student: Daniel Stephen Platt

Student ID: 08015557

School of Environmental and Geographical Sciences

MRes in Environmental and Geographical Sciences

Faculty of Science and Engineering

## Abstract

In Malaysia, land area under oil palm plantation has been increasing. Meanwhile voluntary measures to improve sustainability of palm oil production have been introduced including regulation of land conversion to oil palm plantations. The objective of this project is to assess the utility of Google Earth Engine with the LandTrendr algorithm for classifying land cover, as a first step towards developing a tool for land cover change detection in Peninsula Malaysia to support Roundtable on Sustainable Oil Palm (RSPO) certification. Ground validation data on land cover and disturbance events from satellite imagery were used to calibrate LandTrendr to detect and map change from forest to oilpalm, other vegetation or urban; other vegetation to oilpalm; and oilpalm to oilpalm (replanting). The resulting disturbance rasters were used with a 2019 multispectral Landsat mosaic in a Random Forests supervised classification. The classified maps of 2019 land cover showed an improvement in accuracy with the addition of LandTrendr rasters over using only Landsat imagery. Our results suggest that disturbance history provides useful ancillary information to support remote sensing mapping and LandTrendr could potentially become a useful tool for detecting land cover change in the tropics. The addition of LandTrendr rasters resulted in a 0.453 percentage point increase in overall accuracy from 59.992% to 60.445%. Overall accuracy improved for the target land covers - oil palm and rubber, as well as forest and urban land covers, while decreasing for other land cover classes. Highest accuracy was obtained for forest, oil palm and rice. The main source of error was from other land covers being incorrectly classified as oil palm. Confusion between the 'other vegetation' class and the 'other agriculture' class, and between urban areas and bare ground were also major sources of error.

## Acknowledgements

I would firstly like to thank my supervisor, Dr Alex Lechner, whose patience, guidance and encouragement made the writing of this thesis possible. You helped me not to lose hope and to keep the big picture in mind. My co-supervisors Professor Ahimsa Campos-Arceiz and Dr Simon Jones were also helpful in their support and in suggesting new ideas.

I would like to thank Wild Asia who funded my Masters and especially to Reza Azmi and Su Shen Phan for their help in developing the direction for the research. Many thanks to Dr Badrul Azhar for sharing his expertise in oil palm plantations. I would like to thank Maria Edrish for helping in data collection, and my colleagues at the University of Nottingham, Darrel Tiang, Michelle Ang and Steve Teo for their input in developing the method.

Finally, I would like to thank the student counsellor, my friends and family. I am especially thankful to my parents, for their emotional support, constant encouragement and prayer throughout my thesis.

Contents

List of Tables

List of Figures

# CHAPTER 1. INTRODUCTION

# 1. Chapter 1 Introduction

## 1.2 Research Aims and Objectives

Operationalising the monitoring of oil palm using remote sensing is perhaps one of the most critical applications for remote sensing of the environment in Southeast Asia. The oil palm is a tree that grows within tropical regions, was traditionally planted in small-holder groves in Africa, but in the early 1900s, oil palm was planted on an industrial scale across the world. Since the 1980s, there has been a growing awareness of the environmental impacts caused by oil palm expansion, as these estates are being developed in tropical regions which are dominated by natural forests (Miettinen et al., 2016; Tang & Al Qahtani, 2020). By the early 2000s, the oil palm industry and NGOs had developed a certification system for oil palm growers which was believed to be the answer to halting deforestation of critical natural habitats (Omont, 2005; RSPO, 2015); known as the *Roundtable for Sustainable Palm Oil* (RSPO). In order to qualify for RSPO certification, plantation-owners must conduct a Land use change analysis (LUCA) to show that no virgin forest was cleared for establishing the plantation. By investigating the utility of LandTrendr for land cover mapping, this project contributes towards developing a tool to more efficiently carry out LUCA for RSPO certification.

The aims of this project are to improve monitoring of deforestation by developing a method for mapping land cover in tropical SE Asia using multi-temporal Landsat data describing historical disturbance. The focus is on deforestation driven by expansion of oil palm plantations. We first created satellite image composites to address cloud cover. Then we used the image time series with LandTrendr pixel based trajectory analysis to analyze the temporal characteristics of different land covers in order to differentiate between land covers with similar spectral characteristics, but different land cover change patterns. Finally raster outputs from LandTrendr and a Landsat mosaic are combined then classified using supervised Random Forests to produce a land cover map. We used a case study in Peninsular Malaysia to test and develop the remote sensing approach. We concluded by discussing the results, limitations and application of the novel approach for multi-temporal remote sensing in the tropics and suggestions for further research, especially within the context of mapping oil palm to support RSPO certification.

This study provides a novel demonstration of LandTrendr to mapping oil palm. LandTrendr was expected to improve the classification accuracy of oil palm, forest and rubber by providing additional historical disturbance information which is useful to help the Random Forest classifier to differentiate similar vegetation classes. This is one of the first studies to apply such a novel approach.

## 1.3 Study Area

Malaysia comprises of two portions – East Malaysia, consisting of Sarawak and Sabah on the island of Borneo, and Peninsular Malaysia, connected to mainland Southeast Asia by the Kra isthmus. Peninsular Malaysia, excluding surrounding islands, lies between 1°15'-6°44' N and 100°7'-104°18' E and has an area of 130,690km2 (calculated in Google Earth Engine). It has a tropical equatorial climate influenced largely by the southwestern and northeastern monsoons (Tangang et al., 2012) and an annual average rainfall of 2420mm (Ahmad et al., 2017). In 2020, 58% of land in Malaysia was occupied by forests(FAO, 2020), however deforestation is major issue, with a reduction in tree cover of 8.12Mha between 2002 and 2019(Global Forest Watch, n.d.).

The population of Peninsular Malaysia is concentrated in coastal cities, particularly in the metropolitan areas of Kuala Lumpur, Penang and Johor Bahru(Department of Statistics, 2011). Human land use is dominated by oil palm plantations and urban areas, followed by rubber plantations, rice paddies and other agriculture(Olaniyi et al., 2013; Samat et al., 2020). Land conversion to oilpalm plantations has been steadily increasing since 1974, with a rise in the area of land under oil palm plantation from 565,766ha to 5,900,157ha between 1974 and 2019(Department of Statistics, 2017). Oil palm plantations currently make up about 21% of the total land area in Peninsular Malaysia(Malaysian Palm Oil Board, 2019).

## 1.3 Study Area

# CHAPTER 2. LITERATURE REVIEW

## 2. Chapter 2 Literature Review

Land use change analysis (LUCA) is an approach used by the RSPO for tracking the success of conservation planning and natural resource management activities at site, regional and national scales (RSPO, 2015). Globally freely available spatial data products (e.g. global forest watch forest change) and remote sensing imagery (Landsat, MODIS and Sentinel) are increasing in quantity and quality, making the provision of spatial data no longer the sole responsibility of the government (Lechner et al., 2020). In addition, a huge step change in the provision and application of remote sensing is taking place due to the development of the Google Earth Engine (GEE; http://earthengine.google.org) where data is provided and analysed on the cloud, dramatically reducing processing and development times (Kennedy et al., 2018).

Remote sensing of land cover and land use in tropical South East Asian countries such as Malaysia, Papua New Guinea and Indonesia is challenging due to high incidence of cloud cover and rapid changes in vegetation cover due to regrowth and conversion to other land uses.  The most dominant form of land conversion in South East Asia is for oil palm (Kanniah et al., 2019; Stibig et al., 2014; Tang et al., 2019; Trisasongko & Paull, 2020). However, clear felling and selective logging, shifting agriculture and rubber plantations as well as urbanisation and mining are also common (Razali et al., 2014). A key difficulty for remote sensing in this region is associated with similarity in spectral properties, for example agricultural land uses such as palm oil and rubber being confused with natural forest (Miettinen et al., 2018). While the spectral signatures of these land covers are relatively similar, the temporal change and multitemporal profiles of clearance, disturbance and regrowth (natural and through plantations) can potentially be used in analyses such as with LandTrendR (Kennedy et al., 2010).

LandTrendr is an algorithm for "generating trajectory-based spectral time series data" from Landsat imagery. It operates on a pixel-by-pixel basis on annual mosaic stacks and returns simplified trajectories and segment information. Unlike single image approaches to LUCA, LandTrendr uses satellite data across a broad time period. This allows detection of both long-term and short-term change while reducing inter-annual signal noise. (Kennedy et al., 2010) It has been integrated with Google Earth Engine, making it widely available, allowing for processing very large datasets on the cloud and convenient for carrying out and sharing methods of land cover analysis (Kennedy et al., 2018).

Remote sensing has been used in relation to oil palm for various purposes, including plantation management and carbon stock auditing (Chong et al., 2017; Trisasongko & Paull, 2020), classification of oil palm extent and other land cover (Deilmai et al., 2014) and change detection (Pittman et al.,

2013). Daliman et al. (2014) classified oil palm at the plantation scale using GLCM-SVM and NDVI from Worldview-2 imagery. Pittman et al. (2013) studied the expansion of oil palm across Borneo by decade using Landsat imagery. An overview of studies into using remote sensing to differentiate oil palm from other land covers is given by Trisasongko & Paull (2020). Differentiation of oil palm from other land covers was achieved at plantation scale by Kamiran & Sarker (2014) and at sub-national level by Deilmai, Ahmad & Zabihi (2014) and Razali et al. (2014). Studies using multitemporal data include Razali et al. (2014) who classified land cover in several different years based on MODIS satellite imagery. Razak et al. (2018) used Landsat time series to differentiate rubber from oil palm and other land covers.

Landsat and MODIS are the only freely available datasets which go back far enough to be useful for conducting LUCA for RSPO certification. Studies that attempted to differentiate oil palm, rubber and/or forest used MODIS (Razali et al., 2014; Senf et al., 2013), Landsat (Beckschäfer, 2017; Deilmai et al., 2014; Lee et al., 2016; Razak et al., 2018; Sun et al., 2017), SAR (Trisasongko et al., 2017) and other satellites (Kamiran & Sarker, 2014; Razali et al., 2014). To tackle spectral similarity between rubber and forest, Razak et al. (2018), Beckschäfer (2017) and Senf et al. (2013) used seasonal differences in rubber spectral data and vegetation indices caused by defoliation of rubber trees to differentiate them from other land covers, and specifically from forest and oil palm. A variety of classifiers (CART, RF, Minimum Distance, Maximum Likelihood, SVM) have been used with Landsat imagery (Deilmai et al., 2014; Lee et al., 2016). Sun et al. (2017) used Landsat with a decision tree classifier (C5.0 adaptive boosting algorithm) and additional filtering to remove speckling. Problems included excessive cloud cover (Lee et al., 2016; Razali et al., 2014; Sun et al., 2017), similarity between plantations and forest (Razali et al., 2014; Sun et al., 2017), mixed land cover pixels (Deilmai et al., 2014; Sun et al., 2017) and difficulty gathering historical ground truth from satellite imagery (Beckschäfer, 2017; Razak et al., 2018; Sun et al., 2017). Due to the lack of imagery due to cloud cover, Sun et al. (Sun et al., 2017) used a mixture of imagery from different seasons which introduced spectral variability, but did not choose imagery based on rubber phenology, making it more difficult to differentiate.

Several change detection algorithms have been developed for use with spectral time series, including LandTrendr, BFAST and VCT, using a range of active and passive sensors (Boriah, 2010). LandTrendr is used for disturbance and recovery detection, whereas VCT only detects disturbance and BFAST is used for drought-related vegetation disturbance (Z. Zhu, 2017). For example, annual oil palm extent in Malaysia and Indonesia has been mapped for 2001-2016 by Xu et al. (2020), using ALOS PALSAR, ALOS PALSAR-2 and MODIS NDVI data, with extent mapped using BFAST for those years in which high-resolution imagery is not available. On the other hand, the LandTrendr algorithm

is dependent on Landsat imagery (Kennedy et al., 2010). LandTrendr has been used for land cover classification (Zhu et al., 2019) and change tracking (Bartz et al., 2015), change agent detection (Kennedy et al., 2015), tracking of insect damage (Liang et al., 2014), and monitoring of forest health and extent (Hudak et al., 2013; Wang et al., 2016), among other applications (Zhu, 2017). A variety of methods have been used with LandTrendr, including correlation with ground-based measurements (Meigs et al., 2011; Pflugmacher et al., 2012), magnitude and relative magnitude threshold (Kennedy et al., 2012), sliding threshold (Grogan et al., 2015), change characterization (Zhu et al., 2019), image stabilization (Bartz et al., 2015), and classification of disturbance rasters (Hislop et al., 2019; Rathnayake et al., 2020). While most applications have focused on North America, studies targeting the tropics and Southeast Asia in particular have used LandTrendr for studying forest disturbance related to rubber and timber plantations (Grogan et al., 2015; Shen et al., 2017; Tang et al., 2019), forest cover change (Fragal et al., 2016; Wang et al., 2016; Ye et al., 2021), mining disturbance (Wang et al., 2020), clearance of savannahs (Almeida de Souza et al., 2020), land cover change (Rathnayake et al., 2020) and cultivation patterns in smallholdings (Schneibel et al., 2017).

This study is the first to use LandTrendr in Malaysia or at a national scale, and the first to study oil palm using LandTrendr. It adds to the small body of work on LandTrendr which has been conducted in the tropics (FRAGAL et al., 2016; Grogan et al., 2015; Schneibel et al., 2017; W. Shen et al., 2017; W. J. Shen & Li, 2017; D. Tang et al., 2019; Yang et al., 2018), which have specific challenges associated with the region including high cloud cover (FRAGAL et al., 2016; W. Shen et al., 2017; D. Tang et al., 2019), spectral similarity between dominant tree-based land covers (forests and plantations) (Mohd Najib et al., 2020) and rapid vegetation regrowth after clearance (W. Shen et al., 2017). LandTrendr was employed to help overcome some of these issues as it utilizes the entire historical Landsat record to analyze both long-duration and abrupt change and so helps to identify disturbance events and differentiate similar land covers by characteristics of their spectral history (Kennedy et al., 2010; L. Zhu et al., 2019). Lack of imagery due to cloud cover was tackled by constructing annual image mosaics from imagery taken from all seasons. LandTrendr with GEE makes it possible to develop a tool which can be easily shared for use by non-specialists in GIS for conducting LUCA (Kennedy et al., 2018).

# CHAPTER 3. METHODS

# 3. Chapter 3 Methods

## 3.1 Overview

In this study we used historical disturbance identified with LandTrendr to map land cover for Peninsular Malaysia using a method compatible with RSPO Land Use Change Assessment (LUCA) (RSPO, 2015) which is used to assess compliance for certification . There were four steps to the processing (see Figure 1):

1. LandTrendr disturbance rasters were extracted along with a 2019 multispectral Landsat mosaic and SRTM elevation data to construct raster stacks.
2. Create LandTrendr disturbance rasters using sliding thresholds to optimize LandTrendr parameters for each of five change patterns. Some potential change patterns (such as 'oil palm to urban and other brown' were not included in the study as there was not sufficient ground truth data available for these land covers to accurately conduct the analysis.
    a. *'forest to oil palm'*
    b. *'oil palm to oil palm' (replanting)*
    c. *'forest to urban and other brown'*
    d. *'forest to other green'*
    e. *'other green to oil palm'*
3. Land cover maps of Peninsular Malaysia were produced using a supervised classification with the random forest algorithm.
4. Confusion matrixes were produced to compare accuracies for the land cover maps.
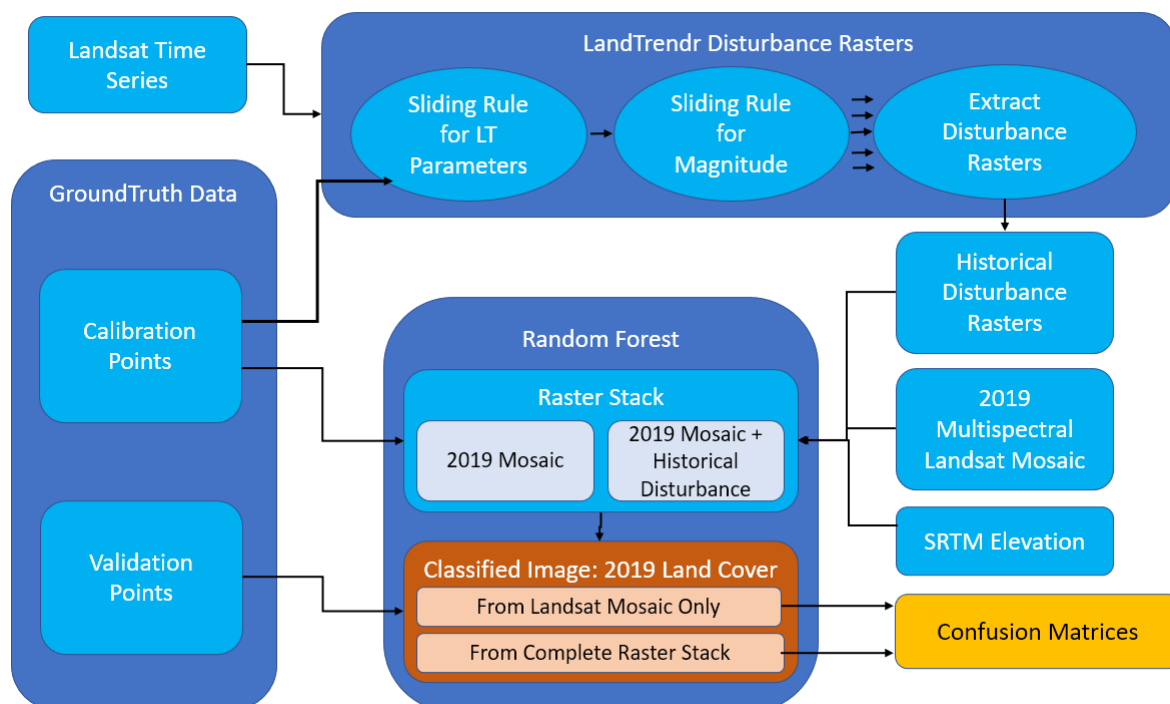


*Figure 1. Flowchart of the process of gathering ground truth data (3.4), calibrating LandTrendr using sliding rules (3.5), extracting disturbance rasters, assembling raster stacks and running Random Forest classification (3.6), and conducting accuracy assessment (3.7).*

## 3.2 Image Preparation

The GEE platform was used to build stacks of Surface Reflectance Tier 1 Landsat TM/ETM+/OLI (Landsat 5, 7 and 8) images from 1988-2019 from the USGS free Landsat archive. An image collection

was created using the Peninsular Malaysia boundary as the region of interest, from across twelve Landsat path/row numbers. The Normalized Burn Ratio (NBR) was chosen as the index for LandTrendr to work on (Grogan et al., 2015; Schneibel et al., 2017; Senf et al., 2015) as qualitative trials found it to be more responsive to clearance events and to track the year of disturbance onset more accurately than other bands and indices during the preliminary calibration. Although NBR is used for detecting fires, it is also excellent at detecting small changes in vegetation intensity (Schneibel et al., 2017). It is calculated from near infrared and short wave infrared as follows:

$$NBR = \frac{NIR - SWIR}{NIR + SWIR}$$

Due to the scarcity of cloud-free images in Peninsular Malaysia, annual median mosaics were created using multispectral images from across the whole year. All 30-m bands were used. Trials with shorter collection periods (i.e. less than 1 year) resulted in large areas with no data. The biannual monsoon and significant regional differences in the timing of the monsoon season (Hashim et al., 2016) also made it challenging to use a single collection period which would capture sufficient imagery for all years and across the whole study area. However, Malaysia's equatorial monsoon climate means that it has little deciduous forest (Zakaria et al., 2020) and so relatively small seasonal variation in phenology of forest vegetation. The collection was masked in GEE for clouds, cloud shadow, snow and water with the CFmask prior to mosaicking. The CFmask uses decision trees and scene-wide statistics to label pixels in the scene and identify cloud cover; and iteratively estimates cloud heights and projects them onto the ground to identify cloud shadow (*CFMask Algorithm*, n.d.). The CFMask was found to be the most accurate out of several cloud detecting algorithms by Foga et al. (2017), including for detecting cloud and cloud shadow over regions of brightness (ice/snow) when thermal data is available. In addition, multi-temporal rasters were derived by compositing several images using the median method which discards the most extreme pixel values such as temporary excessive brightness due to water.

## 3.3 Land Cover Classification Scheme

The land cover classification scheme was designed to represent the key land cover classes found in Malaysia (Yoshino et al., 2010), with consideration for distinctions in spectral appearance and structural differences. Two schemes were employed for the 1) land cover classification for 2019 (9 classes – see Table 1: 2019 Class) and 2) for the classification of historical disturbance patterns (5 classes – see Table 1: Change Pattern Macroclass). We first started by identifying a set of idealized land cover classes (Table 1) and from that identified a subset of classes based on the remote sensing limitations and usefulness for RSPO mapping. Forest was further split according to vegetation coefficient as described in the RSPO guidelines (RSPO, 2015) and disturbance history. Fine land cover classes were grouped thematically into coarse Macro land cover classes (Table 1).

Different schemes were used for the land cover mapping and for use in change detection to create the historical land cover change raster (Table 1). Classes for the supervised classification were grouped together by assumed spectral similarity. For example, bare ground and sand/mud were grouped together as 'Bare Ground' as they have similar spectral characteristics, but 'Urban' was not included as it was assumed to show more permanent characteristics. For the change detection, only the classes relevant to the major change patterns being studied were included, namely *Forest*, *Oil Palm*, *Other Green* and *Urban and Other Brown* (Table 3). We used a smaller number for the change detection as other classes were not sufficiently represented in the groundtruth data.

*Table 1. Idealized land cover classes, RSPO vegetation coefficient, relevant change patterns, and land cover macroclasses used for change detection and supervised classification in this study*

| Macroclass | Land Cover Class | RSPO Vegetation Coefficient | Relevant Change Pattern | Change Pattern Macroclass | 2019 Class |
|---|---|---|---|---|---|
| Forest | Undisturbed Rainforest | 1 | Forest | Forest | Forest |
| | Lightly Logged/ Lightly Disturbed Forest | 1 | Forest | Forest | Forest |
| | Mature Secondary Forest | 1 | Forest | Forest | Forest |
| | Secondary Forest | 0.7 | Forest | Forest | Forest |
| Wetlands | Marsh | 1 | OtherGreen | OtherGreen | OtherVegetation |
| | Swamp | 1 | Forest | Forest | Forest |
| | Mangroves | 1 | Forest | Forest | Forest |
| Agroforestry | Polycultural Orchards and Agroforestry | 0.4 | OtherGreen | OtherGreen | OtherAgriculture |
| Agriculture | Oilpalm | 0 | Oilpalm | Oilpalm | Oilpalm |
| | Rubber | 0 | OtherGreen | OtherGreen | Rubber |
| | Rice | 0 | OtherGreen | OtherGreen | Rice |
| | Monocultural Orchards | 0 | OtherGreen | OtherGreen | OtherAgriculture |
| | Tea Plantation | 0 | OtherGreen | OtherGreen | - |
| | Vegetable Farms | 0 | OtherGreen | OtherGreen | - |
| | Other Agriculture | 0 | OtherGreen | OtherGreen | OtherAgriculture |
| Water | River | - | - | - | - |
| | Lake | - | - | - | - |
| | Pond Farms/Aquaculture | - | - | - | - |
| Degraded | Bare ground/cleared | 0 | UrbanOtherBrown | UrbanOtherBrown | Bare Ground |
| | Grassland | 0 | OtherGreen | OtherGreen | OtherVegetation |
| | Scattered Trees | 0 | OtherGreen | OtherGreen | OtherVegetation |
| | Sand/Mud | 0 | UrbanOtherBrown | UrbanOtherBrown | Bare Ground |
| Urban | Urban | 0 | UrbanOtherBrown | UrbanOtherBrown | Urban |

## 3.4 Groundtruth Data for calibration and accuracy assessment

Reference data was gathered in three batches using visual assessment of hi-resolution Google Earth Pro historical imagery (commonly World View), Landsat imagery, World View Imagery in ArcGIS Pro, Google Timelapse and landcover maps from Malaya Landuse, iPlan and an existing historical Oil Palm mapping product by WRI. A map of the points' locations can be found in Appendix A: Map of Ground Truth Points. The data was digitized by several interpreters, with the bulk of the points digitized by the same independent interpreter. All reference points used a homogenous area of 90 metres squared centred around each point as the relevant area for inspection, equal to the 3x3 pixel window used by the LandTrendr algorithm to reduce the effect of localized abnormalities in spectral value and spectral trajectory, and geometric error between the Landsat pixel and the reference data. Accordingly, the minimum distance allowed between points was set at 180 metres.

The LandTrendr algorithm was used with default LandTrendr parameters to produce a raster showing year of disturbance. The default parameters were used for maximum segments (6), spike threshold (0.9), vertex count overshoot (3), prevent one year recovery (false), recovery threshold (0.25), pval threshold (0.1), best model proportion (1.25) and minimum observations needed (6). The index selected was NBR. However, the annual date range for image compositing was extended to cover the whole year from 01-01 to 12-31. Vegetation change type was kept as 'Loss' and sorted by 'Greatest' disturbance. All filters were set to 'false' except for mmu=11.

The resulting raster was used for stratifying 2000 random points equally according to year of change (including *no change*) between 2001 to 2019 (Table 2). These points were examined and labelled according to the method described in Appendix B: Instructions for Gathering Ground Truth Data. Data was recorded regarding current land cover, land cover in the year 2000, occurrence of change prior to the year 2000, and year of disturbance onset and 'before' and 'after' land cover class for any changes taking place after the year 2000.

To examine the satellite imagery, ground truth points were imported into Google Earth Pro and Google Earth Engine. The annual historical imagery in Google Earth and the high-resolution historical imagery were examined at each point, as well as that of the surrounding landscape for context. An example of the use of context is assessing whether an area of dark green vegetation is surrounded by similar land cover with no roads or settlements, or if it is in an agricultural region near to towns and villages – the former would indicate it is likely forest whereas the latter would suggest it could be oil palm plantation. The original land cover in the year 2000 was examined, with comparison to previous years to determine if it was previously disturbed – particularly important in differentiating primary and secondary forest, and in differentiating forest from plantation. The imagery was also examined up to the present, noting the current land cover as of the year 2019, and any disturbances to the land cover, such as forest clearance, plantation replanting, conversion to built-up areas, flooding which destroys vegetation, extreme drought or draining of land, conversion between different types of agriculture, damming of rivers, erosion and change of river courses, and forest regrowth. The type of change was not explicitly recorded, but the time of disturbance onset was recorded, along with both the land cover present before the disturbance occurred and the stable land cover which the land cover became after recovery from the disturbance. If multiple disturbance events occurred, each disturbance was recorded separately. Google Earth Engine was used for viewing customized Landsat composites when a closer view of the pixels was required or for inspecting a more specific time period to determine whether a disturbance occurred in a certain year or in the following year. The following flowchart (Figure 2) was used as a rough guide to define different land covers:
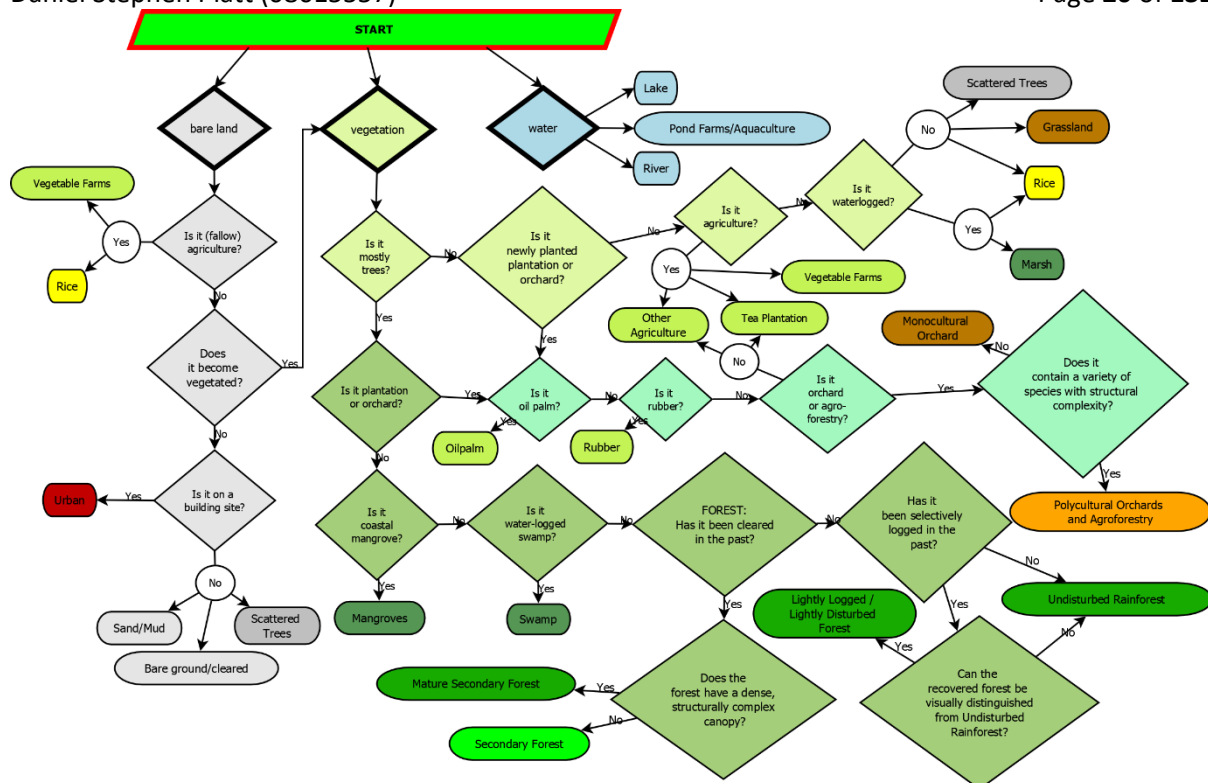
*Figure 2. Flow chart used for deciding which land cover class is present when gathering ground truth data from satellite imagery.*

Of the points examined, 172 were discarded due to falling on areas with heterogeneous land cover or with extremely complicated land cover histories, while 1828 points were kept for use in the analysis. Heterogeneous landcover included areas of part forest mixed with oil palm, rubber or agriculture, or oil palm mixed with rubber or agriculture, as well as some points located on the edge of water bodies. Complicated land cover histories generally involved areas which were cleared or disturbed by flooding or drought multiple times to the point where individual disturbance events could not be clearly differentiated by the interpreter; and where an area of otherwise homogeneous forest was cleared in sections with several years gap between clearance events. As some land cover classes were under-represented, to supplement these points for training and validation, a further 424 points were created and labelled with current land cover only.

An additional set of 333 points targeted towards the 'Other Vegetation', 'Rice', 'Other Agriculture' and 'Bare Ground' land cover classes were created by digitizing polygons in areas dominated by those land cover classes. Points were created randomly within those polygons, maintaining a distance of 180m from each other and all existing points. They were labelled with current land cover only. Points were discarded which fell on mixed land cover ('Other Vegetation', 'Rice' or 'Other Agriculture' mixed with each other, 'Forest', 'Oil Palm' or 'Urban'; and 'Bare Ground' mixed with vegetation classes) or on other land cover classes. Once sufficient points had been digitized for each class any remaining unlabelled points were discarded. A further set of 91 points covering the '*Water*' class were gathered with current land cover to be used for validation only. These points were created manually, making sure to keep a distance of at least 180m between points. A total of 2252 grountruth points were collected of which 1081 were used for calibration/training and 1171 were used in the accuracy assessment.

*Table 2. Calibration and Validation points for each class.*

| Class | Calibration | Validation | Total |
|---|---|---|---|
| Forest | 241 | 219 | 460 |
| Other Vegetation | 64 | 73 | 137 |
| Oilpalm | 443 | 456 | 899 |
| Rubber | 100 | 104 | 204 |
| Rice | 58 | 52 | 110 |
| Other Agriculture | 78 | 70 | 148 |
| Bare Ground | 35 | 34 | 69 |
| Urban | 50 | 59 | 109 |
| Water | 12 | 104 | 116 |
| Total | 1081 | 1171 | 2252 |

## 3.5 LandTrendr historical disturbance mapping

### 3.5.1 Sliding rule

We used sliding thresholds to optimize LandTrendr for each of five key land cover change patterns that dominate Malaysia (Grogan et al., 2015; Kennedy et al., 2010) (Table 3). One of the key challenges with applying LandTrendr to a new location is the need to paramaterise the LandTrendr model, and unlike many Landtrendr studies, we used training data to systematically identify the best parameterisation for running LandTrendr. As LandTrendr only identifies disturbance patterns (i.e. magnitude, length of disturbance and date of disturbance onset) we calibrated LandTrendr separately for each coarse-scale land cover change pattern (Table 3). Calibration points for each change pattern were assigned to a reference and classified dataset values as either Change or No-Change (i.e. disturbance) based on the ground truth data and the LandTrendr greatest disturbance segment data respectively. The reference and classified values were then compared and used to calculate Overall Accuracy for four LandTrendr parameters (i.e. one-year recovery, recovery threshold, and p-value)  to identify the best combination of LandTrendr parameterization which resulted in the most accurate detection of change for a period from 2000 to 2019.

The number of points per change lists produced from the reference data are summarized in Table 3 below.

*Table 3. Number of points used for optimizing parameters per change pattern.*

| | forest to oil palm | oil palm to oil palm (replanting) | forest to urban and other brown | forest to other green | other green to oil palm |
|---|---|---|---|---|---|
| Change | 88 | 310 | 24 | 54 | 25 |
| No Change | 126 | 26 | 126 | 126 | 33 |
| Total | 214 | 336 | 150 | 180 | 58 |

### 3.5.2 Calibration Points

The groundtruth data were converted into change lists for each change pattern, summarized in Table 3. Points were only included in a change list if the original land cover in the year 2000 was of the relevant class. Points were assigned reference values of either 'Change' if they subsequently underwent change to the relevant land cover class or 'No Change' if they remained unchanged with no disturbance having occurred.

### 3.5.3 LandTrendr Parameters

The LandTrendr algorithm was run iteratively with a sliding range of values for each of four LandTrendr parameters: maximum segments, one-year recovery, recovery threshold, and p-value. The remaining LandTrendr parameters were kept at conservative values as they were determined during preliminary calibration to have little effect. The range of values used are summarized in Table 5. The full list of parameterizations is given Appendix C: Table of Parameter Values for Sliding Threshold. A brief description of each parameter is given below:

- Spike threshold – A sudden spike in spectral value may indicate false changes, for example due to clouds. LandTrendr removes spikes where the difference in spectral values before and after the spike is less than a chosen percentage of the magnitude of the spike itself.

- Pval threshold – If the p-of-F value is greater than the chosen threshold, the pixel is considered no-change.

- Maximum segments – The maximum number of segments allowed for the final trajectory.

- Recovery threshold – Rapid recovery after disturbance may be an illusion caused by cloud cover. A segment will be removed if it's rate of recovery relative to the total spectral range is less than 1/recoveryThreshold.

- Vertex count overshoot – The initial model is created with a greater number of segments before undergoing simplification. This number is maximum segments + vertex count overshoot.

- Prevent one year recovery – Complete recovery within a year after vegetation disturbance is considered unlikely in many ecosystems, but does occur in Malaysia. Setting this parameter to *true* will remove those recovery segments.

- Best model proportion – After undergoing simplification, the model is chosen which has the most vertices but with a p value no more than a certain proportion from that of the model with the lowest p value.

- Minimum observations needed – If there are fewer than this number of annual images in a pixel's time series, then it will not be analyzed by LandTrendr and no output will be given.

A sample of some of the LandTrendr parameters used to run LandTrendr for the parameterization is given below in Table 4:

*Table 4. An example of some of the LandTrendr parameters used to extract data for calibrating LandTrendr using a sliding range of values for maximum segments, prevent one year recovery, recovery threshold and pval threshold. The full set of data can be found in Appendix C.*

| Serial Number | 1 | 2 | 3 | 4 | 5 | 6 | 7 | 8 | 9 | 10 |
|---|---|---|---|---|---|---|---|---|---|---|
| maxSegments | 2 | 2 | 4 | 4 | 6 | 6 | 8 | 8 | 2 | 2 |
| spikeThreshold | 0.9 | 0.9 | 0.9 | 0.9 | 0.9 | 0.9 | 0.9 | 0.9 | 0.9 | 0.9 |
| vertexCountOvershoot | 3 | 3 | 3 | 3 | 3 | 3 | 3 | 3 | 3 | 3 |
| preventOneYearRecovery | 1 | 0 | 1 | 0 | 1 | 0 | 1 | 0 | 1 | 0 |
| recoveryThreshold | 0 | 0 | 0 | 0 | 0 | 0 | 0 | 0 | 0 | 0 |
| pvalThreshold | 0.01 | 0.01 | 0.01 | 0.01 | 0.01 | 0.01 | 0.01 | 0.01 | 0.05 | 0.05 |
| bestModelProportion | 0.75 | 0.75 | 0.75 | 0.75 | 0.75 | 0.75 | 0.75 | 0.75 | 0.75 | 0.75 |
| minObservationsNeeded | 6 | 6 | 6 | 6 | 6 | 6 | 6 | 6 | 6 | 6 |

| Serial Number | 11 | 12 | 13 | 14 | 15 | 16 | 17 | 18 | 19 | 20 |
|---|---|---|---|---|---|---|---|---|---|---|
| maxSegments | 4 | 4 | 6 | 6 | 8 | 8 | 2 | 2 | 4 | 4 |
| spikeThreshold | 0.9 | 0.9 | 0.9 | 0.9 | 0.9 | 0.9 | 0.9 | 0.9 | 0.9 | 0.9 |
| vertexCountOvershoot | 3 | 3 | 3 | 3 | 3 | 3 | 3 | 3 | 3 | 3 |
| preventOneYearRecovery | 1 | 0 | 1 | 0 | 1 | 0 | 1 | 0 | 1 | 0 |
| recoveryThreshold | 0 | 0 | 0 | 0 | 0 | 0 | 0 | 0 | 0 | 0 |
| pvalThreshold | 0.05 | 0.05 | 0.05 | 0.05 | 0.05 | 0.05 | 0.1 | 0.1 | 0.1 | 0.1 |
| bestModelProportion | 0.75 | 0.75 | 0.75 | 0.75 | 0.75 | 0.75 | 0.75 | 0.75 | 0.75 | 0.75 |
| minObservationsNeeded | 6 | 6 | 6 | 6 | 6 | 6 | 6 | 6 | 6 | 6 |

| Serial Number | 21 | 22 | 23 | 24 | 25 | 26 | 27 | 28 | 29 | 30 |
|---|---|---|---|---|---|---|---|---|---|---|
| maxSegments | 6 | 6 | 8 | 8 | 2 | 2 | 4 | 4 | 6 | 6 |
| spikeThreshold | 0.9 | 0.9 | 0.9 | 0.9 | 0.9 | 0.9 | 0.9 | 0.9 | 0.9 | 0.9 |
| vertexCountOvershoot | 3 | 3 | 3 | 3 | 3 | 3 | 3 | 3 | 3 | 3 |
| preventOneYearRecovery | 1 | 0 | 1 | 0 | 1 | 0 | 1 | 0 | 1 | 0 |
| recoveryThreshold | 0 | 0 | 0 | 0 | 0.33 | 0.33 | 0.33 | 0.33 | 0.33 | 0.33 |
| pvalThreshold | 0.1 | 0.1 | 0.1 | 0.1 | 0.01 | 0.01 | 0.01 | 0.01 | 0.01 | 0.01 |
| bestModelProportion | 0.75 | 0.75 | 0.75 | 0.75 | 0.75 | 0.75 | 0.75 | 0.75 | 0.75 | 0.75 |
| minObservationsNeeded | 6 | 6 | 6 | 6 | 6 | 6 | 6 | 6 | 6 | 6 |

| Serial Number | 31 | 32 | 33 | 34 | 35 | 36 | 37 | 38 | 39 | 40 |
|---|---|---|---|---|---|---|---|---|---|---|
| maxSegments | 8 | 8 | 2 | 2 | 4 | 4 | 6 | 6 | 8 | 8 |
| spikeThreshold | 0.9 | 0.9 | 0.9 | 0.9 | 0.9 | 0.9 | 0.9 | 0.9 | 0.9 | 0.9 |
| vertexCountOvershoot | 3 | 3 | 3 | 3 | 3 | 3 | 3 | 3 | 3 | 3 |
| preventOneYearRecovery | 1 | 0 | 1 | 0 | 1 | 0 | 1 | 0 | 1 | 0 |
| recoveryThreshold | 0.33 | 0.33 | 0.33 | 0.33 | 0.33 | 0.33 | 0.33 | 0.33 | 0.33 | 0.33 |
| pvalThreshold | 0.01 | 0.01 | 0.05 | 0.05 | 0.05 | 0.05 | 0.05 | 0.05 | 0.05 | 0.05 |
| bestModelProportion | 0.75 | 0.75 | 0.75 | 0.75 | 0.75 | 0.75 | 0.75 | 0.75 | 0.75 | 0.75 |
| minObservationsNeeded | 6 | 6 | 6 | 6 | 6 | 6 | 6 | 6 | 6 | 6 |

Table 5. List of variables used for LandTrendr parameter.

| Parameter | Value(s) |
|---|---|
| maxSegments | 2,4,6,8 |
| spikeThreshold | 0,9 |
| vertexCountOvershoot | 3 |
| preventOneYearRecovery | TRUE, FALSE |
| recoveryThreshold | 0, 0.33, 0.67, 0.99, 1 |
| pvalThreshold | 0.01, 0.05, 0.1 |
| bestModelProportion | 0.75 |
| minObservationsNeeded | 6 |

For each iteration of LandTrendr disturbance rasters were sampled using the calibration points and
values for magnitude and year of disturbance onset were extracted (see Appendix D: GEE Code for
Parameter Optimization). These data were filtered to include only disturbances beginning after the
year 2000.

### 3.5.4 Magnitude Threshold

Each point was assigned a classified value of 'Change' or 'No Change' based on a sliding threshold for
magnitude, from 0 to 500 at intervals of 10. Magnitude refers to the change in spectral value, which
has a possible range of 0 to 1000. If the magnitude of disturbance was greater than the threshold
value then it was counted as 'Change' and if it was less than or equal to the threshold value then it
was counted as 'No Change'. (See Appendix E: R Code for Parameter Optimization.) Given the
average NBR value of forest and oil palm, and that of bare ground, it is unlikely for small
disturbances with magnitude of up to 100 or 200 to represent true clearance. However, disturbances
may show lower magnitudes if the post-disturbance imagery does not capture the bare ground
signature due to rapid regrowth.

### 3.5.5 Accuracy Estimation

For each set of LandTrendr parameters and each magnitude threshold value, Users and Producers
accuracy for change detection was estimated (see Appendix E: R Code for Parameter
Optimization)(Grogan et al., 2015). The equations for calculating accuracy are given below. nA is the
number of points where both the reference value and the classified value are 'Change. nB is the
number of points where the classified value is 'Change'. nC is the number of points where the
reference value is 'Change'.

User's Accuracy was calculated as:

$$UA = \frac{nA}{nB}$$

Producer's Accuracy was calculated as:

$$PA = \frac{nA}{nC}$$

Overall accuracy was calculated as:

$$OA = \frac{UA + PA}{2}$$

The maximum overall accuracy at any magnitude threshold was extracted for each parameterization and was averaged across all change patterns and the best parameterization was used to make the disturbance rasters.

## 3.6 Supervised Random Forest Classification of landcover for 2019

A Random forest supervised classification was conducted using a raster stack which included the disturbance rasters from LandTrendr, a Landsat multi-date 2019 mosaic and SRTM elevation data. The final method was identified from an iterative process which included combining ancillary data to achieve the best classification. In addition, we compared classification results with and without the disturbance rasters. Initially several iterations of the classification were conducted to attempt to improve the accuracy of the output maps, which mainly proved to make little improvement to the overall accuracy. The more useful measures attempted included using a water mask to map the water class and including an elevation layer in the raster stack. These were implemented in the final iteration of the classification. The elevation layer was included as many land covers are spatially concentrated by altitude, such as oil palm and rice in lower elevations and higher elevations dominated by forest (Jarvis, A. et al., 2008).

The Random forest classification was conducted on two image stacks. One stack consisted of a multispectral annual Landsat mosaic for the year 2019 with SRTM elevation data. Seven 30-m resolution Landsat bands were used, including visible light, ultrablue, near infrared and short-wave infrared. The second stack contained additional LandTrendr disturbance rasters representing greatest disturbance segment information extracted for each of the parameterizations chosen in the parameter optimization step. The disturbance rasters consisted of 7 raster layers representing year of disturbance onset, end year, pre-disturbance NBR value, post-disturbance NBR value, magnitude of change in NBR, duration of disturbance and annual rate of disturbance (Hudak et al., 2013).

The calibration points used to train the random forest classifier were the same points used for the parameter optimization step. Each point was assigned a current land cover value. Points assigned to the 'Water' class were removed, as were points which fell on areas with no 2019 Landsat imagery available. The supervised classification was run with 300 trees and a total of 1068 training points (see Appendix F: GEE Code for Classification). After classification, the JRC-GSW layer was used to map areas of the 'Water' class (Pekel et al., 2016). The 'transition' layer was used and pixels labelled 'Permanent', 'New Permanent' or 'Season-to-Permanent' were masked as water. (We found that the seasonal and ephemeral JRC water classes overlapped with rice paddy.)

## 3.7 Validation

The resulting land cover maps were assessed using a separate set of 1171 validation points (see Appendix G: GEE Code for Validation) to produce confusion matrices. Percentage values for User's, Producer's and Overall accuracy were produced (see Appendix H: R Code for Validation). The matrices for the two land cover maps were compared (with and without the inclusion of the LandTrendr disturbance rasters) and areas of confusion between particular land cover classes were identified.

# CHAPTER 4. RESULTS

# 4. Chapter 4 Results

## 4.1 Optimal Parameters

The optimum parameters are presented in Table 6.  These parameters were used in producing the LandTrendr disturbance rasters for the raster stack. Below in Table 7 are the maximum Overall accuracy values obtained with the optimal magnitude threshold along with the User's and Producer's accuracies. Note also that although optimal magnitude threshold values are presented, no magnitude filter was used in producing the disturbance rasters for the supervised classification.

*Table 6. Optimum LandTrendr parameters chosen for extracting disturbances rasters.*

| Parameter | Value |
|---|---|
| Max Segments | 8 |
| spike Threshold | 0.9 |
| vertex Count Overshoot | 3 |
| prevent One Year Recovery | FALSE |
| Recovery Threshold | 1 |
| Pval Threshold | 0.1 |
| Best Model Proportion | 0.75 |
| Min Observations Needed | 6 |

*Table 7. Optimal magnitude threshold and accuracy values for detection of each change pattern when chosen LandTrendr parameters are used.*

| Change Pattern | forest to oil palm | oil palm to oil palm (replanting) | forest to urban and other brown | forest to other green | other green to oil palm |
|---|---|---|---|---|---|
| Magnitude Threshold | 290 | ≤110 | 310 | 150 | ≤140 |
| User's Accuracy (%) | 72.414 | 96.935 | 44.828 | 58.904 | 60.000 |
| Producer's Accuracy (%) | 71.591 | 81.613 | 54.167 | 79.630 | 60.000 |
| Overall Accuracy (%) | 72.002 | 89.274 | 49.497 | 69.267 | 60.000 |

For comparison, the optimal overall accuracy for each individual change pattern when optimized separately are presented in Table 8, and the raw accuracy values for some of the tested iterations of LandTrendr in Table 9. The overall accuracy of detection of each change pattern is slightly lower using the chosen parameters (except for 'other green to oil palm' which remains the same) than if the change pattern were optimized separately. However, as using multiple LandTrendr outputs adds a large number of bands to the raster stack and so reduces accuracy, it is necessary to compromise and use a parameterization that works reasonably well with all five land cover change patterns.

*Table 8. Optimal overall accuracies for detection of individual change patterns separately.*

|  | Overall Accuracy (%) |
|---|---|
| **forest to oil palm** | 72.784 |
| **oil palm to oil palm (replanting)** | 89.294 |
| **forest to urban and other brown** | 50.298 |
| **forest to other green** | 71.701 |
| **other green to oil palm** | 60.000 |

*Table 9 An example of some of the accuracy values obtained for various iterations of LandTrendr, using different magnitude thresholds. The full set of data can be found in Appendix K.*

| | Parameter ID | 1 | 2 | 3 | 4 | 5 | 6 | 7 | 8 | 9 | 10 |
|---|---|---|---|---|---|---|---|---|---|---|---|
| Magnitude Threshold | 0 | 15.34 | 18.37 | 20.45 | 20.45 | 26.70 | 20.45 | 23.13 | 18.37 | 16.70 | 18.37 |
| | 100 | 15.34 | 18.37 | 20.45 | 20.45 | 26.70 | 20.45 | 23.13 | 18.37 | 16.70 | 18.37 |
| | 200 | 15.34 | 18.37 | 20.45 | 20.45 | 26.70 | 20.45 | 23.13 | 18.37 | 16.70 | 18.37 |
| | 300 | 15.34 | 18.37 | 20.45 | 20.45 | 26.70 | 20.45 | 23.13 | 18.37 | 16.70 | 18.37 |
| | 400 | 7.71 | 10.57 | 7.71 | 7.71 | 13.07 | 10.57 | 10.57 | 8.90 | 8.90 | 10.57 |
| | 500 | 10.57 | 13.07 | 10.57 | 13.07 | 25.57 | 25.57 | 17.23 | 17.23 | 10.57 | 13.07 |

| | Parameter ID | 11 | 12 | 13 | 14 | 15 | 16 | 17 | 18 | 19 | 20 |
|---|---|---|---|---|---|---|---|---|---|---|---|
| Magnitude Threshold | 0 | 22.27 | 24.49 | 31.70 | 30.84 | 26.70 | 27.27 | 16.70 | 18.37 | 18.37 | 24.49 |
| | 100 | 22.27 | 24.49 | 31.70 | 30.84 | 26.70 | 27.27 | 16.70 | 18.37 | 18.37 | 24.49 |
| | 200 | 22.27 | 24.49 | 31.70 | 30.84 | 26.70 | 27.27 | 16.70 | 18.37 | 18.37 | 24.49 |
| | 300 | 22.27 | 24.49 | 31.70 | 30.84 | 26.70 | 27.27 | 16.70 | 18.37 | 18.37 | 24.49 |
| | 400 | 8.90 | 10.57 | 17.23 | 13.07 | 13.07 | 10.57 | 8.90 | 10.57 | 8.90 | 10.57 |
| | 500 | 10.57 | 13.07 | 25.57 | 25.57 | 17.23 | 17.23 | 10.57 | 13.07 | 10.57 | 13.07 |

| | Parameter ID | 21 | 22 | 23 | 24 | 25 | 26 | 27 | 28 | 29 | 30 |
|---|---|---|---|---|---|---|---|---|---|---|---|
| Magnitude Threshold | 0 | 25.57 | 42.27 | 17.23 | 35.61 | 16.45 | 12.27 | 71.51 | 68.92 | 74.81 | 75.14 |
| | 100 | 25.57 | 42.27 | 17.23 | 35.61 | 16.45 | 12.27 | 72.73 | 70.86 | 76.84 | 77.12 |
| | 200 | 25.57 | 42.27 | 17.23 | 35.61 | 12.27 | 10.04 | 70.86 | 68.92 | 75.39 | 75.62 |
| | 300 | 25.57 | 42.27 | 17.23 | 35.61 | 14.77 | 12.42 | 65.98 | 63.84 | 72.29 | 72.40 |
| | 400 | 25.57 | 25.57 | 17.23 | 17.23 | 5.11 | 5.57 | 53.75 | 52.75 | 63.07 | 62.13 |
| | 500 | 25.57 | 25.57 | 17.23 | 17.23 | 6.82 | 7.71 | 49.13 | 46.84 | 53.98 | 52.10 |

| | Parameter ID | 31 | 32 | 33 | 34 | 35 | 36 | 37 | 38 | 39 | 40 |
|---|---|---|---|---|---|---|---|---|---|---|---|
| Magnitude Threshold | 0 | 76.57 | 77.62 | 16.45 | 12.27 | 70.77 | 68.18 | 74.81 | 75.14 | 75.86 | 76.91 |
| | 100 | 78.51 | 79.50 | 16.45 | 12.27 | 72.00 | 70.12 | 76.41 | 76.70 | 77.01 | 78.02 |
| | 200 | 78.86 | 79.10 | 12.27 | 10.04 | 70.40 | 68.46 | 74.92 | 75.17 | 77.27 | 77.54 |
| | 300 | 77.12 | 77.24 | 14.77 | 12.42 | 65.37 | 63.23 | 71.69 | 71.82 | 76.02 | 76.18 |
| | 400 | 66.72 | 65.13 | 5.11 | 5.57 | 52.75 | 51.81 | 62.13 | 61.24 | 65.04 | 63.49 |
| | 500 | 55.68 | 53.93 | 6.82 | 7.71 | 46.84 | 44.80 | 52.10 | 50.38 | 53.93 | 52.32 |

| | Parameter ID | 41 | 42 | 43 | 44 | 45 | 46 | 47 | 48 | 49 | 50 |
|---|---|---|---|---|---|---|---|---|---|---|---|
| Magnitude Threshold | 0 | 16.45 | 12.27 | 70.77 | 68.18 | 74.43 | 74.05 | 75.86 | 76.91 | 16.45 | 12.27 |
| | 100 | 16.45 | 12.27 | 72.00 | 70.12 | 76.41 | 76.00 | 77.01 | 78.02 | 16.45 | 12.27 |
| | 200 | 12.27 | 10.04 | 70.40 | 68.46 | 74.92 | 74.46 | 77.27 | 77.54 | 12.27 | 10.04 |
| | 300 | 14.77 | 12.42 | 65.37 | 63.23 | 71.69 | 71.82 | 76.02 | 76.18 | 14.77 | 12.42 |
| | 400 | 5.11 | 5.57 | 52.75 | 51.81 | 62.13 | 61.24 | 65.04 | 63.49 | 5.11 | 5.57 |
| | 500 | 6.82 | 7.71 | 46.84 | 44.80 | 52.10 | 50.38 | 53.93 | 52.32 | 6.82 | 7.71 |

## 4.2 Land Cover Maps

Figure 3 show the classified maps of land cover using Landsat, elevation and LandTrendr data, and
using only Landsat and elevation data. Larger versions are attached in Appendix I: Land Cover Maps.
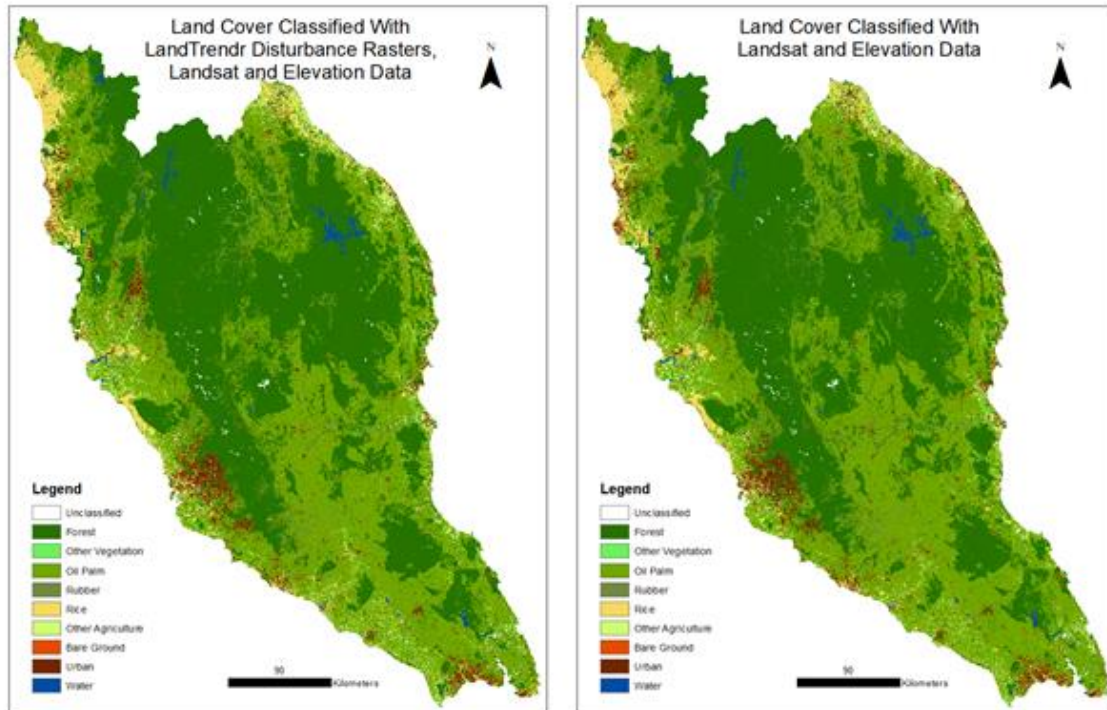


*Figure 3 a) Land cover map classified with LandTrendr disturbance rasters, Landsat and elevation data. b) Land
cover map classified with Landsat and elevation data.*

In Table 10 and Table 11 below are the confusion matrices for the land cover maps which were
classified using raster stacks of LandTrendr disturbance rasters, Landsat and elevation data; and
Landsat and elevation data without LandTrendr disturbance rasters. As can be seen from the last
column of Table 10 and Table 11, the number of points varies greatly between land cover classes. Oil
Palm and Forest, as the dominant land covers in Malaysia, have the most points. This imbalance
affects the classification, skewing the output map to favour oil palm, as shown by the high number
of points misclassified as oil palm among other classes.

*Table 10. Confusion matrix for image classified with LandTrendr disturbance rasters, Landsat and elevation data.*

| | | Classified | | | | | | | | | |
|---|---|---|---|---|---|---|---|---|---|---|---|
| | | Forest | Other Vegetation | Oil Palm | Rubber | Rice | Other Agriculture | Bare Ground | Urban | Water | Total |
| Reference | Forest | **151** | 1 | 57 | 3 | 2 | 0 | 2 | 1 | 1 | 218 |
| | Other Vegetation | 4 | **18** | 27 | 1 | 3 | 16 | 1 | 3 | 0 | 73 |
| | Oil Palm | 30 | 1 | **407** | 3 | 1 | 9 | 4 | 1 | 0 | 456 |
| | Rubber | 20 | 0 | 62 | **16** | 0 | 0 | 4 | 2 | 0 | 104 |
| | Rice | 1 | 1 | 2 | 0 | **42** | 4 | 0 | 2 | 0 | 52 |
| | Other Agriculture | 2 | 9 | 16 | 0 | 5 | **31** | 6 | 1 | 0 | 70 |
| | Bare Ground | 2 | 2 | 3 | 3 | 0 | 4 | **12** | 7 | 0 | 33 |
| | Urban | 0 | 0 | 9 | 1 | 3 | 1 | 10 | **35** | 0 | 59 |
| | Water | 3 | 1 | 0 | 0 | 0 | 0 | 1 | 0 | **99** | 104 |
| | Total | 213 | 33 | 583 | 27 | 56 | 65 | 40 | 52 | 100 | 1169 |

*Table 11. Confusion matrix for image classified with Landsat and elevation data.*

| | | Classified | | | | | | | | | |
|---|---|---|---|---|---|---|---|---|---|---|---|
| | | Forest | Other Vegetation | Oil Palm | Rubber | Rice | Other Agriculture | Bare Ground | Urban | Water | Total |
| Reference | Forest | **144** | 2 | 56 | 11 | 1 | 0 | 2 | 1 | 1 | 218 |
| | Other Vegetation | 3 | **21** | 28 | 0 | 3 | 14 | 1 | 3 | 0 | 73 |
| | Oil Palm | 29 | 0 | **399** | 8 | 2 | 12 | 2 | 4 | 0 | 456 |
| | Rubber | 28 | 0 | 54 | **17** | 0 | 0 | 2 | 3 | 0 | 104 |
| | Rice | 0 | 1 | 5 | 0 | **44** | 2 | 0 | 0 | 0 | 52 |
| | Other Agriculture | 3 | 11 | 13 | 0 | 5 | **32** | 5 | 1 | 0 | 70 |
| | Bare Ground | 4 | 2 | 4 | 1 | 0 | 5 | **12** | 5 | 0 | 33 |
| | Urban | 6 | 1 | 9 | 0 | 1 | 0 | 9 | **33** | 0 | 59 |
| | Water | 3 | 1 | 0 | 0 | 0 | 0 | 0 | 1 | **99** | 104 |
| | Total | 220 | 39 | 568 | 37 | 56 | 65 | 33 | 51 | 100 | 1169 |

## 4.3 Accuracy Assessment

User's, Producer's and Overall accuracy were calculated for both land cover maps (Table 12).

*Table 12. Accuracy values by land cover class and general for both classified images.*

|  | With LandTrendr | | | | Without LandTrendr | | |
|---|---|---|---|---|---|---|---|
|  | UA | PA | OA | | UA | PA | OA |
| **Forest** | 70.892% | 69.266% | 70.079% | | 65.455% | 66.055% | 65.755% |
| **Other Vegetation** | 54.545% | 24.658% | 39.601% | | 53.846% | 28.767% | 41.307% |
| **Oil Palm** | 69.811% | 89.254% | 79.533% | | 70.246% | 87.500% | 78.873% |
| **Rubber** | 59.259% | 15.385% | 37.322% | | 45.946% | 16.346% | 31.146% |
| **Rice** | 75.000% | 80.769% | 77.885% | | 78.571% | 84.615% | 81.593% |
| **Other Agriculture** | 47.692% | 44.286% | 45.989% | | 49.231% | 45.714% | 47.473% |
| **Bare Ground** | 30.000% | 36.364% | 33.182% | | 36.364% | 36.364% | 36.364% |
| **Urban** | 67.308% | 59.322% | 63.315% | | 64.706% | 55.932% | 60.319% |
| **Water** | 99.000% | 95.192% | 97.096% | | 99.000% | 95.192% | 97.096% |
| **Total** | 63.723% | 57.166% | **60.445%** | | 62.596% | 57.387% | **59.992%** |

The map produced using Landsat, elevation data and LandTrendr disturbance rasters had an Overall accuracy of 60.445%, with User's and Producer's accuracy of 63.723% and 57.166% respectively. User's, Producer's and Overall accuracy was calculated for each land cover class. Water had the highest accuracy for all measures. After Water, the class with the highest overall accuracy was Oil Palm (79.533%), followed by Rice (77.885%) and Forest (70.079%). The same pattern was followed for Producer's Accuracy, with 89.254%, 80.769% and 69.266% respectively. User's accuracy was highest for Rice (75.000%), then Forest (70.892%) and Oil Palm (69.811%). Bare Ground scored the lowest overall, with 30.000%, 36.364% and 33.182% User's, Producer's and Overall accuracy respectively. However, Rubber and Other Vegetation had the lowest Producer's Accuracies at 15.385% and 24.658%.

In the map produced using only Landsat and elevation data, the relative accuracies of the classes were about the same, although User's accuracy was considerably lower for Rubber (45.946%) and Forest (65.755%). The Overall accuracy of Bare Ground, while remaining amongst the lowest two classes, was much higher at 36.364%, as was Rice at 81.593%.

Table 13 and Table 14 below show the confusion matrices with percentages instead of number of points for the map which used LandTrendr data in the input raster stack. Percentages are calculated for Table 13 based on the total number of reference points for each land cover class, while percentages for Table 14 are calculated based on the total number of classified points for each land cover. The totals calculated under 'Omission Error' and 'Commission Error' are the sum of percentages for each column/row excluding correctly classified points. The bolded values running diagonally from top-left to bottom-right are the percentage of correctly classified points. In Table 13 these values represent Producer's Accuracy, while in Table 14 they represent User's Accuracy.

*Table 13. The percentages of validation points by reference class for the map using LandTrendr data. The last column shows the total percentage of misclassified points for that class (omission error).*

| | | **Classified** | | | | | | | | | **Omission Error** |
|---|---|---|---|---|---|---|---|---|---|---|---|
| | | **Forest** | **Other Vegetation** | **Oil Palm** | **Rubber** | **Rice** | **Other Agriculture** | **Bare Ground** | **Urban** | **Water** | |
| **Reference** | **Forest** | **69%** | 0% | 26% | 1% | 1% | 0% | 1% | 0% | 0% | **31%** |
| | **Other Vegetation** | 5% | **25%** | 37% | 1% | 4% | 22% | 1% | 4% | 0% | **75%** |
| | **Oil Palm** | 7% | 0% | **89%** | 1% | 0% | 2% | 1% | 0% | 0% | **11%** |
| | **Rubber** | 19% | 0% | 60% | **15%** | 0% | 0% | 4% | 2% | 0% | **85%** |
| | **Rice** | 2% | 2% | 4% | 0% | **81%** | 8% | 0% | 4% | 0% | **19%** |
| | **Other Agriculture** | 3% | 13% | 23% | 0% | 7% | **44%** | 9% | 1% | 0% | **56%** |
| | **Bare Ground** | 6% | 6% | 9% | 9% | 0% | 12% | **36%** | 21% | 0% | **64%** |
| | **Urban** | 0% | 0% | 15% | 2% | 5% | 2% | 17% | **59%** | 0% | **41%** |
| | **Water** | 3% | 1% | 0% | 0% | 0% | 0% | 1% | 0% | **95%** | **5%** |

*Table 14. The percentages of validation points by classified map class for the map using LandTrendr data. The last row shows the total percentage of validation points which were misclassified as a certain land cover (commission error).*

| | | **Classified** | | | | | | | | |
|---|---|---|---|---|---|---|---|---|---|---|
| | | **Forest** | **Other Vegetation** | **Oil Palm** | **Rubber** | **Rice** | **Other Agriculture** | **Bare Ground** | **Urban** | **Water** |
| **Reference** | **Forest** | **71%** | 3% | 10% | 11% | 4% | 0% | 5% | 2% | 1% |
| | **Other Vegetation** | 2% | **55%** | 5% | 4% | 5% | 25% | 3% | 6% | 0% |
| | **Oil Palm** | 14% | 3% | **70%** | 11% | 2% | 14% | 10% | 2% | 0% |
| | **Rubber** | 9% | 0% | 11% | **59%** | 0% | 0% | 10% | 4% | 0% |
| | **Rice** | 0% | 3% | 0% | 0% | **75%** | 6% | 0% | 4% | 0% |
| | **Other Agriculture** | 1% | 27% | 3% | 0% | 9% | **48%** | 15% | 2% | 0% |
| | **Bare Ground** | 1% | 6% | 1% | 11% | 0% | 6% | **30%** | 13% | 0% |
| | **Urban** | 0% | 0% | 2% | 4% | 5% | 2% | 25% | **67%** | 0% |
| | **Water** | 1% | 3% | 0% | 0% | 0% | 0% | 3% | 0% | **99%** |
| **Commission Error** | | 29% | 45% | 30% | 41% | 25% | 52% | 70% | 33% | 1% |

The highest source of omission error is from misclassification as oil palm for all other classes except bare ground and rice. This is partly due to the over-representation of oil palm in the training data, and also to the similarity between oil palm and rubber, other vegetation and forest, which were the classes that were most often misclassified as oil palm. The highest sources of commission error are from confusion between 'other agriculture' and 'other vegetation' and confusion between 'urban' and 'bare ground'. The confusion between these classes is likely caused by the similarity in their spectral appearances.

*Table 15. The percentages of validation points by reference class for the map without LandTrendr data. The last column shows the total percentage of misclassified points for that class (omission error).*

| | | Classified | | | | | | | | | Omission Error |
|---|---|---|---|---|---|---|---|---|---|---|---|
| | | Forest | Other Vegetation | Oil Palm | Rubber | Rice | Other Agriculture | Bare Ground | Urban | Water | |
| Reference | Forest | 66% | 1% | 26% | 5% | 0% | 0% | 1% | 0% | 0% | 34% |
| | Other Vegetation | 4% | 29% | 38% | 0% | 4% | 19% | 1% | 4% | 0% | 71% |
| | Oil Palm | 6% | 0% | 88% | 2% | 0% | 3% | 0% | 1% | 0% | 13% |
| | Rubber | 27% | 0% | 52% | 16% | 0% | 0% | 2% | 3% | 0% | 84% |
| | Rice | 0% | 2% | 10% | 0% | 85% | 4% | 0% | 0% | 0% | 15% |
| | Other Agriculture | 4% | 16% | 19% | 0% | 7% | 46% | 7% | 1% | 0% | 54% |
| | Bare Ground | 12% | 6% | 12% | 3% | 0% | 15% | 36% | 15% | 0% | 64% |
| | Urban | 10% | 2% | 15% | 0% | 2% | 0% | 15% | 56% | 0% | 44% |
| | Water | 3% | 1% | 0% | 0% | 0% | 0% | 0% | 1% | 95% | 5% |

*Table 16. The percentages of validation points by classified map class for the map without LandTrendr data. The last row shows the total percentage of validation points which were misclassified as a certain land cover (commission error).*

| | | Classified | | | | | | | | |
|---|---|---|---|---|---|---|---|---|---|---|
| | | Forest | Other Vegetation | Oil Palm | Rubber | Rice | Other Agriculture | Bare Ground | Urban | Water |
| Reference | Forest | 65% | 5% | 10% | 30% | 2% | 0% | 6% | 2% | 1% |
| | Other Vegetation | 1% | 54% | 5% | 0% | 5% | 22% | 3% | 6% | 0% |
| | Oil Palm | 13% | 0% | 70% | 22% | 4% | 18% | 6% | 8% | 0% |
| | Rubber | 13% | 0% | 10% | 46% | 0% | 0% | 6% | 6% | 0% |
| | Rice | 0% | 3% | 1% | 0% | 79% | 3% | 0% | 0% | 0% |
| | Other Agriculture | 1% | 28% | 2% | 0% | 9% | 49% | 15% | 2% | 0% |
| | Bare Ground | 2% | 5% | 1% | 3% | 0% | 8% | 36% | 10% | 0% |
| | Urban | 3% | 3% | 2% | 0% | 2% | 0% | 27% | 65% | 0% |
| | Water | 1% | 3% | 0% | 0% | 0% | 0% | 0% | 2% | 99% |
| Commission Error | | 35% | 46% | 30% | 54% | 21% | 51% | 64% | 35% | 1% |

Table 15 and Table 16 show confusion matrices with percentages for the map produced without LandTrendr data. The main difference in commission error was in rubber – commission went from 54% down to 41% with the addition of LandTrendr data. When LandTrendr was added, User's Accuracy improved for Forest, Other Vegetation, Rubber and Urban. It remained the same for Oil Palm, and decreased for Rice, Other Agriculture and Bare Ground. Producer's Accuracy averaged across all land covers decreased slightly, but improved for Forest, Oil Palm and Urban. It remained the same for Bare Ground, and decreased for Other Vegetation, Rubber, Rice and Other Agriculture.

Overall accuracy improved for the land covers of interest for mapping oil palm – Forest, Oil Palm and Rubber (as it is spectrally similar). Therefore, while overall accuracy for the map as a whole was only minimally affected by addition LandTrendr data, it has made a larger improvement to differentiation of these key land covers.

## 4.4 LandTrendr

In order to determine whether historical disturbance identified with LandTrendr is useful for land cover mapping in Malaysia it is necessary to answer two questions:

- Is Landsat data sufficient to differentiate different land covers present in Malaysia?
- Is the LandTrendr algorithm capable of detecting changes relevant to differentiating different land covers?

Historical land use and land cover change analysis using only Landsat historical satellite imagery is a challenging task for a human interpreter. The low resolution of the satellite imagery, high variation in appearance within land cover classes and high similarity in appearance between certain land covers makes it difficult to say with certainty what class of land cover is present and what change has taken place. However, with time and experience, a human interpreter could probably make a reasonable attempt to digitize land use and land cover change using the available Landsat bands and supplementary data (Cohen et al., 2010). But this would be difficult to scale to the national level without losing spatial resolution or taking a very long time.

Using LandTrendr disturbance rasters for supervised classification increased overall accuracy by 0.453 percentage points. This suggests that historical disturbance data from LandTrendr may be of some value for land cover change mapping in Malaysia. Preliminary analysis showed that LandTrendr is capable of detecting disturbance due to several different change patterns (see Appendix J: Graphs from Preliminary Investigation 2). It is too soon to say conclusively that it is feasible to use LandTrendr to differentiate types and timing of change in Malaysia. However, it will certainly require further research before LandTrendr can be used to this purpose.

# CHAPTER 5. DISCUSSION

# 5. Chapter 5 Discussion

## 5.1 Overview

The method used in this study for mapping land cover  LandTrendr to study land use and land cover change. However, these previous studies have mostly focused on a limited range of land cover classes or types of change, such as disturbances affecting forest (Hislop et al., 2019) or abandonment of cropland (Dara et al., 2018). They also tend to have already identified land cover distribution in the base year (Zhu et al., 2019) or restrict the study to an area with a narrow range of land cover change patterns present (Grogan et al., 2015; Kennedy et al., 2012). In addition, LandTrendr applications in the tropics for detecting disturbance (Grogan et al., 2015) and recovery (W. Shen et al., 2017) in forests and timber plantations and conversion to rubber plantations (Tang et al., 2019).

Other studies used LandTrendr output rasters for supervised classification, however they used them to identify specific land covers or change patterns, rather than for general land cover classification – or else they targeted a much smaller study area (Rathnayake et al., 2020). In this thesis the method was also modified to suit the tropics – utilizing full-year image collections for creating annual mosaics to reduce cloud cover without affecting coverage, following Grogan et al. (2015), and calibrating LandTrendr to change patterns prevalent in the region.

The results in this thesis did not show a clear advantage in using LandTrendr over using only Landsat and elevation data, nor did it show conclusive evidence that LandTrendr is a viable tool for land cover change mapping. However, it does suggest that LandTrendr has potential to be developed into such a tool. The use of LandTrendr improved overall accuracy for oil palm, rubber and forest detection, and specifically user's accuracy improved for forest and rubber, while producer's accuracy improved for forest and oil palm. This means that use of LandTrendr improves differentiation of these three very similar land covers and therefore careful use of LandTrendr could have a positive impact on attempts to map change from forest to oil palm. In contrast there was unexpected decreases in accuracy for certain land covers when LandTrendr was used, such as increased confusion between bare ground and rubber, and bare ground and urban, decrease in producer's accuracy for rubber, and the overall decrease in accuracy for rice and other agriculture. It may be that LandTrendr outputs may have more relevance to the change patterns being targeted.

## 5.2 Parameterization

The parameters used were found to have a large effect on the accuracy of change detection, with overall accuracy values ranging from below 10% for some change patterns up to above 80% depending on the parameters and magnitude threshold used (see Appendix K: Tables of Selected Accuracy Values from Parameter Optimization). The overall accuracy under optimal conditions varied from 50.298% for 'forest to urban and other brown' to 89.294% for 'oil palm to oil palm' (replanting). Lower accuracy may reflect a lack of calibration points as the change patterns with the three lowest overall accuracy values were also those with the fewest calibration points. The variability in change events may also be a factor, with forest clearance and replanting of oil palm widely following standard patterns of management, whereas urban development may have a variety of time periods and spectral appearances following clearance.

Only one LandTrendr parameter was used for producing disturbance rasters, as it was found that including additional parameterizations had a negative impact on map accuracy, likely due to having too many bands with too few training points. Therefore, the algorithm hasn't been able to detect each type of change equally well. In choosing the optimum parameters, each change pattern was weighted equally even though 'Forest to Oil Palm' and 'Oil Palm to Oil Palm' (replanting) are both

the most prevalent change patterns and the patterns being studied. However, a compromise seems better as it allows detection of all change patterns and reduces the complexity of the classification. It would be useful in further studies to know in which years conversion to oil palm is most prevalent. However, from the ground truth data we cannot accurately determine an overall temporal pattern in forest to oil palm conversion.

## 5.3 Mapping

The two land cover maps produced with and without LandTrendr didn't appear very noticeably different from each other, with major areas of land cover remaining largely the same in both. Out of 145.9 million total pixels, only 7.5% (10.9 million pixels) differed between the two land cover maps. This is approximately 9913km$^2$. Most of the differences were due to differences in the classification of oil palm and forest.  Only 1.7 million pixels (1563km$^2$) represented net differences between the two methods. At a smaller scale, differences are visible in small groups of pixels with differences between similar land cover classes and in mixed landscapes. Two examples are given below from Negeri Sembilan and the coast of Pahang.



*Figure 4 Examples of areas which show differences between land cover maps classified from an input raster stack consisting of Landsat imagery, elevation data and LandTrendr outputs (A1 and B1), and produced from a raster stack consisting of only Landsat imagery and elevation data (A2 and B2). The locations are in Pahang (A) and Negeri Sembilan (B)*
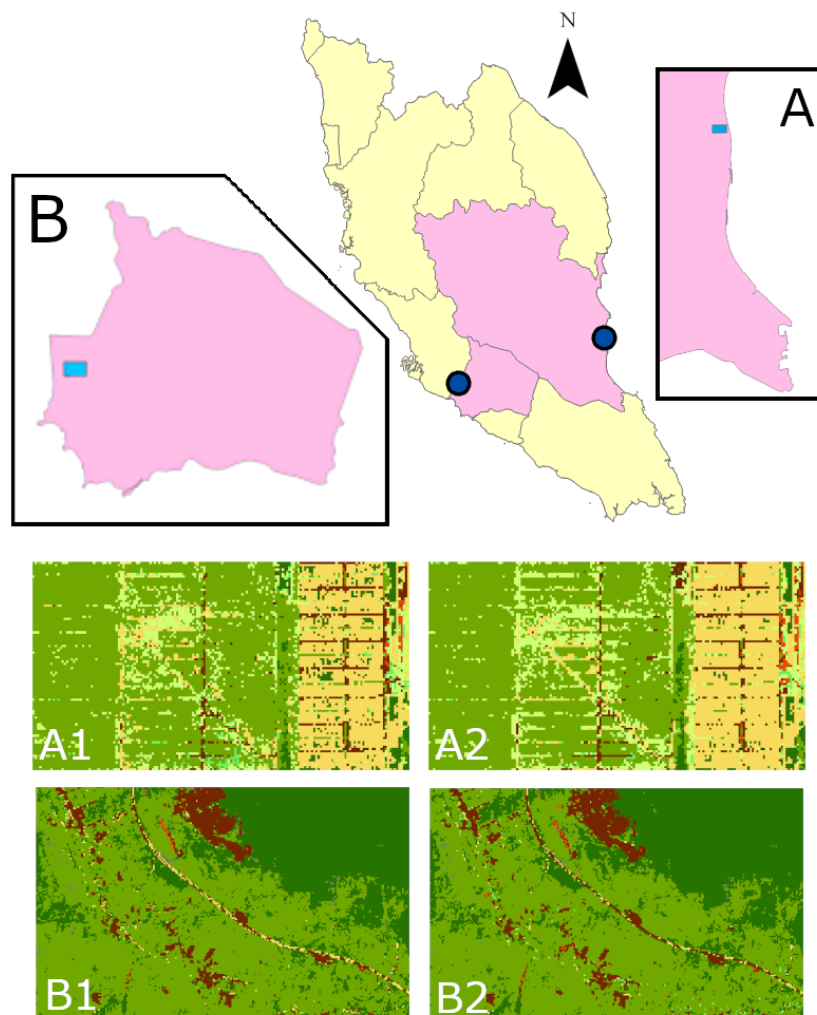
In Figure 4 Examples of areas which show differences between land cover maps classified from an input raster stack consisting of Landsat imagery, elevation data and LandTrendr outputs (A1 and B1), and produced from a raster stack consisting of only Landsat imagery and elevation data (A2 and B2). The locations are in Pahang (A) and Negeri Sembilan (B), the scene from Pahang shows rice and oil palm fields (A), with an area of denser vegetation between them and paths. The two images show differences in distribution of the pixels making up the paths (classified as 'urban') between rows of vegetation. The scene from Negeri Sembilan (B) shows a linear settlement with agriculture that runs parallel to a highway with forest in the northeastern corner. The two images differ in their distribution of 'forest' and 'oil palm' pixels in the transition zone, and the image with LandTrendr (B1) shows a section of road ('urban') misclassified as 'rice'.

For the map classified using LandTrendr, the greatest sources of confusion were between 'other vegetation' and 'other agriculture' (orchards and miscellaneous other types of agriculture such as large home gardens and banana fields – see Table 1: 2019 Land Cover), and between 'bare ground' and 'urban'. In terms of the number of misclassified points, the most frequently confused land covers were 'rubber', 'oil palm' and 'forest' as also found in previous studies (Mohd Najib et al., 2020). A major source of commission errors for 'forest' and 'oil palm' were 'oil palm' or 'rubber' being classified as 'forest', and 'rubber' or 'forest' being classified as 'oil palm'. Other sources of error were 'other agriculture' being classified as 'bare ground'. The greatest source of omission was misclassification of land covers as 'oil palm', particularly misclassification of 'rubber', 'other vegetation' and 'forest'. While 'oil palm' and 'forest' maintained accuracy values all above 69%, 'rubber' had a poor producer's accuracy at only 15%. This may be due to the difficulty encountered during ground truthing as rubber was difficult to differentiate from forest and oil palm, while being less common than either class.

The map classified using LandTrendr data is slightly more accurate than the one using only Landsat and elevation data, although producer's accuracy decreased slightly. There was a large increase in overall accuracy for 'rubber' and 'forest' and a smaller increase for 'oil palm' and 'urban', but a decrease in overall accuracy for 'other vegetation', 'rice', 'other agriculture' and 'bare ground'. As LandTrendr detects disturbance by analyzing temporal change, the improvement in detection of rubber and forest may be attributed to the ability to detect past clearance and differentiate it from undisturbed forest. The decrease in accuracy of detecting bare ground may be due to associating recent disturbance with a bare ground signal, whereas vegetation in the tropics may recover rapidly, hiding the bare ground signal in as little time as a year. Likewise, detection of rice may have been confounded by temporary changes in spectral value due to seasonal flooding and harvest patterns being interpreted as change by LandTrendr.

## 5.4 Limitations and Future Research

While the results indicate that LandTrendr is useful for helping to map land cover and investigating historical land cover change, the accuracy of the land cover map is still quite low and will require further research to potentially improve it. The results might be improved by increasing the number and quality of training points (Kanniah et al., 2015; Li et al., 2014; Shaharum et al., 2020). The ground truth data may not have been labelled accurately, as some land covers are difficult to differentiate from satellite imagery, and high resolution imagery is not uniformly available for all areas and time periods. The constraints in selecting more numerous, reliable training points for this study were time and cost, and difficulty of reliably interpreting historical satellite imagery. As high quality imagery over the complete time period is scarce and land covers are difficult to differentiate, it requires an expert interpreter with experience in the task and in the land cover patterns present in the target area.

The similarity of many common land covers in Malaysia is partly due to the domination of the landscape by trees, including natural forest and oil palm and rubber plantations, which have similar spectral appearances to one another. These classes are difficult to differentiate visually or using random forests as they are spectrally similar. We found from a small sample of points for bare land, forest, oil palm, water and urban that the NDVI and NBR of forest, oil palm and bare land all overlapped with each other (see Appendix L: Graphs from Preliminary Investigation 1). The large study area and fine level of land cover classes used in the analysis were also limiting as it increased the potential variability in land cover patterns. To simplify the study, land covers were not differentiated into different stages of growth, despite vast differences in appearance and spectral value between newly planted and mature oil palm, and between dry and flooded rice fields.

Other challenges encountered were due to the local climate. Located in the equatorial region, Malaysia experiences high rainfall and cloud cover. An attempt was made to identify periods of low cloud incidence to focus on. However, using a cloud mapping tool (Appendix M: Cloud Cover Mapper) it was found that different regions of Peninsular Malaysia have different seasonal patterns of cloud cover due to the influence of the two monsoons. It may be possible to separate and map different areas of the peninsula according to their seasonal pattern, thereby reducing the chance of spectral variation due to short-term changes in vegetation. The tropical climate also means that vegetation may change appearance rapidly after rainfall, especially after a dry period; and rapid vegetation regrowth may obscure disturbance signals from being detected by LandTrendr, which operates at a temporal scale of one year.

One of the limitations of using LandTrendr is that disturbance data only applies to a small proportion of the whole study area. Furthermore, we have not identified which LandTrendr outputs are most important for identifying land cover. Further research to investigate the significance of individual segment characteristics and spectral bands or indices (Hudak et al., 2013), and the use of recovery information and data from multiple disturbances (Kennedy et al., 2012) per pixel may help to develop LandTrendr for land use and land cover change mapping for tropical South East Asia.

# CHAPTER 6. CONCLUSION

## 6. Chapter 6 Conclusion

This study is the first to use LandTrendr in Malaysia and the first use it for mapping land cover classes in South East Asia. Land cover maps have been produced with user's accuracy for oil palm and forest of 69.81% and 70.89%, and which show that LandTrendr disturbance data can be used to improve supervised classification of land cover in Malaysia. With further research it may be possible for this capability to be developed into a useful tool for mapping land conversion to oil palm plantation, conducting LUCA assessments and for conservation planning.

# 7. Chapter 7 Bibliography

Ahmad, F., Ushiyama, T., & Sayama, T. (2017). Determination of Z-R Relationship and Inundation Analysis for Kuantan River. *Research Publication No. 2*, 1–39. http://www.met.gov.my/data/research/researchpapers/2017/researchpaper_201702.pdf

Almeida de Souza, A., Galvão, L. S., Korting, T. S., & Prieto, J. D. (2020). Dynamics of savanna clearing and land degradation in the newest agricultural frontier in Brazil. *GIScience and Remote Sensing*, *57*(7). https://doi.org/10.1080/15481603.2020.1835080

Bartz, K. K., Ford, M. J., Beechie, T. J., Fresh, K. L., Pess, G. R., Kennedy, R. E., Rowse, M. L., & Sheer, M. (2015). Trends in developed land cover adjacent to habitat for threatened salmon in Puget Sound, Washington, U.S.A. *PLoS ONE*, *10*(4). https://doi.org/10.1371/journal.pone.0124415

Beckschäfer, P. (2017). Obtaining rubber plantation age information from very dense Landsat TM & ETM + time series data and pixel-based image compositing. *Remote Sensing of Environment*, *196*, 89–100. https://doi.org/10.1016/j.rse.2017.04.003

Boriah, S. (University of M. (2010). *Time Series Change Detection: Algorithms for Land Cover Change* [University of Minnesota]. https://conservancy.umn.edu/handle/11299/90706

*CFMask Algorithm*. (n.d.). USGS. Retrieved May 26, 2021, from https://www.usgs.gov/core-science-systems/nli/landsat/cfmask-algorithm

Chong, K. L., Kanniah, K. D., Pohl, C., & Tan, K. P. (2017). A review of remote sensing applications for oil palm studies. *Geo-Spatial Information Science*, *20*(2). https://doi.org/10.1080/10095020.2017.1337317

Cohen, W. B., Yang, Z., & Kennedy, R. (2010). Detecting trends in forest disturbance and recovery using yearly Landsat time series: 2. TimeSync - Tools for calibration and validation. *Remote Sensing of Environment*, *114*(12). https://doi.org/10.1016/j.rse.2010.07.010

Daliman, S., Rahman, S. A., Bakar, S. A., & Busu, I. (2014). Segmentation of oil palm area based on GLCMSVM and NDVI. *IEEE TENSYMP 2014 - 2014 IEEE Region 10 Symposium*. https://doi.org/10.1109/tenconspring.2014.6863113

Dara, A., Baumann, M., Kuemmerle, T., Pflugmacher, D., Rabe, A., Griffiths, P., Hölzel, N., Kamp, J., Freitag, M., & Hostert, P. (2018). Mapping the timing of cropland abandonment and recultivation in northern Kazakhstan using annual Landsat time series. *Remote Sensing of Environment*, *213*. https://doi.org/10.1016/j.rse.2018.05.005

Deilmai, B. R., Ahmad, B. Bin, & Zabihi, H. (2014). Comparison of two Classification methods (MLC and SVM) to extract land use and land cover in Johor Malaysia. *IOP Conference Series: Earth and Environmental Science*, *20*(1). https://doi.org/10.1088/1755-1315/20/1/012052

Department of Statistics. (2017). *Malaysia economics statistics—Time series 2016.* https://www.dosm.gov.my/v1/index.php?r=column/ctimeseries&menu_id=NHJlaGc2Rlg4ZXlGTjh1SU1kaWY5UT09

FAO. (2020). *Global Forest Resources Assessment (FRA) 2020 Malaysia*. http://www.fao.org/3/cb0033en/cb0033en.pdf

Foga, S., Scaramuzza, P. L., Guo, S., Zhu, Z., Dilley, R. D., Beckmann, T., Schmidt, G. L., Dwyer, J. L., Joseph Hughes, M., & Laue, B. (2017). Cloud detection algorithm comparison and validation for operational Landsat data products. *Remote Sensing of Environment*, *194*, 379–390. https://doi.org/10.1016/j.rse.2017.03.026

Fragal, E. H., Silva, T. S. F., & Novo, E. M. L. de M. (2016). Reconstrução histórica de mudanças na
     cobertura florestal em várzeas do baixo amazonas utilizando o algoritmo landtrendr. *Acta
     Amazonica*, *46*(1). https://doi.org/10.1590/1809-4392201500835

FRAGAL, E. H., SILVA, T. S. F., & NOVO, E. M. L. de M. (2016). Reconstructing historical forest cover
     change in the Lower Amazon floodplains using the LandTrendr algorithm. *Acta Amazonica*,
     *46*(1). https://doi.org/10.1590/1809-4392201500835

Global Forest Watch. (n.d.). *Tree cover loss in Malaysia*. Retrieved January 30, 2021, from
     www.globalforestwatch.org

Grogan, K., Pflugmacher, D., Hostert, P., Kennedy, R., & Fensholt, R. (2015). Cross-border forest
     disturbance and the role of natural rubber in mainland Southeast Asia using annual Landsat
     time series. *Remote Sensing of Environment*, *169*. https://doi.org/10.1016/j.rse.2015.03.001

Hislop, S., Jones, S., Soto-Berelov, M., Skidmore, A., Haywood, A., & Nguyen, T. H. (2019). A fusion
     approach to forest disturbance mapping using time series ensemble techniques. *Remote
     Sensing of Environment*, *221*. https://doi.org/10.1016/j.rse.2018.11.025

Hudak, A. T., Bright, B. C., & Kennedy, R. E. (2013). Predicting live and dead basal area from
     LandTrendr variables in beetle-affected forests. *MultiTemp 2013 - 7th International Workshop
     on the Analysis of Multi-Temporal Remote Sensing Images: "Our Dynamic Environment",
     Proceedings*. https://doi.org/10.1109/Multi-Temp.2013.6866024

Jarvis, A., Reuter, H. I., Nelson, A., & Guevara, E. (2008). *Hole-filled SRTM for the globe Version 4*.
     https://srtm.csi.cgiar.org

Kamiran, N., & Sarker, M. L. R. (2014). Exploring the potential of high resolution remote sensing data
     for mapping vegetation and the age groups of oil palm plantation. *IOP Conference Series: Earth
     and Environmental Science*, *18*(1). https://doi.org/10.1088/1755-1315/18/1/012181

Kanniah, K. D., Cracknell, A. P., & Yu, L. (2019). Preface. In *International Journal of Remote Sensing*
     (Vol. 40, Issue 19). https://doi.org/10.1080/01431161.2019.1613069

Kanniah, K. D., Sheikhi, A., Cracknell, A. P., Goh, H. C., Tan, K. P., Ho, C. S., & Rasli, F. N. (2015).
     Satellite images for monitoring mangrove cover changes in a fast growing economic region in
     southern Peninsular Malaysia. *Remote Sensing*, *7*(11), 14360–14385.
     https://doi.org/10.3390/rs71114360

Kennedy, R. E., Yang, Z., Braaten, J., Copass, C., Antonova, N., Jordan, C., & Nelson, P. (2015).
     Attribution of disturbance change agent from Landsat time-series in support of habitat
     monitoring in the Puget Sound region, USA. *Remote Sensing of Environment*, *166*.
     https://doi.org/10.1016/j.rse.2015.05.005

Kennedy, R. E., Yang, Z., & Cohen, W. B. (2010). Detecting trends in forest disturbance and recovery
     using yearly Landsat time series: 1. LandTrendr - Temporal segmentation algorithms. *Remote
     Sensing of Environment*, *114*(12). https://doi.org/10.1016/j.rse.2010.07.008

Kennedy, R. E., Yang, Z., Cohen, W. B., Pfaff, E., Braaten, J., & Nelson, P. (2012). Spatial and temporal
     patterns of forest disturbance and regrowth within the area of the Northwest Forest Plan.
     *Remote Sensing of Environment*, *122*, 117–133. https://doi.org/10.1016/j.rse.2011.09.024

Kennedy, R. E., Yang, Z., Gorelick, N., Braaten, J., Cavalcante, L., Cohen, W. B., & Healey, S. (2018).
     Implementation of the LandTrendr algorithm on Google Earth Engine. In *Remote Sensing* (Vol.
     10, Issue 5). https://doi.org/10.3390/rs10050691

Lechner, A. M., Foody, G. M., & Boyd, D. S. (2020). Applications in Remote Sensing to Forest Ecology

and Management. *One Earth*, *2*(5). https://doi.org/10.1016/j.oneear.2020.05.001

Lee, J. S. H., Wich, S., Widayati, A., & Koh, L. P. (2016). Detecting industrial oil palm plantations on
    Landsat images with Google Earth Engine. *Remote Sensing Applications: Society and
    Environment*, *4*(March 2015), 219–224. https://doi.org/10.1016/j.rsase.2016.11.003

Li, C., Wang, J., Wang, L., Hu, L., & Gong, P. (2014). Comparison of classification algorithms and
    training sample sizes in urban land classification with landsat thematic mapper imagery.
    *Remote Sensing*, *6*(2), 964–983. https://doi.org/10.3390/rs6020964

Liang, L., Hawbaker, T. J., Chen, Y., Zhu, Z., & Gong, P. (2014). Characterizing recent and projecting
    future potential patterns of mountain pine beetle outbreaks in the Southern Rocky Mountains.
    *Applied Geography*, *55*. https://doi.org/10.1016/j.apgeog.2014.09.012

Malaysian Palm Oil Board. (2019). *Oil Palm Planted Area 2019*.
    http://bepi.mpob.gov.my/images/area/2019/Area_summary.pdf

Meigs, G. W., Kennedy, R. E., & Cohen, W. B. (2011). A Landsat time series approach to characterize
    bark beetle and defoliator impacts on tree mortality and surface fuels in conifer forests.
    *Remote Sensing of Environment*, *115*(12). https://doi.org/10.1016/j.rse.2011.09.009

Miettinen, J., Gaveau, D. L. A., & Liew, S. C. (2018). Comparison of visual and automated oil palm
    mapping in Borneo. *International Journal of Remote Sensing*, *40*(21), 8174–8185.
    https://doi.org/10.1080/01431161.2018.1479799

Miettinen, J., Shi, C., & Liew, S. C. (2016). Land cover distribution in the peatlands of Peninsular
    Malaysia, Sumatra and Borneo in 2015 with changes since 1990. *Global Ecology and
    Conservation*, *6*, 67–78. https://doi.org/10.1016/j.gecco.2016.02.004

Mohd Najib, N. E., Kanniah, K. D., Cracknell, A. P., & Yu, L. (2020). Synergy of active and passive
    remote sensing data for effective mapping of oil palm plantation in Malaysia. *Forests*, *11*(8).
    https://doi.org/10.3390/F11080858

Olaniyi, A. O., Abdullah, A. M., Ramli, M. F., & Sood, A. M. (2013). Agricultural land use in Malaysia:
    An historical overview and implications for food security. *Bulgarian Journal of Agricultural
    Science*, *19*(1).

Omont, H. (2005). Roundtable on sustainable palm oil - RSPO. The second RSPO meeting in Jakarta in
    October 2004. In *OCL - Oleagineux Corps Gras Lipides* (Vol. 12, Issue 2).
    https://doi.org/10.1051/ocl.2005.0125

Pekel, J. F., Cottam, A., Gorelick, N., & Belward, A. S. (2016). High-resolution mapping of global
    surface water and its long-term changes. *Nature*, *540*(7633).
    https://doi.org/10.1038/nature20584

Pflugmacher, D., Cohen, W. B., & Kennedy, R. E. (2012). Using Landsat-derived disturbance history
    (1972-2010) to predict current forest structure. *Remote Sensing of Environment*, *122*.
    https://doi.org/10.1016/j.rse.2011.09.025

Pittman, A. M. (Stanford U., Curran, L. M. (Stanford U., Carlson, K. M. (New Y. U., & Ponette-
    Gonzalez, A. G. (University of N. T. (2013). NASA Satellite Data Used to Study the Impact of Oil
    Palm Expansion Across Indonesian Borneo. *The Earth Observer (NASA)*, 12–16.

Rathnayake, C. W. M., Jones, S., & Soto-Berelov, M. (2020). Mapping land cover change over a 25-
    year period (1993-2018) in Sri Lanka using landsat time-series. *Land*, *9*(1).
    https://doi.org/10.3390/land9010027

Razak, J. A. binti A., Shariff, A. R. bin M., Ahmad, N. bin, & Ibrahim Sameen, M. (2018). Mapping
    rubber trees based on phenological analysis of Landsat time series data-sets. *Geocarto
    International*, *33*(6), 627–650. https://doi.org/10.1080/10106049.2017.1289559

Razali, S. M., Marin, A., Nuruddin, A. A., Shafri, H. Z. M., & Hamid, H. A. (2014). Capability of
    integrated MODIS imagery and ALOS for oil palm, rubber and forest areas mapping in tropical
    forest regions. *Sensors (Switzerland)*, *14*(5). https://doi.org/10.3390/s140508259

RSPO. (2015). *RSPO Remediation and Compensation Procedures Related to Land Clearance without
    Prior HCV Assessment*.
    http://www.rspo.org/file/2_RSPORemediationandCompensationProcedures_May2014.pdf

Samat, N., Mahamud, M. A., Tan, M. L., Tilaki, M. J. M., & Tew, Y. L. (2020). Modelling land cover
    changes in peri-urban areas: A case study of george town conurbation, malaysia. *Land*, *9*(10).
    https://doi.org/10.3390/land9100373

Schneibel, A., Stellmes, M., Röder, A., Frantz, D., Kowalski, B., Haß, E., & Hill, J. (2017). Assessment of
    spatio-temporal changes of smallholder cultivation patterns in the Angolan Miombo belt using
    segmentation of Landsat time series. *Remote Sensing of Environment*, *195*.
    https://doi.org/10.1016/j.rse.2017.04.012

Senf, C., Pflugmacher, D., van der Linden, S., & Hostert, P. (2013). Mapping rubber plantations and
    natural forests in Xishuangbanna (Southwest China) using multi-spectral phenological metrics
    from modis time series. *Remote Sensing*, *5*(6), 2795–2812. https://doi.org/10.3390/rs5062795

Senf, C., Pflugmacher, D., Wulder, M. A., & Hostert, P. (2015). Characterizing spectral-temporal
    patterns of defoliator and bark beetle disturbances using Landsat time series. *Remote Sensing
    of Environment*, *170*. https://doi.org/10.1016/j.rse.2015.09.019

Shaharum, N. S. N., Shafri, H. Z. M., Ghani, W. A. W. A. K., Samsatli, S., Al-Habshi, M. M. A., & Yusuf,
    B. (2020). Oil palm mapping over Peninsular Malaysia using Google Earth Engine and machine
    learning algorithms. *Remote Sensing Applications: Society and Environment*, *17*(October 2019),
    100287. https://doi.org/10.1016/j.rsase.2020.100287

Shen, W. J., & Li, M. S. (2017). Mapping disturbance and recovery of plantation forests in southern
    China using yearly landsat time series observations. *Shengtai Xuebao/ Acta Ecologica Sinica*,
    *37*(5). https://doi.org/10.5846/stxb201510142074

Shen, W., Li, M., & Wei, A. (2017). Spatio-temporal variations in plantation forests' disturbance and
    recovery of northern Guangdong Province using yearly Landsat time series observations (1986–
    2015). *Chinese Geographical Science*, *27*(4). https://doi.org/10.1007/s11769-017-0880-z

Stibig, H. J., Achard, F., Carboni, S., Raši, R., & Miettinen, J. (2014). Change in tropical forest cover of
    Southeast Asia from 1990 to 2010. *Biogeosciences*, *11*(2). https://doi.org/10.5194/bg-11-247-
    2014

Sun, Z., Leinenkugel, P., Guo, H., Huang, C., & Kuenzer, C. (2017). Extracting distribution and
    expansion of rubber plantations from Landsat imagery using the C5.0 decision tree method.
    *Journal of Applied Remote Sensing*, *11*(2), 026011. https://doi.org/10.1117/1.jrs.11.026011

Tang, D., Fan, H., Yang, K., & Zhang, Y. (2019). Mapping forest disturbance across the China–Laos
    border using annual Landsat time series. *International Journal of Remote Sensing*, *40*(8).
    https://doi.org/10.1080/01431161.2018.1533662

Tang, K. H. D., & Al Qahtani, H. M. S. (2020). Sustainability of oil palm plantations in Malaysia. In
    *Environment, Development and Sustainability* (Vol. 22, Issue 6).

https://doi.org/10.1007/s10668-019-00458-6

Tangang, F. T., Juneng, L., Salimun, E., Sei, K. M., Le, L. J., & Muhamad, H. (2012). Climate change and variability over Malaysia: Gaps in science and research information. *Sains Malaysiana*, *41*(11).

Trisasongko, B. H., Panuju, D. R., Paull, D. J., Jia, X., & Griffin, A. L. (2017). Comparing six pixel-wise classifiers for tropical rural land cover mapping using four forms of fully polarimetric sar data. *International Journal of Remote Sensing*, *38*(11), 3274–3293. https://doi.org/10.1080/01431161.2017.1292072

Trisasongko, B. H., & Paull, D. (2020). A review of remote sensing applications in tropical forestry with a particular emphasis in the plantation sector. In *Geocarto International* (Vol. 35, Issue 3). https://doi.org/10.1080/10106049.2018.1516245

Wang, X., Huang, H., Gong, P., Biging, G. S., Xin, Q., Chen, Y., Yang, J., & Liu, C. (2016). Quantifying multi-decadal change of planted forest cover using airborne LiDAR and Landsat imagery. *Remote Sensing*, *8*(1). https://doi.org/10.3390/rs8010062

Wang, Z., Lechner, A. M., Yang, Y., Baumgartl, T., & Wu, J. (2020). Mapping the cumulative impacts of long-term mining disturbance and progressive rehabilitation on ecosystem services. *Science of the Total Environment*, *717*. https://doi.org/10.1016/j.scitotenv.2020.137214

Xu, Y., Yu, L., Li, W., Ciais, P., Cheng, Y., & Gong, P. (2020). Annual oil palm plantation maps in Malaysia and Indonesia from 2001 to 2016. *Earth System Science Data*, *12*(2). https://doi.org/10.5194/essd-12-847-2020

Yang, Y., Erskine, P. D., Lechner, A. M., Mulligan, D., Zhang, S., & Wang, Z. (2018). Detecting the dynamics of vegetation disturbance and recovery in surface mining area via Landsat imagery and LandTrendr algorithm. *Journal of Cleaner Production*, *178*. https://doi.org/10.1016/j.jclepro.2018.01.050

Ye, L., Liu, M., Liu, X., & Zhu, L. (2021). Developing a new disturbance index for tracking gradual change of forest ecosystems in the hilly red soil region of southern China using dense Landsat time series. *Ecological Informatics*, *61*. https://doi.org/10.1016/j.ecoinf.2021.101221

Yoshino, K., Ishida, T., Nagano, T., & Setiawan, Y. (2010). LANDCOVER PATTERN ANALYSIS OF TROPICAL PEAT SWAMP LANDS IN SOUTHEAST ASIA. *Networking the World with Remote Sensing*, *38*.

Zhu, L., Liu, X., Wu, L., Tang, Y., & Meng, Y. (2019). Long-term monitoring of cropland change near Dongting Lake, China, using the landtrendr algorithm with landsat imagery. *Remote Sensing*, *11*(10). https://doi.org/10.3390/rs11101234

Zhu, Z. (2017). Change detection using landsat time series: A review of frequencies, preprocessing, algorithms, and applications. In *ISPRS Journal of Photogrammetry and Remote Sensing* (Vol. 130). https://doi.org/10.1016/j.isprsjprs.2017.06.013

# Appendices

## Appendix A: Map of Ground Truth Points

Appendix B: Instructions for Gathering Ground Truth Data
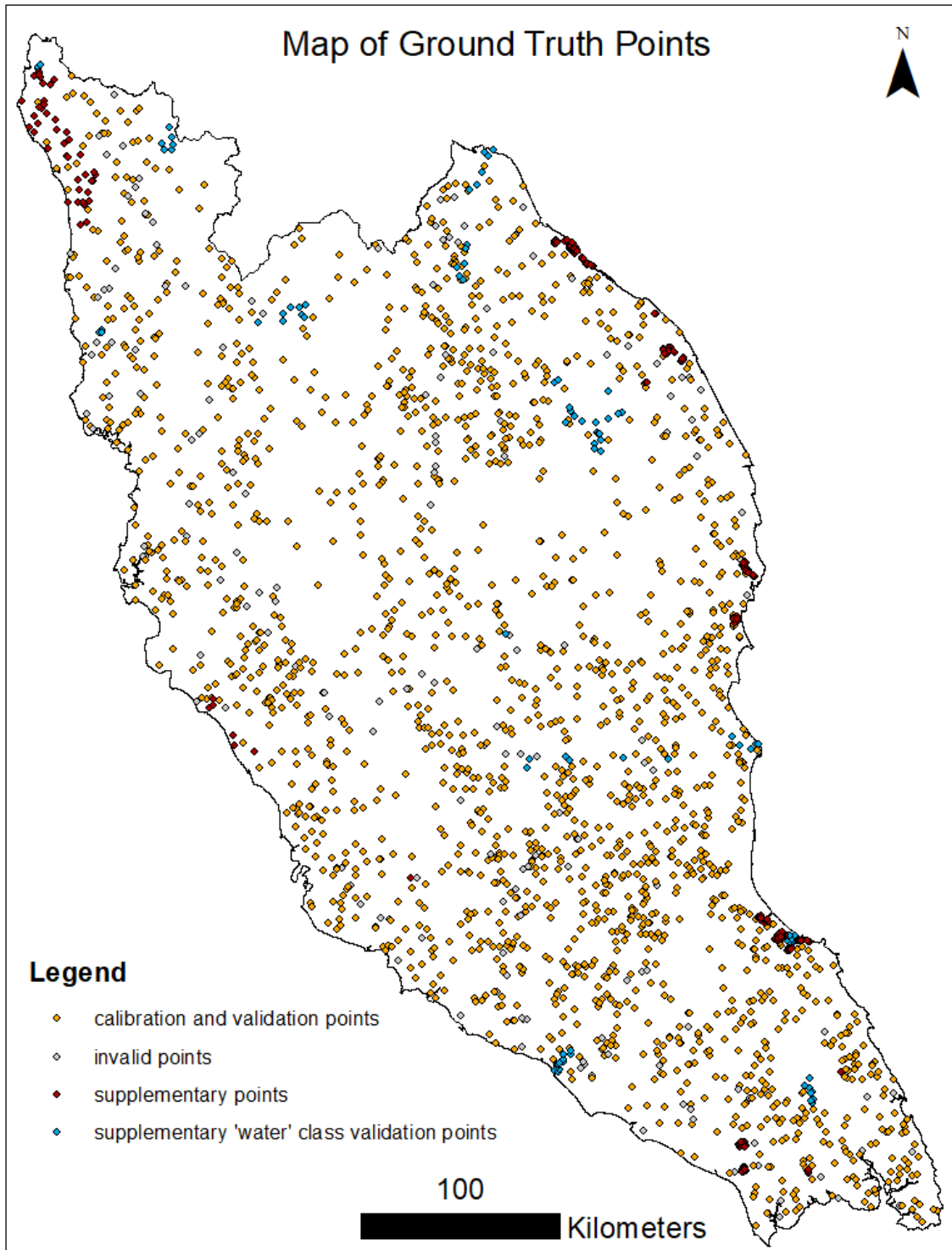
Documents Included in Instruction Package:

1. instructions.pdf
   - Main document describing how to inspect the satellite imagery and label the points.
2. datakeys.pdf
   - Keys explaining what values to input for each field when labelling the points.
   - Additional notes related to the data keys.
3. landcover-screenshots.ppt
   - Example images for various landcover classes.
4. classification scheme.xls
   - List and descriptions of the coarse (macro) and fine landcover classes.
5. landcover-flowchart.png
   - A visual aid to differentiating landcover classes.

Also see the demonstration videos on YouTube:
https://www.youtube.com/playlist?list=PLUDezM3HQXofRhfvtlvmZsk6PJZVu_phf

Video 1 – How to set columns as Read-Only.
Video 2 – Add ArcGIS Basemap and check date.
Video 3 – Set up Google Earth.
Video 4 – Starting to examine and label points.
Video 5 – Classifying a group of nearby points at once.
Video 6 – Labelling multiple clearances and no clearance.
Video 7 – Long demonstration of labelling a large set of points.

You should start by reading the Instructions.pdf, to get a full idea of what to do. The videos will also help get an idea of how to carry out the instructions, particularly Videos 1, 2 3 and 4.

The data keys and classification scheme will be necessary to refer to when actually labelling the points. You should read these carefully before starting classification and refer back to them as necessary.

The landcover flowchart will be useful initially to get a general idea of how to differentiate landcover classes, and may help with particularly challenging points. However, you will not need it when classifying every single point.

You should have a look at the example images in landcover-screenshots.ppt before you start classification.

**Instructions**

To manually label points from satellite imagery, to be used for calibrating a landcover change model and assessing its accuracy.

**Background**

Point data is needed for developing a model that can produce annual change maps of areas where forest clearance and other landcover change has occurred. There are three types of change pattern being looked at:

- Forest to oilpalm plantation
- Forest to urban/other
- Oilpalm plantation to oilpalm plantation (clearance and replanting)
- Oilpalm to other
- Other to oilpalm

Calibration points are needed as well as accuracy points. However, as far as your task goes, there is no difference between the two.

The points will be labelled with information regarding any clearance events which have taken place from Year 2000 onwards, as well as more brief information about pre-2000 disturbance, and some information regarding landcover. (See below).

This information will be determined based on visual assessment of historical satellite imagery from various sources, including Google Earth Pro, Google Timelapse, the ArcGIS basemap(s) and Google Earth Engine. Additional documents are also included (see readme.doc). See the following link for demonstration videos:
https://www.youtube.com/playlist?list=PLUDezM3HQXofRhfvtlvmZsk6PJZVu_phf.

More details about this are given below.

**Files:**

The initial files include:

- peninsular.shp – a boundary polygon for Peninsular Malaysia
- rawpoints.shp – random points with blank attribute columns for filling in groundtruth information

**Steps:**

SECTION I: SETTING UP AND USING DIFFERENT TOOLS
FOR EXAMINING SATELLITE IMAGERY

1.  ArcGIS Pro

    a)  Open ArcGIS Pro with no template. (See Video
        1 and Data Keys). Insert a New Map. Under
        the Map tab, add the 'Imagery' basemap[1].
        (See Fig I:1a(i) and Fig I:1a(ii). This will be one
        of the ground truth sources.



*Fig I:1a(i) Add 'Imagery' Basemap to ArcMap.*



*Fig I:1a(ii) Add 'Imagery' Basemap to ArcMap.*
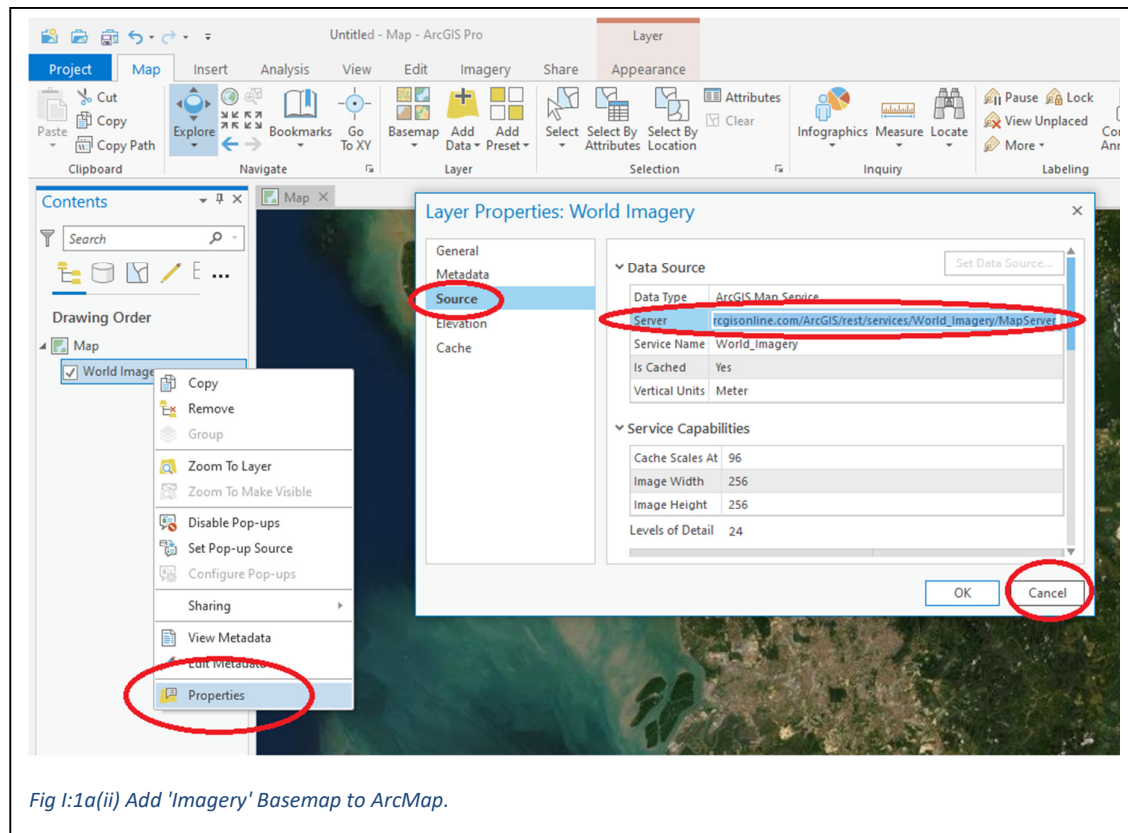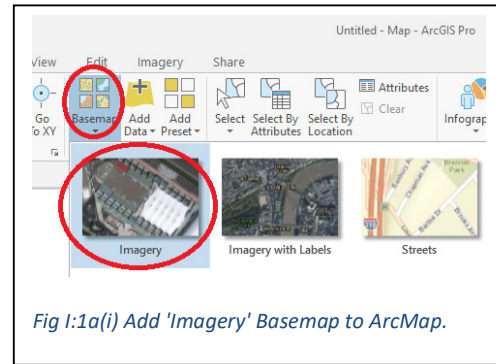
    b)  The basemap is a mosaic of multiple images. To check the date of an image you will need to
        copy the Source: Server URL from the basemap properties. Then Add Data from Path using
        the URL with '/0' added at the end of the string. Finally click on the image near the point
        being examined to get the date of the image. See Fig I:1b.

---

[1] See Video 2.
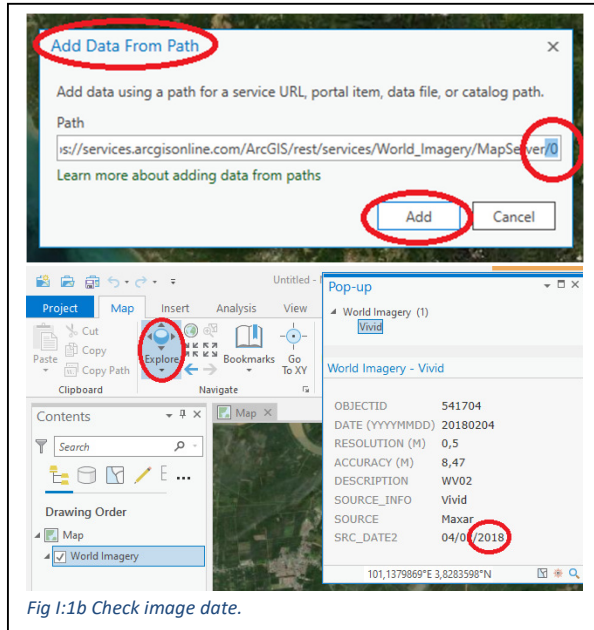
Fig I:1b Check image date.

c)    Import the random points (and boundary file for Peninsular Malaysia) into ArcGIS Pro. Set columns "CID", "YID" and "Class" to Read-Only.

2. Google Earth Pro

   a. An important ground truth source will be from Google Earth Pro[2]. This programme can be downloaded from https://www.google.com/earth/versions/#earth-pro. Import rawpoints as a .shp file. See Fig I:2a(i) and (ii).

   b. A dialog box will ask about setting a design template. Select 'No.' See Fig I:2b.
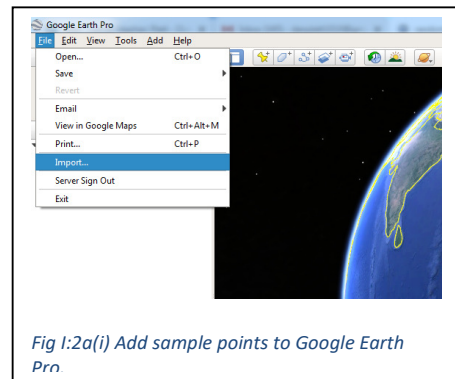


Fig I:2a(i) Add sample points to Google Earth Pro
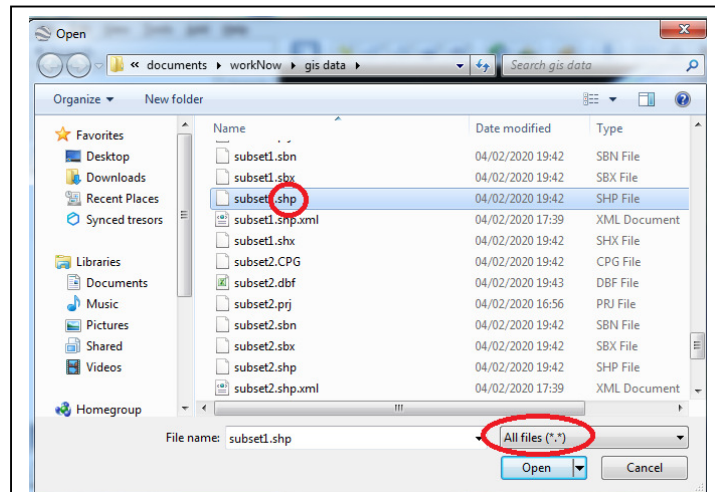


Fig I:2a(ii) Make sure to set file type to 'All files' when selecting the shapefile (centre image).
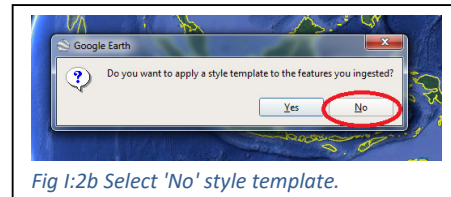


Fig I:2b Select 'No' style template.

---

[2] See Video 3.

c. Switch on the layer and set the symbology to a hollow circle ◎ See Fig I:2c.

d. It is important to look at the whole range of historical imagery available in Google Earth. This includes more recent hi-res imagery at close zoom and annual low-res images from 1984 to 2016 at lower zoom levels. To access historical imagery select the clock icon in the toolbar. You need to be at the right zoom level to view all the Landsat imagery. See Fig I:2d.



Fig I:2c Set symbol to a circle.
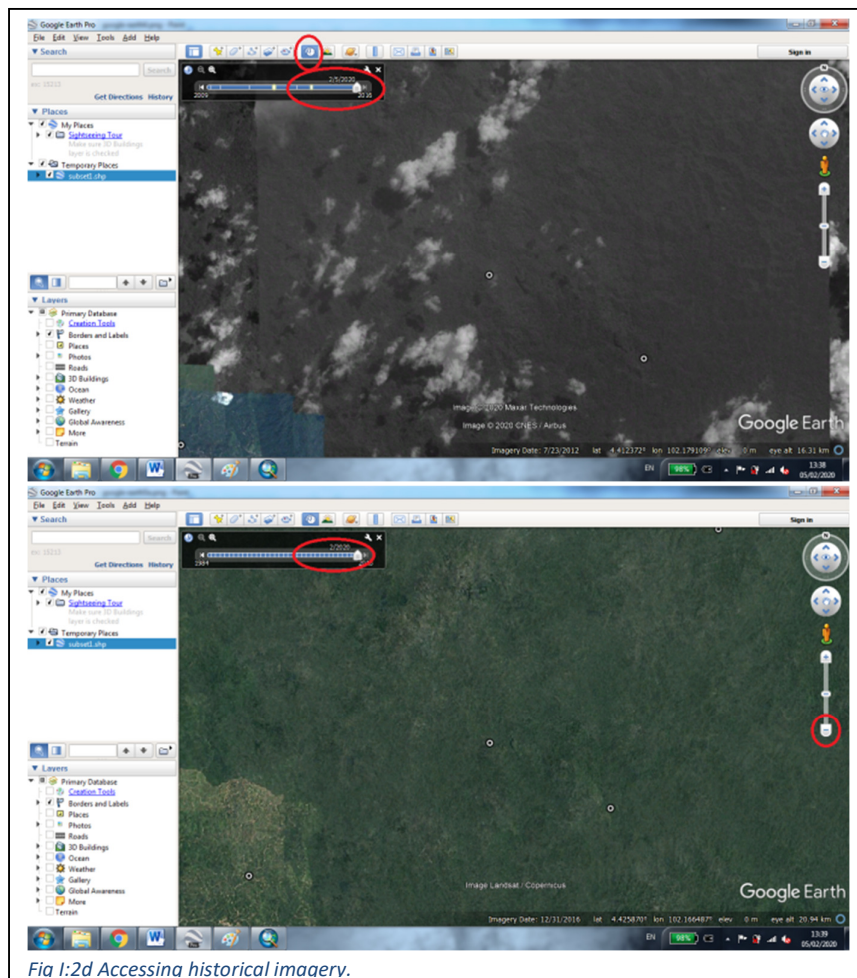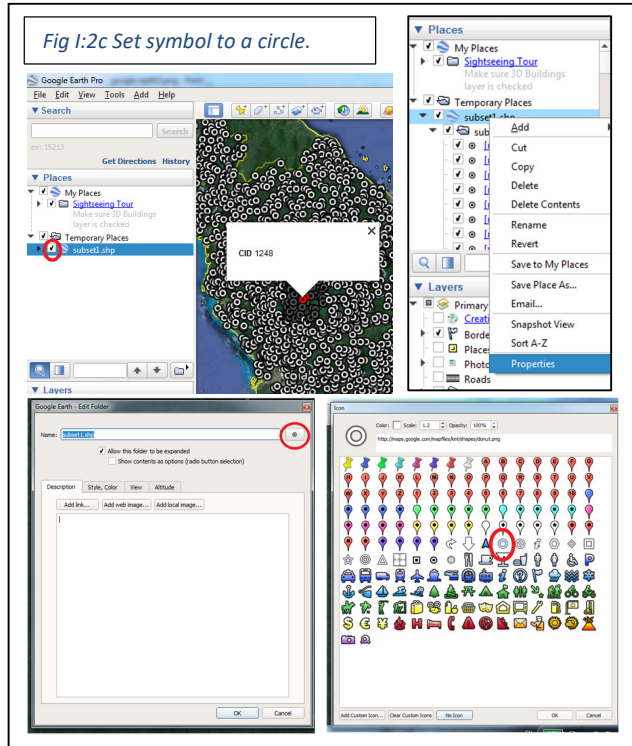


Fig I:2d Accessing historical imagery.

e.  It is important to use the Windows Magnifier tool to view the imagery at the pixel level (See Fig I:2e(i) – set View to 'Docked', Tracking to 'Follow the keyboard focus' and Zoom to 500%. To set the view, rightclick on a point and mouse over the nearest menu option; then left-click anywhere on the map. See Fig I:2e(ii).
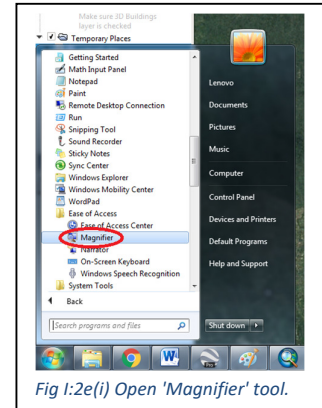

Fig I:2e(i) Open 'Magnifier' tool.
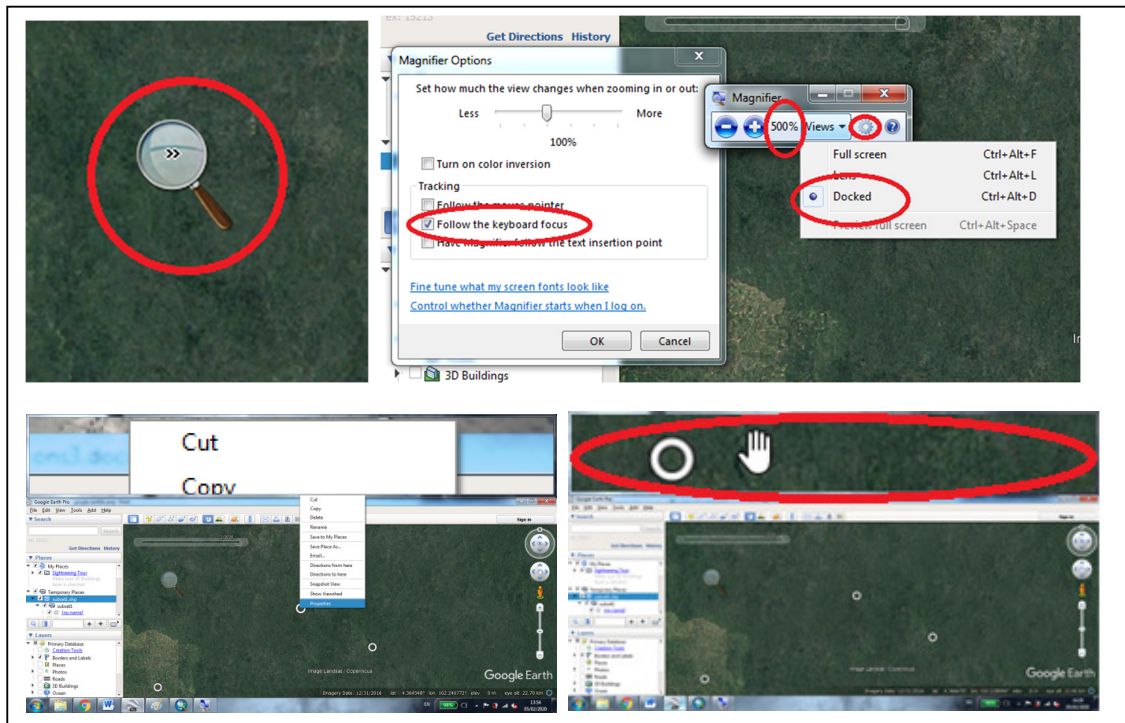

Fig I:2e(ii) Change the 'Magnifier' Settings.

f.  Finally, in order to view high-resolution satellite imagery, (which is only available for more recent years,) zoom in. This imagery makes it possible to see individual trees and determine the type of vegetation/plantation which is present. You may need to click forward on the timeline slider after zooming in. See Video 3.

3.  Google Timelapse

Google Timelapse may also be useful for quickly viewing large-scale changes over time in an area: https://earthengine.google.com/timelapse/. You can navigate to an area by typing in the coordinates in decimal degrees.

4.  Google Earth Engine

More temporally-detailed imagery can be viewed from Landsat using Google Earth Engine (GEE). This will be useful for looking at rapid changes (less than a year) as individual Landsat

images can be viewed. It will only be used as a supplement when Goggle Earth Pro imagery is not sufficient, for example to identify the month(s) when change began/ended, and to pinpoint small areas of disturbance.

In order to use the GEE code editor (https://code.earthengine.google.com), you will need to have a Google account and will need to apply for access to GEE which may take a few days to be approved. I will then share scripts and assets which can be run to visualize multitemporal Landsat mosaics.

The following describes how to use Google Earth Engine to create and examine cloudfree mosaics from Landsat 5, 7 and 8 imagery. [3]

a) After opening the script, go to the section titled 'Set parameters'. Choose the point that you wish to inspect according to its CID number; and the date range (YYYY-MM-DD) for the satellite imagery which will be used to form the mosaic. Click Run.

b) Wait for the map to load. It will display a cloudfree mosaic of Landsat 5, 7 and/or 8 images. Under 'Layers' you can also view NDWI and NDVI maps for the same area.

SECTION II: EXAMINING GROUNDTRUTH DATA (SATELLITE IMAGERY) [4]



Fig II:1 Three-by-three pixel area corresponding to one point.

1. Examine the ground truth sources. You are looking to find out what changes in landcover have occurred and when clearance took place. For each point, examine the imagery mentioned in Section I ("SETTING UP AND USING DIFFERENT TOOLS FOR EXAMINING SATELLITE IMAGERY"). The area to be examined should roughly correspond to a 3x3 Landsat pixel region (~90x90m) around the point. (See Fig II:-)

2. Each disturbance event is to be noted. Only disturbances which occurred after the year 2000 need to be labelled in more detail (see Data Keys). Disturbance events include clearance, selective logging, replanting, permanent flooding or drainage, and temporary flooding which has causes significant damage to the vegetation. Regrowth after clearance is considered to be part of the same change event as the clearance, rather than a separate change event in itself. For example, forest clearance and subsequent regrowth will be classified as forest-to-secondaryforest, not forest-to-bare and bare-to-secondaryforest.

3. If the area covers the boundary between several different landcovers, ignore the point and move on to the next point. If the point falls on a narrow road or river that doesn't make up a significant proportion of the area being examined, the point can be examined and labelled as usual with a note added mentioning the presence of the road/river.

4. In Google Earth, the hi-res imagery can be used to differentiate similar-looking landcovers. Once the landcover has been identified, the hi-res imagery should then be compared with low-res imagery or Landsat mosaics from the same year; and with images from preceding and following years. The low-res historical imagery is probably the most important source of information, particularly when clear hi-res imagery is scarce. The presence or absence of change (eg. clearance or recovery) can be used to determine what landcover was present
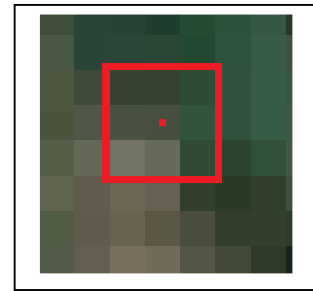
---

[3] See Video 6.
[4] See Video 4.

during years for which hi-res imagery is not available. Temporal patterns in the appearance of the satellite images are very important for identifying the landcover.

> For example, if forest if visible in 2010 hi-res imagery, and no clearance has occurred in the past, then it is probably Undisturbed Rainforest or Lightly Logged / Lightly Disturbed Rainforest. If it has been disturbed in the past then it is likely Secondary Forest or Mature Secondary Forest. Alternatively, you might suspect that it was converted to rubber plantation after the clearance event.

The landcover can also be determined from context. Using your judgement, you can look at the surrounding landscape – such as whether it is deep forest, forest edge, agricultural land, urban, oilpalm-dominated, etc. – and decide which landcover classes make the most sense.

5. Also see the "landcover-screenshots.ppt" and "landcover-flowcharts.png" documents for help in differentiating the various landcovers.

SECTION III: LABELLING THE POINTS

1. In ArcGIS Pro, use the attribute table to label the points (rawpoints.shp) with the data gathered from the satellite imagery. The data keys to input is described in "datakeys.pdf" and the landcover classes are described in "classification scheme.xls".

2. If a point has undergone multiple disturbance events[5], duplicate the point, and label each copy with a different disturbance event. (See Fig III:2b-d). The 'Year', 'Duration', 'Before' and 'After' (See datakeys.pdf; sections k, l, & m) will need changing but the other attributes ('Change', 'Pre200', 'Post2000', 'Orig', 'Curr' and 'Multi') remain the same for all copies of the point.

    a. Label the point completely for the first change/disturbance event, as per screenshots and instructions below.

    b. Save changes from the Edit tab. From the Edit tab click 'Copy'.

    c. From the same tab, click 'Paste'. It will appear as the last object in the Attributes table.

    d. Change the relevant attributes for the new point (Year, Duration, Before, After).



*Fig III:2b-d Copying a point which has undergone multiple disturbances.*

    e. Repeat as many times as needed.

3. Some points may be classified simultaneously, if they fall within an area that has undergone the same or similar change pattern. See Video 5 for an example of this.

---

[5] See Video 6.

DATA KEYS

Make sure the input is case-sensitive with no spaces before or after the word/phrase.

(The default values for not-yet-labelled points are 9999 for numeric fields and a blank for text fields.)

a) [Attribute Field] CID [serial number of the point – DO NOT CHANGE]

b) YID [secondary serial number of the point – DO NOT CHANGE]

c) Class [year of change used in stratifying the random points – DO NOT CHANGE]

d) Change [whether or not change has occurred here):
   a. 0 = no change
   b. 1 = change

e) Pre2000 [whether or not any disturbance was observed prior to year 2000]
   a. 0 = no change
   b. 1 = change
   c. 2 = only minor change (such as selective logging or repeated light disturbance)

f) Post2000 [whether or not any disturbance was observed between year 2000 and the present]
   a. 0 = no change
   b. 1 = change
   c. 2 = only minor change (such as selective logging or repeated light disturbance)

g) Orig [original land cover as of 1999 or most recent imagery prior to year 2000; see Landcover Class Definitions; use the ID number for the FINE landcover class]

h) Curr [current landcover or landcover present in most recent imagery; see Landcover Class Definitions; use the ID number for the FINE landcover class]

i) Multi [whether more than one disturbance event occurred from year 2000 onwards]:
   a. 0 = one or no disturbance events
   b. 1 = two or more disturbance events

j) Year [year of onset of disturbance, ONLY from year 2000 onwards]: Eg. 2003. If multiple disturbance events occurred, label the year of greatest disturbance. **See Step 5**.

k) Duration [number of years before the disturbed land begins to recover]

l) Before [landcover before change event; see Landcover Class Definitions; use the ID number for the FINE landcover class]

m) After [landcover the disturbed area converts to after disturbance; see Landcover Class Definitions; use the ID number for the FINE landcover class]. Note that, if further disturbance events occur (**See i**), this landcover only refers to the fate of the landcover until the next clearance event. Also, a cleared area may undergo further clearance before regrowth occurs – in this case input 'Bare'.

n) Notes [commentary and annotations]: for example, if a point has been ignored due to falling on the boundary between several different landcover classes, it could be labelled as 'landcover boundary'. If a point falls exactly on a road or a narrow stream, which does not make up a significant portion of the area being examined, it can be labelled as 'on road' or 'on stream'. Other major ambiguities in the imagery can also be noted.

Important Notes:

- The 'Change', 'Pre2000' and 'Post2000' columns all refer to occurrence of change, but in different time periods. 'Change' refers to the whole period, and so should only be labelled as '0=no change' if both Pre2000 and Post2000 also show no change.

- Orig and Curr refer to the overall time period – Orig is landcover before year 2000 and Curr is the most recent landcover.
- All other columns refer to specific clearance events – ie. If multiple clearances take place (Multi=1) at one point, these columns will have different values for each duplicate of that point (see Step 5). So 'Before' refers specifically to the landcover immediately before clearance and 'After' refers to the landcover the land converts to after that specific clearance event.
- When identifying landcover for Orig, Curr, Before and After, it is important to consider temporal patterns across the whole range of available imagery and how this relates to real events; and to not just look only at the imagery from the particular year of interest.
- Where no change events are explicitly visible in pre-2000 imagery, the value for Pre2000 will be 0, even if the landcover is non-natural (eg. Rubber plantation).
- Only put Multi=1 if more than one clearance event occurred after year 2000. If one clearance occurred after year 2000 and another before year 2000, the value for Multi will still be 0.
- Minimum value for Duration is 1. If 0 is put in it means that no change has occurred.

## Appendix C: Table of Parameter Values for Sliding Threshold

| Serial Number | 1 | 2 | 3 | 4 | 5 | 6 | 7 | 8 | 9 | 10 |
|---|---|---|---|---|---|---|---|---|---|---|
| maxSegments | 2 | 2 | 4 | 4 | 6 | 6 | 8 | 8 | 2 | 2 |
| spikeThreshold | 0.9 | 0.9 | 0.9 | 0.9 | 0.9 | 0.9 | 0.9 | 0.9 | 0.9 | 0.9 |
| vertexCountOvershoot | 3 | 3 | 3 | 3 | 3 | 3 | 3 | 3 | 3 | 3 |
| preventOneYearRecovery | 1 | 0 | 1 | 0 | 1 | 0 | 1 | 0 | 1 | 0 |
| recoveryThreshold | 0 | 0 | 0 | 0 | 0 | 0 | 0 | 0 | 0 | 0 |
| pvalThreshold | 0.01 | 0.01 | 0.01 | 0.01 | 0.01 | 0.01 | 0.01 | 0.01 | 0.05 | 0.05 |
| bestModelProportion | 0.75 | 0.75 | 0.75 | 0.75 | 0.75 | 0.75 | 0.75 | 0.75 | 0.75 | 0.75 |
| minObservationsNeeded | 6 | 6 | 6 | 6 | 6 | 6 | 6 | 6 | 6 | 6 |

| Serial Number | 11 | 12 | 13 | 14 | 15 | 16 | 17 | 18 | 19 | 20 |
|---|---|---|---|---|---|---|---|---|---|---|
| maxSegments | 4 | 4 | 6 | 6 | 8 | 8 | 2 | 2 | 4 | 4 |
| spikeThreshold | 0.9 | 0.9 | 0.9 | 0.9 | 0.9 | 0.9 | 0.9 | 0.9 | 0.9 | 0.9 |
| vertexCountOvershoot | 3 | 3 | 3 | 3 | 3 | 3 | 3 | 3 | 3 | 3 |
| preventOneYearRecovery | 1 | 0 | 1 | 0 | 1 | 0 | 1 | 0 | 1 | 0 |
| recoveryThreshold | 0 | 0 | 0 | 0 | 0 | 0 | 0 | 0 | 0 | 0 |
| pvalThreshold | 0.05 | 0.05 | 0.05 | 0.05 | 0.05 | 0.05 | 0.1 | 0.1 | 0.1 | 0.1 |
| bestModelProportion | 0.75 | 0.75 | 0.75 | 0.75 | 0.75 | 0.75 | 0.75 | 0.75 | 0.75 | 0.75 |
| minObservationsNeeded | 6 | 6 | 6 | 6 | 6 | 6 | 6 | 6 | 6 | 6 |

| Serial Number | 21 | 22 | 23 | 24 | 25 | 26 | 27 | 28 | 29 | 30 |
|---|---|---|---|---|---|---|---|---|---|---|
| maxSegments | 6 | 6 | 8 | 8 | 2 | 2 | 4 | 4 | 6 | 6 |
| spikeThreshold | 0.9 | 0.9 | 0.9 | 0.9 | 0.9 | 0.9 | 0.9 | 0.9 | 0.9 | 0.9 |
| vertexCountOvershoot | 3 | 3 | 3 | 3 | 3 | 3 | 3 | 3 | 3 | 3 |
| preventOneYearRecovery | 1 | 0 | 1 | 0 | 1 | 0 | 1 | 0 | 1 | 0 |
| recoveryThreshold | 0 | 0 | 0 | 0 | 0.33 | 0.33 | 0.33 | 0.33 | 0.33 | 0.33 |
| pvalThreshold | 0.1 | 0.1 | 0.1 | 0.1 | 0.01 | 0.01 | 0.01 | 0.01 | 0.01 | 0.01 |
| bestModelProportion | 0.75 | 0.75 | 0.75 | 0.75 | 0.75 | 0.75 | 0.75 | 0.75 | 0.75 | 0.75 |
| minObservationsNeeded | 6 | 6 | 6 | 6 | 6 | 6 | 6 | 6 | 6 | 6 |

| Serial Number | 31 | 32 | 33 | 34 | 35 | 36 | 37 | 38 | 39 | 40 |
|---|---|---|---|---|---|---|---|---|---|---|
| maxSegments | 8 | 8 | 2 | 2 | 4 | 4 | 6 | 6 | 8 | 8 |
| spikeThreshold | 0.9 | 0.9 | 0.9 | 0.9 | 0.9 | 0.9 | 0.9 | 0.9 | 0.9 | 0.9 |
| vertexCountOvershoot | 3 | 3 | 3 | 3 | 3 | 3 | 3 | 3 | 3 | 3 |
| preventOneYearRecovery | 1 | 0 | 1 | 0 | 1 | 0 | 1 | 0 | 1 | 0 |
| recoveryThreshold | 0.33 | 0.33 | 0.33 | 0.33 | 0.33 | 0.33 | 0.33 | 0.33 | 0.33 | 0.33 |
| pvalThreshold | 0.01 | 0.01 | 0.05 | 0.05 | 0.05 | 0.05 | 0.05 | 0.05 | 0.05 | 0.05 |
| bestModelProportion | 0.75 | 0.75 | 0.75 | 0.75 | 0.75 | 0.75 | 0.75 | 0.75 | 0.75 | 0.75 |
| minObservationsNeeded | 6 | 6 | 6 | 6 | 6 | 6 | 6 | 6 | 6 | 6 |

| Serial Number | 41 | 42 | 43 | 44 | 45 | 46 | 47 | 48 | 49 | 50 |
|---|---|---|---|---|---|---|---|---|---|---|
| maxSegments | 2 | 2 | 4 | 4 | 6 | 6 | 8 | 8 | 2 | 2 |
| spikeThreshold | 0.9 | 0.9 | 0.9 | 0.9 | 0.9 | 0.9 | 0.9 | 0.9 | 0.9 | 0.9 |
| vertexCountOvershoot | 3 | 3 | 3 | 3 | 3 | 3 | 3 | 3 | 3 | 3 |
| preventOneYearRecovery | 1 | 0 | 1 | 0 | 1 | 0 | 1 | 0 | 1 | 0 |
| recoveryThreshold | 0.33 | 0.33 | 0.33 | 0.33 | 0.33 | 0.33 | 0.33 | 0.33 | 0.67 | 0.67 |
| pvalThreshold | 0.1 | 0.1 | 0.1 | 0.1 | 0.1 | 0.1 | 0.1 | 0.1 | 0.01 | 0.01 |
| bestModelProportion | 0.75 | 0.75 | 0.75 | 0.75 | 0.75 | 0.75 | 0.75 | 0.75 | 0.75 | 0.75 |
| minObservationsNeeded | 6 | 6 | 6 | 6 | 6 | 6 | 6 | 6 | 6 | 6 |

| Serial Number | 51 | 52 | 53 | 54 | 55 | 56 | 57 | 58 | 59 | 60 |
|---|---|---|---|---|---|---|---|---|---|---|
| maxSegments | 4 | 4 | 6 | 6 | 8 | 8 | 2 | 2 | 4 | 4 |
| spikeThreshold | 0.9 | 0.9 | 0.9 | 0.9 | 0.9 | 0.9 | 0.9 | 0.9 | 0.9 | 0.9 |
| vertexCountOvershoot | 3 | 3 | 3 | 3 | 3 | 3 | 3 | 3 | 3 | 3 |
| preventOneYearRecovery | 1 | 0 | 1 | 0 | 1 | 0 | 1 | 0 | 1 | 0 |
| recoveryThreshold | 0.67 | 0.67 | 0.67 | 0.67 | 0.67 | 0.67 | 0.67 | 0.67 | 0.67 | 0.67 |
| pvalThreshold | 0.01 | 0.01 | 0.01 | 0.01 | 0.01 | 0.01 | 0.05 | 0.05 | 0.05 | 0.05 |
| bestModelProportion | 0.75 | 0.75 | 0.75 | 0.75 | 0.75 | 0.75 | 0.75 | 0.75 | 0.75 | 0.75 |
| minObservationsNeeded | 6 | 6 | 6 | 6 | 6 | 6 | 6 | 6 | 6 | 6 |

| Serial Number | 61 | 62 | 63 | 64 | 65 | 66 | 67 | 68 | 69 | 70 |
|---|---|---|---|---|---|---|---|---|---|---|
| maxSegments | 6 | 6 | 8 | 8 | 2 | 2 | 4 | 4 | 6 | 6 |
| spikeThreshold | 0.9 | 0.9 | 0.9 | 0.9 | 0.9 | 0.9 | 0.9 | 0.9 | 0.9 | 0.9 |
| vertexCountOvershoot | 3 | 3 | 3 | 3 | 3 | 3 | 3 | 3 | 3 | 3 |
| preventOneYearRecovery | 1 | 0 | 1 | 0 | 1 | 0 | 1 | 0 | 1 | 0 |
| recoveryThreshold | 0.67 | 0.67 | 0.67 | 0.67 | 0.67 | 0.67 | 0.67 | 0.67 | 0.67 | 0.67 |
| pvalThreshold | 0.05 | 0.05 | 0.05 | 0.05 | 0.1 | 0.1 | 0.1 | 0.1 | 0.1 | 0.1 |
| bestModelProportion | 0.75 | 0.75 | 0.75 | 0.75 | 0.75 | 0.75 | 0.75 | 0.75 | 0.75 | 0.75 |
| minObservationsNeeded | 6 | 6 | 6 | 6 | 6 | 6 | 6 | 6 | 6 | 6 |

| Serial Number | 71 | 72 | 73 | 74 | 75 | 76 | 77 | 78 | 79 | 80 |
|---|---|---|---|---|---|---|---|---|---|---|
| maxSegments | 8 | 8 | 2 | 2 | 4 | 4 | 6 | 6 | 8 | 8 |
| spikeThreshold | 0.9 | 0.9 | 0.9 | 0.9 | 0.9 | 0.9 | 0.9 | 0.9 | 0.9 | 0.9 |
| vertexCountOvershoot | 3 | 3 | 3 | 3 | 3 | 3 | 3 | 3 | 3 | 3 |
| preventOneYearRecovery | 1 | 0 | 1 | 0 | 1 | 0 | 1 | 0 | 1 | 0 |
| recoveryThreshold | 0.67 | 0.67 | 0.99 | 0.99 | 0.99 | 0.99 | 0.99 | 0.99 | 0.99 | 0.99 |
| pvalThreshold | 0.1 | 0.1 | 0.01 | 0.01 | 0.01 | 0.01 | 0.01 | 0.01 | 0.01 | 0.01 |
| bestModelProportion | 0.75 | 0.75 | 0.75 | 0.75 | 0.75 | 0.75 | 0.75 | 0.75 | 0.75 | 0.75 |
| minObservationsNeeded | 6 | 6 | 6 | 6 | 6 | 6 | 6 | 6 | 6 | 6 |

| Serial Number | 81 | 82 | 83 | 84 | 85 | 86 | 87 | 88 | 89 | 90 |
|---|---|---|---|---|---|---|---|---|---|---|
| maxSegments | 2 | 2 | 4 | 4 | 6 | 6 | 8 | 8 | 2 | 2 |
| spikeThreshold | 0.9 | 0.9 | 0.9 | 0.9 | 0.9 | 0.9 | 0.9 | 0.9 | 0.9 | 0.9 |
| vertexCountOvershoot | 3 | 3 | 3 | 3 | 3 | 3 | 3 | 3 | 3 | 3 |
| preventOneYearRecovery | 1 | 0 | 1 | 0 | 1 | 0 | 1 | 0 | 1 | 0 |
| recoveryThreshold | 0.99 | 0.99 | 0.99 | 0.99 | 0.99 | 0.99 | 0.99 | 0.99 | 0.99 | 0.99 |
| pvalThreshold | 0.05 | 0.05 | 0.05 | 0.05 | 0.05 | 0.05 | 0.05 | 0.05 | 0.1 | 0.1 |
| bestModelProportion | 0.75 | 0.75 | 0.75 | 0.75 | 0.75 | 0.75 | 0.75 | 0.75 | 0.75 | 0.75 |
| minObservationsNeeded | 6 | 6 | 6 | 6 | 6 | 6 | 6 | 6 | 6 | 6 |

| Serial Number | 91 | 92 | 93 | 94 | 95 | 96 | 97 | 98 | 99 | 100 |
|---|---|---|---|---|---|---|---|---|---|---|
| maxSegments | 4 | 4 | 6 | 6 | 8 | 8 | 2 | 2 | 4 | 4 |
| spikeThreshold | 0.9 | 0.9 | 0.9 | 0.9 | 0.9 | 0.9 | 0.9 | 0.9 | 0.9 | 0.9 |
| vertexCountOvershoot | 3 | 3 | 3 | 3 | 3 | 3 | 3 | 3 | 3 | 3 |
| preventOneYearRecovery | 1 | 0 | 1 | 0 | 1 | 0 | 1 | 0 | 1 | 0 |
| recoveryThreshold | 0.99 | 0.99 | 0.99 | 0.99 | 0.99 | 0.99 | 1 | 1 | 1 | 1 |
| pvalThreshold | 0.1 | 0.1 | 0.1 | 0.1 | 0.1 | 0.1 | 0.01 | 0.01 | 0.01 | 0.01 |
| bestModelProportion | 0.75 | 0.75 | 0.75 | 0.75 | 0.75 | 0.75 | 0.75 | 0.75 | 0.75 | 0.75 |
| minObservationsNeeded | 6 | 6 | 6 | 6 | 6 | 6 | 6 | 6 | 6 | 6 |

| Serial Number | 101 | 102 | 103 | 104 | 105 | 106 | 107 | 108 | 109 | 110 |
|---|---|---|---|---|---|---|---|---|---|---|
| maxSegments | 6 | 6 | 8 | 8 | 2 | 2 | 4 | 4 | 6 | 6 |
| spikeThreshold | 0.9 | 0.9 | 0.9 | 0.9 | 0.9 | 0.9 | 0.9 | 0.9 | 0.9 | 0.9 |
| vertexCountOvershoot | 3 | 3 | 3 | 3 | 3 | 3 | 3 | 3 | 3 | 3 |
| preventOneYearRecovery | 1 | 0 | 1 | 0 | 1 | 0 | 1 | 0 | 1 | 0 |
| recoveryThreshold | 1 | 1 | 1 | 1 | 1 | 1 | 1 | 1 | 1 | 1 |
| pvalThreshold | 0.01 | 0.01 | 0.01 | 0.01 | 0.05 | 0.05 | 0.05 | 0.05 | 0.05 | 0.05 |
| bestModelProportion | 0.75 | 0.75 | 0.75 | 0.75 | 0.75 | 0.75 | 0.75 | 0.75 | 0.75 | 0.75 |
| minObservationsNeeded | 6 | 6 | 6 | 6 | 6 | 6 | 6 | 6 | 6 | 6 |

| Serial Number | 111 | 112 | 113 | 114 | 115 | 116 | 117 | 118 | 119 | 120 |
|---|---|---|---|---|---|---|---|---|---|---|
| maxSegments | 8 | 8 | 2 | 2 | 4 | 4 | 6 | 6 | 8 | 8 |
| spikeThreshold | 0.9 | 0.9 | 0.9 | 0.9 | 0.9 | 0.9 | 0.9 | 0.9 | 0.9 | 0.9 |
| vertexCountOvershoot | 3 | 3 | 3 | 3 | 3 | 3 | 3 | 3 | 3 | 3 |
| preventOneYearRecovery | 1 | 0 | 1 | 0 | 1 | 0 | 1 | 0 | 1 | 0 |
| recoveryThreshold | 1 | 1 | 1 | 1 | 1 | 1 | 1 | 1 | 1 | 1 |
| pvalThreshold | 0.05 | 0.05 | 0.1 | 0.1 | 0.1 | 0.1 | 0.1 | 0.1 | 0.1 | 0.1 |
| bestModelProportion | 0.75 | 0.75 | 0.75 | 0.75 | 0.75 | 0.75 | 0.75 | 0.75 | 0.75 | 0.75 |
| minObservationsNeeded | 6 | 6 | 6 | 6 | 6 | 6 | 6 | 6 | 6 | 6 |

## Appendix D: GEE Code for Parameter Optimization

```
//##############################################################################
##########################
//#                                                    #\\
//#                   RANDOM FOREST CLASSIFIER                         #\\
//#           USING SEGMENT INFORMATION FROM MULTIPLE PARAMETERIZATIONS
#\\
//#                   WITH ACCURACY ASSESSMENT                         #\\
//#             based on LANDTRENDR GREATEST DISTURBANCE MAPPING           #\\
//#                                                    #\\
//##############################################################################
##########################




//##############################################################################
##########
// START INPUTS
//##############################################################################
##########


// VARIABLES
//choose input points
//GEE will run out of memory if you try to extract data for all the points at once.
//The shapefile contains an attribute field of serial numbers named 'CID'.
//Select a range of CID values and run the script multiple times, increasing the startCID and endCID
values each time.
var table = ee.FeatureCollection("users/danplatt1010/random3_uploadtogee"); //Import the
shapefile of sample points.
var startCID = 1900; //This is the lower CID value. The filter is inclusive of this point.
var endCID = 2000; //This is the higher CID value. The filter is exclusive of this point.
var points = table.select('CID').filterMetadata("CID","less_than",
endCID).filterMetadata("CID","not_less_than", startCID); //Filters the points by CID.


//choose export name
```

var date = ee.Date(Date.now()).format('yyyyMMdd_HHMM', 'Asia/Kuala_Lumpur'); //Automatically selects the current date.

var run = ee.String('9'); //Set a number to differentiate subsequent exports from the same day.

print(date); //Prints the date to check if it is correct.

// END OF VARIABLES

//(SEE BELOW FOR LANDTRENDR PARAMETERS)


//The LandTrendr script has been modified to only operate on the area relevant to the sample points. This speeds up the process.

// buffer points to polygons

var bufferFunction = function(feature){ //Define the function for buffering points.

  return feature.buffer(85).bounds(); //The buffer distance encompasses the 3x3 pixel area used by LandTrendr.

};

var roi = points.map(bufferFunction); //Apply the buffer function to the points and set the buffered polygons as the region of interest.

print(roi); //Check the function has been executed.


//Parameters for LandTrendr

// define collection parameters

var startYear = 1988;

var endYear = 2019;

var startDay = '01-01';

var endDay = '12-31';

var aoi = roi;

var index = 'NBR';

var maskThese = ['cloud', 'shadow', 'snow', 'water'];


// define change parameters

var changeParams = {

  delta:  'loss', //detects disturbance (instead of recovery) by setting LandTrendr to select only segments with negative change

```
  sort:   'greatest', //tells LandTrendr to select the disturbance segment with the greatest change in NBR

  year:   {checked:false, start:1986, end:2017}, //year, mag, dur and preval are unfiltered

  mag:    {checked:false, value:250,  operator:'>'},

  dur:    {checked:false, value:4,    operator:'<'},

  preval: {checked:false, value:500,  operator:'>'},

  mmu:    {checked:true, value:11}, //Masks groups of change pixels with fewer than 11 connected pixels sharing the same year of disturbance onset.

  };
```

//############################################################################################
##########

// END INPUTS

//############################################################################################
##########

```
// load the LandTrendr.js module

var ltgee = require('users/danplatt1010/tut1:LandTrendr2.js'); //Calls custom LandTrendr script. This script creates annual mosaics clipped to buffers around the sample points.


// add index to changeParams object

changeParams.index = index;


var setltparams = function() { //Since LandTrendr is being run multiple times, some parameters need changing each time.

  var runParams = {

    maxSegments:         maxSegmentsList[i], //This parameter will be called from a list using a for loop. See below.

    spikeThreshold:      0.9,

    vertexCountOvershoot:  3,

    preventOneYearRecovery: preventOneYearRecoveryList[l], //This parameter will be called from a list using a for loop. See below.

    recoveryThreshold:    recoveryThresholdList[m], //This parameter will be called from a list using a for loop. See below.
```

```
  pvalThreshold:       pvalThresholdList[n], //This parameter will be called from a list using a for loop. See below.

  bestModelProportion:   0.75,

  minObservationsNeeded:  6

 };

  return runParams;

};
```

```
// run landtrendr

var annualLTcollection = function(){ //Customized LandTrendr function to annual Landsat mosaic time series.

  return ltgee.makeLTcollection(startYear, endYear, startDay, endDay, aoi, index, [], maskThese);

};

var annualLTcollection = annualLTcollection();

print(annualLTcollection);
```

```
var lt = function(){ //Customized LandTrendr function to get LandTrendr outputs.

  return ltgee.runLT(annualLTcollection, setltparams()); //Requires inputs of a timeseries and landtrendr parameters

};
```

```
// get the change map layers*/

var changeImg = function(){ //Function to convert the LandTrendr outputs into a change map (of greatest disturbance).

  return ltgee.getChangeMap(lt(), changeParams); //Requires inputs of LandTrendr outputs and change parameters

};
```

```
//These are the lists of parameter values for the sliding threshold. See setltparams above

var maxSegmentsList = {0: 2, 1: 4, 2: 6, 3: 8};

var preventOneYearRecoveryList = {0: true, 1: false};

var recoveryThresholdList = {0: 0, 1: 0.33, 2: 0.67, 3: 0.99, 4: 1};

var pvalThresholdList = {0: 0.01, 1: 0.05, 2: 0.1};
```

```
// create multiple stacks

// The for loops cycle through each parameterization and produce change images which are sampled
by points.

for (var m = 0; m < ee.Dictionary(recoveryThresholdList).size().getInfo(); m++) { //Separate export file
will be created for each variant of these two parameters.

  for (var n = 0; n < ee.Dictionary(pvalThresholdList).size().getInfo(); n++) {

   // open individual stack

   var paramLists = ee.List([[0,0,0,0,0,0,0,0]]); //Creates a blank list for the parameters to be added
to. This will be added as a property to the export file later to help in identifying files.

   var stack = ee.Image([]); //Creates a blank image stack to add the change images to.

    for (var i = 0; i < ee.Dictionary(maxSegmentsList).size().getInfo(); i++) { //These two parameters will
be varied while the resulting data are combined into a single export file.

     for (var l = 0; l < ee.Dictionary(preventOneYearRecoveryList).size().getInfo(); l++) { //Convert 0
and 1 to false and true

     var newbands = changeImg().select(['mag','yod']); //Select the magnitude and year of
disturbance bands

     var stack = stack.addBands(newbands); //Add the bands to the image stack.


     //Extract the parameter dictionary and add it to the list of parameters

     var params = ee.Dictionary(setltparams());

     var booleanValue = ee.String(params.get('preventOneYearRecovery').getInfo().toString());

     var params = params.set('preventOneYearRecovery', booleanValue.compareTo('true').eq(0));

     var keys = params.keys();

     var params = params.toArray(keys).toList();

     var paramLists = paramLists.add(params);
  //close stack

   }}

   var stack = stack.unmask().clip(roi); //Unmask the image stack and clip it to the buffered area
around the sample points.


   //The data is sampled point by point, to reduce likelihood of GEE crashing

   var thesePoints = points.filterMetadata('CID','equals',startCID); //Sample the first point.
```

```
    var theseAccuracy = stack.sampleRegions({

        collection: thesePoints,

        properties: ['change'],

        scale: 30

    });

    for (var q = startCID+1; q < endCID; q++) { //Sample the rest of the points using a for loop.

      var thisPoint = points.filterMetadata('CID','equals',q);

      var thisAccuracy = stack.sampleRegions({

        collection: thisPoint,

        properties: ['change'],

        scale: 30

      });

      var theseAccuracy = theseAccuracy.merge(thisAccuracy).set('parameters',paramLists); //Merge
the samples into a single feature collection.

    }

    print(theseAccuracy);

    print(paramLists);

    //Automatically assign codes to the export files based on the parameters for variables m and n
(recoveryThreshold and pvalThreshold)

    var exportvariantm = {0: 'a', 1: 'b', 2: 'c', 3: 'd', 4: 'e'};

    var exportvariantn = {0: 'a', 1: 'b', 2: 'c', 3: 'd', 4: 'e'};

    var exportname = date.cat('_').cat(run).cat(exportvariantm[m]).cat(exportvariantn[n]); //Name
the export file with date/time, serial number and variable code

//Export the magnitude and yod data.

    Export.table.toDrive({

      collection: theseAccuracy,

      description: exportname.getInfo(),

      folder: 'sliding-threshold3',

      fileFormat: 'CSV',

    });

}}
```

## Appendix E: R Code for Parameter Optimization

The R Code used for parameter optimization consists of four data preparation scripts and two analysis scripts:

Data Preparation

1. Rename Export Files
2. Compile LandTrendr Data
3. Subset Ground Truth Data
4. Subset LandTrendr Data

Analysis

5. Make Change Lists
6. Get Optimal Parameters

## Data Preparation

### *Rename Export Files*

```
## Rename export files so that they appear in the correct order.

setwd("D:/documents/workNow/code-testing/sliding-threshold2/gee-exports/renamed")

library('stringr')



# Remove time from filenames.

oldNames <- list.files(full.names = TRUE) # Get list of filenames.

newNames <- str_replace(oldNames, pattern = "_\\d+\\_", replacement = "_") # Create list of new
names, removing the portion of the name describing the time of creation.



# Make serial numbers all the same length.

shortnames <- newNames[str_length(newNames)==18] # Select files with serial numbers below 10.

newNames[str_length(newNames)==18] <- str_replace(shortnames, pattern = "_", replacement =
"_0") # Insert a 0 before the serial number to make it two-digit.

#file.rename(from = oldNames, to = newNames) # Rename the files with their new names.

#list.files() # Check the new filenames are correct.
```

### *Compile LandTrendr Data*

```
## Combine LTdata.

## Combine the various GEE export files into a single dataset.

setwd("D:/documents/workNow/code-testing/sliding-threshold3/gee-exports/renamed")

setSize <- 15

filelist <- list.files()
```

```r
numberOfFiles <- length(filelist)

numberOfSets <- numberOfFiles/setSize


# Make lists of column names to assign to new dataset.

getnames <- function(prefix) {

  names <- c(prefix)

  for (i in 1 : 119) {

    names <- c(names,paste(prefix,"_",i,sep=""))

  }

  return(names)

}


combineLTdata <- function() {

  magnames <- getnames("mag")

  yodnames <- getnames("yod")

  listofcolnames <- c(magnames,yodnames)

  # Rename columns and append to dataframe.

  # Create template for main data frame.

  LTdata <- read.csv(file = filelist[1])[c(2:17)] # Create data frame with first file to which to append
other columns. Exclude the first and last columns.

  # Rename and append remaining columns.

  for (j in 2 : setSize) {

    tempData <- read.csv(file = filelist[j])[c(2:17)]

    colnames(tempData) <- listofcolnames[c((((j-1)*8)+1):(j*8),(((j+setSize-1)*8)+1):((j+setSize)*8))] #
Rename columns

    LTdata <- cbind(LTdata,tempData) # Append to main dataset.

  }

  # Append remaining rows.

  if (numberOfSets>1) {

  for (i in 2 : numberOfSets) {

    allColumns <- read.csv(file = filelist[(((i-1)*setSize)+1)])[c(2:17)] # Create temporary dataset for
each group of points.
```

```
  for (j in 2 : setSize) {

    tempData <- read.csv(file = filelist[(((i-1)*setSize)+j)])[c(2:17)] # Read each export file.

    colnames(tempData) <- listofcolnames[c((((j-1)*8)+1):(j*8),(((j+setSize-1)*8)+1):((j+setSize)*8))] #
Rename the columns

      allColumns <- cbind(allColumns,tempData) # Append to the temporary dataset.

   }

    LTdata <- rbind(LTdata,allColumns) # Append the new rows to the main dataset.

  }} else {}

  return (LTdata)

}

?ifelse

LTdata <- combineLTdata() # Run the function to get all the data into one dataset.

LTdata <- cbind(data.frame("CID"=c(0:1999)),LTdata) # Add the CID numbers.


# Save dataset

#setwd("D:/documents/workNow/code-testing/sliding-threshold3/datasets")

#write.csv(LTdata, file = "LTdata.csv", row.names = FALSE)
```

*Subset Ground Truth Data*

```
#### DO NOT RUN - THIS WILL CREATE ANOTHER UNIQUE CALIBRATION AND VALIDATION SET

## subset-groundtruth.txt

## 1. Removes points which fall on landcover boundaries.

## 2. Creates unique subsets of groundtruth data for calibration and validation.


setwd("D:/documents/workNow/code-testing/sliding-threshold2/datasets")

filename <- "Ground.csv" ## Choose name of groundtruth file

percentage <- 0.3 ## Choose percentage of points to use for calibration. The remaining points will be
used for validation.

library("tidyr")

library("prodlim")


replace.na <- function(Data) {  # Define function to replace NA values with '9999'.

  null.list <- as.list(rep(9999,each=length(Data)))
```

```
  names(null.list) <- names(Data)

  return (replace_na(Data,null.list))

}
```

```
remove.nullrows <- function(Data) { # Remove null rows (points which fall on landcover boundaries).

  null.list <- Data[1,c(-1:-2,-13)]

  null.list[1,] <- rep(9999,each=length(null.list))

  return (Data[((row.match(Data[,c(3:12)], null.list, nomatch=0))==0),])

}
```

# Import data and call functions replace.na and remove.nullrows.

Data <- remove.nullrows(replace.na(read.csv(file = filename, sep = ";")[,c(-3,-4)]))  #Import groundtruth dataset without 'YID' and 'Class' columns and remove null rows (points which fall on landcover boundaries).

# Subset data into calibration and validation samples.

CIDlist <- sort(Data$CID[!duplicated(Data$CID)]) # Make list of CID without duplicates.

calibrationCIDlist <- sort((sample(CIDlist, length(CIDlist)*percentage))) # Randomly sample X% of the points.

Data.calibration <- Data[Data$CID %in% calibrationCIDlist,] # Select these points as the calibration subset.

Data.validation <- subset(Data, !(Data$FID %in% Data.calibration$FID)) # Select the remaining points as the validation subset.

# Save subsets.

#write.csv(Data.calibration, file = "Ground.calibration.csv", row.names = FALSE)

#write.csv(Data.validation, file = "validation/Ground.validation.csv", row.names = FALSE)

*Subset LandTrendr Data*

## Subset LandTrendr data into calibration and validation datasets corresponding to how the groundtruth data has been subset.

setwd("D:/documents/workNow/code-testing/sliding-threshold2/datasets")

# Import data

```
LTdata <- read.csv("LTdata.csv") # Import LTdata
```
```
calibrationCIDlist <- read.csv("Ground.calibration.csv")$CID # Get CID values of the grountruth points
assigned for calibration.
```

```
# Filter by year
```
```
getnames <- function(prefix) {
```
```
  names <- c(prefix)
```
```
  for (i in 1 : 119) {
```
```
    names <- c(names,paste(prefix,"_",i,sep=""))
```
```
  }
```
```
  return(names)
```
```
}
```
```
magnames <- getnames("mag")
```
```
yodnames <- getnames("yod")
```
```
yodData <- LTdata[,match(yodnames,names(LTdata))]
```
```
LTdata[,match(magnames,names(LTdata))][yodData<2000] <- 0
```
```
LTdata[,match(yodnames,names(LTdata))][yodData<2000] <- 0
```

```
# Subset the LTdata
```
```
LTdata.calibration <- LTdata[(LTdata$CID %in% calibrationCIDlist),] # Subset the LTdata for
calibration by selecting only the calibration CID values.
```
```
LTdata.validation <- LTdata[!(LTdata$CID %in% calibrationCIDlist),] # Subset the LTdata for validation
by excluding the calibration CID values.
```

```
# Save subsets.
```
```
#write.csv(LTdata.calibration, file = "LTdata.calibration.csv", row.names = FALSE)
```
```
#write.csv(LTdata.validation, file = "validation/LTdata.validation.csv", row.names = FALSE)
```

## Analysis

### Make Change Lists
```
## Makes change lists for every viable combination of landcover classes (including change back to
original landcover), and saves them as csv.
```
```
## Tabulates frequencies of Change and Non-Change for each change pattern and saves it as a csv.
```

```
## WARNING: Abbreviations for landcover classes must be specified in the correct order. Preferably choose unique, two-character abbreviations. See 'textstring.abb'.

setwd("D:/documents/workNow/code-testing/sliding-threshold2/datasets/")


# Define macro-classes

textstring <- strsplit(paste('

  Forest <- c(11, 12, 13, 14, 22, 23)

  Oilpalm <- 41

  OtherGreen <- c(21, 31, 42, 43, 44, 45, 46, 47, 62, 63)

  UrbanOtherBrown <- c(61, 64, 71)'

),'\n  ')[[1]][-1]

textstring.names <- textstring

for (i in 1 : length(textstring)) {

  eval(parse(text=textstring[i]))

  textstring.names[i] <- strsplit(textstring[i],' <-')[[1]][1]

}

textstring.abb <- c('ft','op','og','ub')


# Import Data

Data <- read.csv("Ground.calibration.csv")

#Data <- Data[Data$Before==41,] # Only select rows with a certain Before landcover class.

Data <- Data[order(Data$CID),]


getdefinitions <- function(timing,landcover) {

  command <- paste("Data$",timing,"==",landcover[1],sep="")

  if (length(landcover)>1) {

    for (i in 2 : length(landcover)) {

      command <- paste(command," | Data$",timing,"==",landcover[i],sep="")

    }

  }

  return(command)
```

```
}


getcommand <- function(before, after) {

  command <- paste("Data$Before==",before[1],sep="")

  if (length(before)>1) {

   for (i in 2 : length(before)) {

     command <- paste(command," | Data$Before==",before[i],sep="")

   }

  }

  command <- paste("(",command,")"," & (Data$After==",after[1],sep="")

  if (length(after)>1) {

   for (i in 2 : length(after)) {

     command <- paste(command," | Data$After==",after[i],sep="")

   }

  }

  command <- paste(command,")",sep="")

  return(command)

}



getdata <- function(before, after) {

  return(Data[eval(parse(text=paste(getcommand(before, after)))),])

}



getchangelist <- function(before,after) {

  Data <- Data[eval(parse(text=paste('(',getcommand(before,after),') |
((',getdefinitions('Orig',before),') & ',getdefinitions('Post2000',0),')',sep=""))),]

  changelist <- data.frame(table(Data$CID))

  names(changelist) <- c("CID","Freq")

  changelist$Change <- FALSE

  pulldata <- getdata(before,after)

  for (i in 1 : 10) {
```

```
   if(dim(pulldata)[1]!=0) {

     index <- match(changelist[,1],pulldata$CID, nomatch = NA)

     for (j in 1 : dim(changelist)[1]) {

       changelist[j,paste('Yr',i,sep='')] <- pulldata$Year[index[j]]

     }

     pulldata <- pulldata[duplicated(pulldata$CID),]

   } else {

     changelist$Change<-is.na(changelist$Yr1)==FALSE

     return(changelist)}

 }

}


# Create change lists.

textstring.objects <- c()

textstring.objects.full <- c()

for (j in 1 : length(textstring.names)) {

  for (i in 1 : length(textstring.names)) {

    tryCatch({

assign(paste(textstring.abb[i],textstring.abb[j],'list',sep=''),getchangelist(eval(parse(text=paste(textstring.names[i]))),eval(parse(text=paste(textstring.names[j])))))

      textstring.objects[length(textstring.objects)+1] <-
paste(textstring.abb[i],textstring.abb[j],'list',sep='')

      textstring.objects.full[length(textstring.objects.full)+1] <- paste(textstring.names[i],'-
',textstring.names[j],sep='')

    }, error=function(e){cat("ERROR :",paste(textstring.abb[i],textstring.abb[j],'list',' does not
exist.',sep=''), "\n")})

  }}

textstring.objects # List of successfully created change lists.

textstring.objects.full

#write.csv(textstring.objects, 'changelists/list-of-patterns.csv', row.names=FALSE)


# Save change lists as csv.
```

```r
for (i in 1 : length(textstring.objects)) {

  #write.csv(eval(parse(text=paste(textstring.objects[i]))), file =
paste('changelists/',textstring.objects[i],'.csv',sep=""),row.names = FALSE)

}
```

```r
# Get statistics on change and no-change points for each pattern.

changevnochange <- matrix(nrow=2,ncol=length(textstring.objects)) # Create blank matrix to save outputs to.

for (i in 1 : length(textstring.objects)) { # For loop cycles through the change lists for each change pattern.

  print(table(eval(parse(text=paste(textstring.objects[i],'$Change',sep=""))))) # Print frequency table for Change/No-Change.

  print(textstring.objects.full[i]) # Print name of change pattern.

  changevnochange[,i] <- table(eval(parse(text=paste(textstring.objects[i],'$Change',sep="")))) # Copies frequency table to the matrix.

}

changevnochange <- data.frame(changevnochange) # Convert matrix to a dataframe.

total <- table(Data[!duplicated(Data$CID),]$Post2000==0)

changevnochange[,length(textstring.objects)+1] <- c(total[2],total[1]) # Add total for all change patterns.

changevnochange[3,] <- changevnochange[1,]+changevnochange[2,] # Add total for each change pattern.

names(changevnochange)<-c(textstring.objects.full,'Total') # Change the column names to the name of the change list.

rownames(changevnochange)<-c('No-Change','Change','Total') # Change row names to Change/No-Change.

#write.csv(changevnochange,'changelists/change-frequencies-by-pattern.csv')
```

*Get Optimal Parameters*
```r
setwd("D:/documents/workNow/code-testing/sliding-threshold3/datasets/")

library('tidyverse')

changepattern <- 'ftub' #Choose change pattern

filename <- paste('changelists/',changepattern,'list.csv',sep="")

changelist <- read.csv(file = filename)

LTdata <- read.csv(file = "LTdata.calibration.csv")
```

```
LTdata <- LTdata[LTdata$CID %in% changelist$CID,]

summary(changelist$CID==LTdata$CID) #Check that CID values match and are in order.


magList <- seq(0,500,10)#c(0,50,100,200,300,400,500)


getnames <- function(prefix) {

  names <- c(prefix)

  for (i in 1 : 119) {

    names <- c(names,paste(prefix,"_",i,sep=""))

  }

  return(names)

}

magnames <- getnames("mag")

LTdata <- LTdata[,names(LTdata) %in% magnames]


CallByParams <- function(magname) {

  compareTable <- data.frame(LTdata[,names(LTdata)==magname])

  compareTable$GroundChange <- changelist$Change

  names(compareTable)

  names(compareTable) <- c("LTChange","GroundChange")

  Tally <- matrix(nrow=length(magList),ncol=5)

  Tally[,1] <- magList

  Accuracy <- matrix(nrow=length(magList),ncol=4) ##colnames=("Mag",User","Producer","Overall")

  Accuracy[,1] <- magList



  countinstance <- function(outcome) {

    length(compareTable$compare[(compareTable$compare==outcome)])

  }


  for (i in 1 : length(magList)) {
```

```r
    replacement <- parse(text=(paste("LTdata$",magname)))

    compareTable$LTChange <- eval(replacement)>magList[i]

    compareTable$compare <- paste(compareTable$LTChange,compareTable$GroundChange,sep="")

    Tally[i,c(2:5)] <-
c(countinstance("TRUETRUE"),countinstance("TRUEFALSE"),countinstance("FALSETRUE"),countinstance("FALSEFALSE"))

    Accuracy[i,2] <- Tally[i,2]/(Tally[i,2]+Tally[i,3])*100 ##User's Accuracy

    Accuracy[i,3] <- Tally[i,2]/(Tally[i,2]+Tally[i,4])*100 ##Producer's Accuracy

    Accuracy[i,4] <- (Accuracy[i,2]+Accuracy[i,3])/2 #Overall Accuracy

  }

  return(Accuracy)

}


Overall <- matrix(nrow=length(magnames), ncol=length(magList))

for (j in 1 : length(magnames)) {

  ThisAccuracy <- CallByParams(magnames[j])

  for (k in 1 : length(magList)) {

    Overall[j,k]<-ThisAccuracy[k,4]

  }

}


positions <- which(Overall==max(Overall,na.rm=TRUE))

for (i in 1 : length(positions)) {

 x <- positions[i] %% 120

 if (x==0) {

   x <- 120

   y <- floor(positions[i]/120)

 } else {

   y <- floor(positions[i]/120)+1

 }

 if (max(Overall,na.rm=TRUE)!=Overall[x,y]) {
```

```
  stop('Incorrect calculation for position of maximum overall accuracy value within accuracy table.')

 }}
```

```
#Optimal <- data.frame(c('ftop','opop','ftog','ogop','ftub'))

#Optimal[5,2] <- x

#names(Optimal)<-c('pattern','optimalParam')

#setwd("D:/documents/workNow/code-testing/sliding-threshold3/r-outputs/")

#write.csv(Optimal,'optimal.csv')
```

## Appendix F: GEE Code for Classification

```
var imageCollection = ee.ImageCollection("LANDSAT/LC08/C01/T1_SR"), // Landsat 8 image collection for creating 2019 mosaic.

    table = ee.FeatureCollection("users/danplatt1010/Peninsular"), // Peninsular Malaysia boundary shapefile for clipping final map

    aoi = // Polygon drawn in GEE loosely around Peninsular Malaysia. If table is used LandTrendr doesn't work.

    /* color: #d63000 */

    /* shown: false */

    ee.Geometry.Polygon(

       [[[99.96538830291695, 6.876396183398622],

        [100.44878674041695, 3.6166336939411026],

        [102.09673595916695, 1.8828589558484479],

        [103.72271252166695, 1.0262094706927138],

        [104.60161877166695, 1.3996602673062004],

        [103.70073986541695, 3.243768415360292],

        [103.56890392791695, 5.325221526141702],

        [102.14068127166695, 6.483574127483413]]]),

    imageVisParam = {"opacity":1,"min":0,"max":9,"palette":["000000","267300","6df15c","70a800","728944","f7db5d","d1ff73","e64c00","732600","004da8"]}, // Display settings for land cover map.

    table2 = ee.FeatureCollection("users/danplatt1010/calibration20210326"), // calibration/training points for random forest

    image = ee.Image("CGIAR/SRTM90_V4"); // SRTM elevation data



//##############################################################################################################
//#                                                                          #\\
//#                 LANDTRENDR GREATEST DISTURBANCE MAPPING                   #\\
//#                                                                          #\\
//##############################################################################################################
```

```
// date: 2018-10-07

// author: Justin Braaten | jstnbraaten@gmail.com

//      Zhiqiang Yang  | zhiqiang.yang@oregonstate.edu

//      Robert Kennedy | rkennedy@coas.oregonstate.edu

// parameter definitions: https://emapr.github.io/LT-GEE/api.html#getchangemap

// website: https://github.com/eMapR/LT-GEE

// notes:

//   - you must add the LT-GEE API to your GEE account to run this script.

//     Visit this URL to add it:

//     https://code.earthengine.google.com/?accept_repo=users/emaprlab/public

//   - use this app to help parameterize:

//     https://emaprlab.users.earthengine.app/view/lt-gee-change-mapper




//###############################################################################
##########
// START LANDTRENDR INPUTS

//###############################################################################
##########


// define collection parameters

// See LandTrendr documentation for more information.

var startYear = 1988; // Create annual image time series for LandTrendr from 1988 to 2019

var endYear = 2019;

var startDay = '01-01'; //select imagery range from whole of each year (1 Jan - 31 Dec)

var endDay = '12-31';

//var aoi = //see imports

var index = 'NBR'; // Normalized Burn Ratio

var maskThese = ['cloud', 'shadow', 'snow', 'water']; //mask all


// define all landtrendr parameters
```

```
var allparams = ee.Array([ // List each set of parameters in a separate list.

  // The first number in the list is the id number assigned to that set of parameter values

  //id number, maxSegments, spikeThreshold, vertexCountOvershoot, preventOneYearRecovery, ...

  //...recoveryThreshold, pvalThreshold, bestModelProportion, minObservationsNeeded

  [32,8,0.9,3,0,0.33,0.01,0.75,6],

  [87,8,0.9,3,1,0.99,0.05,0.75,6],

  [29,6,0.9,3,1,0.33,0.01,0.75,6]

  ]);
```

var boolean = ee.Dictionary({0: false, 1: true}); // Arrays can only hold numbers, so preventOneYearRecovery must be converted to boolean.

var paramsets = ee.List.sequence(0, allparams.length().get([0]).subtract(1)); // Count number of parameterizations (ie. number of times LandTrendr must run).

```
// define change parameters

// See LandTrendr documentation for more information.

var changeParams = {

  delta:  'loss', // Identify disturbance (not recovery)

  sort:   'greatest', // Select the disturbance of the greatest magnitude

  year:   {checked:false, start:1986, end:2019}, // no filters for year, mag, dur or preval.

  mag:    {checked:false, value:200,  operator:'>'},

  dur:    {checked:false, value:4,    operator:'<'},

  preval: {checked:false, value:300,  operator:'>'},

  mmu:    {checked:true, value:11}, // Filter out isolated change pixels with less than 11 px in a cluster.


};
```

```
//###################################################################################
##########

// END LANDTRENDR INPUTS

//###################################################################################
##########
```

```
//############################################################################
##########

// START FUNCTIONS

//############################################################################
##########

// These functions have been taken (and modified) from LandTrendr.js to allow the script to be
customized for supervised classification.

var getChangeMap = function(lt, changeParams){ // Function to extract disturbance rasters

  // call functions from ltgee

  var makeBoolean = ltgee.makeBoolean;


  // since dsnr is a new addition make this function back compatible by auto-setting dsnr to false

  if(changeParams.mag.dsnr === undefined){changeParams.mag.dsnr = false}


  // get the segment info

  var segInfo = ltgee.getSegmentData(lt, changeParams.index, changeParams.delta);

  changeParams.segInfo = segInfo;


  // sort by dist type

  var sortByThis;

  switch (changeParams.sort.toLowerCase()){

    case 'greatest':

      sortByThis = changeParams.segInfo.arraySlice(0,4,5).multiply(-1); // need to flip the delta here,
since arraySort is working by ascending order

      break;

    case 'least':

      sortByThis = changeParams.segInfo.arraySlice(0,4,5);

      break;

    case 'newest':

      sortByThis = changeParams.segInfo.arraySlice(0,0,1).multiply(-1); // need to flip the delta here,
since arraySort is working by ascending order

      break;
```

```
  case 'oldest':

    sortByThis = changeParams.segInfo.arraySlice(0,0,1);

    break;

  case 'fastest':

    sortByThis = changeParams.segInfo.arraySlice(0,5,6);

    break;

  case 'slowest':

    sortByThis = changeParams.segInfo.arraySlice(0,5,6).multiply(-1); // need to flip the delta here,
since arraySort is working by ascending order

    break;

 }


 var segInfoSorted = changeParams.segInfo.arraySort(sortByThis); // sort the array by magnitude


 var distArray = segInfoSorted.arraySlice(1, 0, 1); // get the first


 // make an image from the array of attributes for the greatest disturbance

 // choose which segment information to include in the raster stack

 var distImg =
ee.Image.cat(distArray.arraySlice(0,0,1).arrayProject([1]).arrayFlatten([['yod']]).toShort(),

              distArray.arraySlice(0,1,2).arrayProject([1]).arrayFlatten([['endYr']]),

              distArray.arraySlice(0,2,3).arrayProject([1]).arrayFlatten([['startVal']]), //Mis-labelled
in early outputs (from an older version of this script) as 'startYr'

              distArray.arraySlice(0,3,4).arrayProject([1]).arrayFlatten([['endVal']]),

              distArray.arraySlice(0,4,5).arrayProject([1]).arrayFlatten([['mag']]),

              distArray.arraySlice(0,5,6).arrayProject([1]).arrayFlatten([['dur']]),

              distArray.arraySlice(0,6,7).arrayProject([1]).arrayFlatten([['rate']]));


  // start a mask based on magnitudes greater than 0 to get rid of the masked pixels from the orginal
collection

 var mask = distImg.select('mag').gt(0);

 mask = ee.Image(1).mask(mask);
```

```
// filter by year
var addMask;
if(makeBoolean(changeParams.year.checked) === true){
  var yod = distImg.select('yod');
  addMask = yod.gte(changeParams.year.start).and(yod.lte(changeParams.year.end));
  mask = mask.updateMask(addMask);
}


// filter by mag
var magBand = 'mag';
if(makeBoolean(changeParams.mag.checked) === true){
  if(makeBoolean(changeParams.mag.dsnr) === true){magBand = 'dsnr'}
  if(changeParams.mag.operator == '<'){
    addMask = distImg.select(magBand).lt(changeParams.mag.value);
  } else if(changeParams.mag.operator == '>'){
    addMask = distImg.select(magBand).gt(changeParams.mag.value);
  } else {
    print("Error: provided mag operator does match either '>' or '<'");
  }
  mask = mask.updateMask(addMask);
}


// filter by dur
if(makeBoolean(changeParams.dur.checked) === true){
  if(changeParams.dur.operator == '<'){
    addMask = distImg.select('dur').lt(changeParams.dur.value);
  } else if(changeParams.mag.operator == '>'){
    addMask = distImg.select('dur').gt(changeParams.dur.value);
  } else {
    print("Error: provided dur operator does match either '>' or '<'");
```

```
  }

  mask = mask.updateMask(addMask);

 }


 // filter by preval
 if(makeBoolean(changeParams.preval.checked) === true){

  if(changeParams.preval.operator == '<'){

    addMask = distImg.select(['preval']).lt(changeParams.preval.value);

  } else if(changeParams.preval.operator == '>'){

    addMask = distImg.select(['preval']).gt(changeParams.preval.value);

  } else{

    print("Error: provided preval operator does match either '>' or '<'");

  }

  mask = mask.updateMask(addMask);

 }


 // filter by mmu
 if(makeBoolean(changeParams.mmu.checked) === true){

  if(changeParams.mmu.value > 1){

    addMask = distImg.select(['yod'])

            .mask(mask)

            .connectedPixelCount(changeParams.mmu.value, true)

            .gte(changeParams.mmu.value)

            .unmask(0);

    mask = mask.updateMask(addMask);

  }

 }


 // apply the filter mask
 return distImg.mask(mask).clip(table);

};
```

```
//######################################################################
##########

// END FUNCTIONS

//######################################################################
##########


// load the LandTrendr.js module

var ltgee = require('users/emaprlab/public:Modules/LandTrendr.js');


// add index to changeParams object

changeParams.index = index;


var getChangeImg = function() { // Function to run LandTrendr and turn LandTrendr outputs into
disturbance rasters.

  // run landtrendr

  var lt = ltgee.runLT(startYear, endYear, startDay, endDay, aoi, index, [], runParams, maskThese);


  // get the change map layers

  var changeImg = getChangeMap(lt, changeParams);


  return(changeImg);
};


// Create true colour image for 2019.

var geometry = table; // Set boundary

var maskL8sr = function (image) { // Mask out clouds and cloud shadow.

  // Bits 3 and 5 are cloud shadow and cloud, respectively.

  var cloudShadowBitMask = (1 << 3);

  var cloudsBitMask = (1 << 5);

  // Get the pixel QA band.

  var qa = image.select('pixel_qa');
```

```
  // Both flags should be set to zero, indicating clear conditions.

  var mask = qa.bitwiseAnd(cloudShadowBitMask).eq(0)

        .and(qa.bitwiseAnd(cloudsBitMask).eq(0));

  return image.updateMask(mask);};

// Filter by date to 1 Jan 2019 - 31 Dec 2019, and by boundary to Peninsular Malaysia

var l8_t1_sr = imageCollection.filterDate("2019-01-01","2019-12-31").filterBounds(geometry);

// Applying the cloud removal function to Landsat collection

var truecolour =
l8_t1_sr.map(maskL8sr).median().select(["B1","B2","B3","B4","B5","B6","B7"]).clip(geometry);

// Create a mask of available Landsat imagery to apply to the raster stack.

var themask = truecolour.select('B1').not().not().unmask();


// Clip the elevation layer to Peninsular Malaysia.

var elevation = image.clip(table);


var changeImg = truecolour.addBands(elevation); // Add the multispectral Landsat mosaic and
elevation data to the raster stack.

for (var m = 0; m < paramsets.length().getInfo(); m++) { // Runs LandTrendr for each
parameterization.

  var runParams = {

    maxSegments:          allparams.get([m,1]),

    spikeThreshold:       allparams.get([m,2]),

    vertexCountOvershoot:  allparams.get([m,3]),

    preventOneYearRecovery: boolean.get(allparams.get([m,4]).int()),

    recoveryThreshold:     allparams.get([m,5]),

    pvalThreshold:        allparams.get([m,6]),

    bestModelProportion:   allparams.get([m,7]),

    minObservationsNeeded:  allparams.get([m,8]),

  };

  var newImg = getChangeImg(); // Get disturbance rasters for one parameterization.

  var changeImg = changeImg.addBands(newImg); // Add the disturbance rasters for all
parameterizations to the raster stack.
```

```
}
```

var changeImg = changeImg.mask(themask); // Mask out areas with no Landsat imagery from the raster stack.

print(changeImg); // Check all bands are present.

var bands = changeImg.bandNames(); // Make a list of image bands to select when training the classifier.

print('bands',bands);

// CLASSIFICATION

// The calibration points will be used to sample the raster stack to produce training points for the classifier.

var calibration = table2.select(['tempID','Change']).filter(ee.Filter.neq('Change',9)); // Remove points labelled 'water'.

print('table2/calibration',calibration);

var cids = calibration.aggregate_array('tempID'); // Make a list of the id numbers of each point.

// Divide the points into batches to prevent GEE crashing when sampling.

var cid1 = cids.slice(0,360); // Subsets the first 360 points.

var cid2 = cids.slice(360,720);

var cid3 = cids.slice(720); // Subsets the 720th point and any following points.

print('cids',cids);

print(cid1);

print(cid2);

// The points are sampled one at a time to speed up the processing.

// The first point is sampled to create a feature collection to append the following points to.

var thesepoints = calibration.filterMetadata('tempID','equals',cid1.get(0)); // Select the first point.

var training1 = changeImg.sampleRegions({ // Sample regions

  collection: thesepoints,

  scale: 30, // Set the scale to the resolution of Landsat (30m)

  //geometries: true // the coordinates of the point are not needed as they will retain their cid number.

```
});

// The following points are sampled one by one using a for loop.

for (var i = 1; i < cid1.length().getInfo(); i++) {

  var thesepoints = calibration.filterMetadata('tempID','equals',cid1.get(i));

  var furthertraining = changeImg.sampleRegions({

    collection: thesepoints,

    scale: 30,

    //geometries: true

  });

  var training1 = training1.merge(furthertraining); // Merge each new training point to the feature collection.

}


// Repeat for the following batches of points.

var thesepoints = calibration.filterMetadata('tempID','equals',cid2.get(0));

var training2 = changeImg.sampleRegions({

  collection: thesepoints,

  scale: 30,

  //geometries: true

});

for (var i = 1; i < cid2.length().getInfo(); i++) {

  var thesepoints = calibration.filterMetadata('tempID','equals',cid2.get(i));

  var furthertraining = changeImg.sampleRegions({

    collection: thesepoints,

    scale: 30,

    //geometries: true

  });

  var training2 = training2.merge(furthertraining);

}


var thesepoints = calibration.filterMetadata('tempID','equals',cid3.get(0));
```

```
var training3 = changeImg.sampleRegions({

  collection: thesepoints,

  scale: 30,

  //geometries: true

});

for (var i = 1; i < cid3.length().getInfo(); i++) {

  var thesepoints = calibration.filterMetadata('tempID','equals',cid3.get(i));

  var furthertraining = changeImg.sampleRegions({

    collection: thesepoints,

    scale: 30,

    //geometries: true

  });

  var training3 = training3.merge(furthertraining);

}


// Combine all the training points into one feature collection.

var training = training1.merge(training2).merge(training3).filter(ee.Filter.neq('tempID',1078));

print('training1',training1);

print('training2',training2);

print('training3',training3);

print('training',training);

print('trainingLandsatvalue',training.aggregate_array('B4').sort());


//CHANGE CLASS IN .TRAIN

// Train the Random Forest classifier with 300 trees on the training points.

// The 'Change' property of the training points is the current (2019) land cover class.

// All bands in the image stack are selected.

var trained = ee.Classifier.smileRandomForest(300).train(training,'Change',bands);

print('trained',trained);

print(changeImg);

// Classify the raster stack and clip the classified image to the boundary of Peninsular Malaysia.
```

```
var classified = changeImg.classify(trained).clip(table);

print('classified',classified);

// View the classified map.

Map.addLayer(classified,imageVisParam2,"classified");


// Export the classified map. It will be used to extract point data for validation.

Export.image.toDrive({

  image: classified,

  description: 'classifiedImage1',

  folder: 'randomforest4',

  region: table,

  maxPixels: 4e8,

  scale: 30

});
```

## Appendix G: GEE Code for Validation

```
var image = ee.Image("JRC/GSW1_2/GlobalSurfaceWater"), // Water dataset for masking water land cover class.

  imageVisParam = {"opacity":1,"min":0,"max":9,"palette":["000000","267300","6df15c","70a800","728944","f7db5d","d1ff73","e64c00","732600","004da8"]}, // Display settings for the classified map.

  table2 = ee.FeatureCollection("users/danplatt1010/Peninsular"), // Boundary shapefile for Peninsular Malaysia

  table = ee.FeatureCollection("users/danplatt1010/validation20210326"), // Validation points

  classified = ee.Image("users/danplatt1010/rf4classifiedImage3"); // The classified image.



var water = image.select('transition').clip(table2).unmask(); // Select the transition layer of the water dataset. Clip it to the boundaries of Peninsular Malaysia and unmask it.

var mask = water.eq(1).max(water.eq(2)).max(water.eq(7)); // Create a mask for Permanent, New Permanent and Seasonal-to-Permanent water.

var watermask = mask.mask(mask).multiply(9); // Set the value of the masked pixels as 9 which is the value for the water land cover class.

var waterlayer = watermask.mask(watermask.connectedPixelCount(11).gte(11)).unmask(); // Filter out small areas of water with fewer than 11 connected pixels.

print(classified);

print(waterlayer);

var map = classified.max(waterlayer); // Add the water class from the JRC-GSW layer to the classified map.

print(map);

Map.addLayer(map,imageVisParam); // View the classified image with water.

var table = table.select(['tempID','Change']); // Select the serial number and reference land cover values of the validation points.

//Sample the classified image by regions using the validation points.
var validation = map.sampleRegions({

  collection: table,

  properties: ['Change'], // Include the reference land cover values.

  scale: 30 // Set the scale to the resolution of Landsat (30m)

});

print('validation',validation);
```

```
// Export the validation points.

Export.table.toDrive({

  collection: validation,

  description: 'rf4validation-results3',

  folder: 'randomforest4'

});

// Export the classified map with water.

Export.image.toDrive({

  image: map,

  description: 'rf4classifiedImage1',

  folder: 'randomforest4',

  region: table2,

  scale:30,

  maxPixels: 4e8

});
```

## Appendix H: R Code for Validation

```
setwd("D:/documents/workNow/code-testing/randomforests4/") # Set the root directory.

Raw <- read.csv('validation/rf4validation-results1.csv')[,c(2:3)] # Read the file containing reference
and classified data from validation samples.

TwoDigit <- Raw

TwoDigit[,3] <- paste(TwoDigit[,1],TwoDigit[,2],sep="") # Concatenate the reference and classified
land cover values

Frequencies <- data.frame(table(TwoDigit[,3])) # Calculate the frequencies of each pair of values

Confusion <- data.frame(matrix(nrow=10,ncol=10)) # Create a blank dataframe to sort the
frequencies into.

row.names(Confusion) <- c('0','1','2','3','4','5','6','7','8','9') # Set the row names according to the
serial number of the land cover classes.

names(Confusion) <- row.names(Confusion) # Set the column names identical to the row names.

for (i in 1 : 10) { # Match each pair of land cover classes (reference and classified) to it's position in
the confusion matrix.

  for (j in 1 : 10) {

    Position <- match(paste(row.names(Confusion)[i],names(Confusion)[j],sep=""),Frequencies[,1])

# Paste the frequency of each pair of occurence of land cover classes.

    if (is.na(Position)) { # If the pair of classes isn't present, set the value to 0.

      Confusion[i,j] <- 0

    } else {

      Confusion[i,j] <- Frequencies[Position,2]

    }

  }

}

length(table(Confusion>=0))==1 # Check that all values in the table are positive or 0.


for (i in 1 : 10) { # Calculate Total number of reference and classified points for each land cover class.

  Confusion[11,i] <- sum(Confusion[c(1:10),i]) # Total number of classified points per land cover class.

  Confusion[i,11] <- sum(Confusion[i,c(1:10)]) # Total number of reference points per land cover
class.

  Confusion[12,i] <- Confusion[i,i]/Confusion[11,i] # User's Accuracy

  Confusion[i,12] <- Confusion[i,i]/Confusion[i,11] # Producer's Accuracy
```

}


# Rename the rows/columns with the correct land cover names.

names(Confusion) <- c('Blank','Forest', 'OtherVegetation', 'Oilpalm', 'Rubber', 'Rice', 'OtherAgriculture', 'BareGround', 'Urban', 'Water', 'TotalGround', 'Producers')

row.names(Confusion) <- c('Blank','Forest', 'OtherVegetation', 'Oilpalm', 'Rubber', 'Rice', 'OtherAgriculture', 'BareGround', 'Urban', 'Water', 'TotalClassified', 'Users')


# Export the confusion table as a csv file.

#write.csv(Confusion, 'confusion/confusion-matrix15.csv') # Keep this line commented out until you have checked the data.

Appendix I: Land Cover Maps



Land Cover Classified With LandTrendr Disturbance Rasters, Landsat and Elevation Data

**Legend**

- Unclassified
- Forest
- Other Vegetation
- Oil Palm
- Rubber
- Rice
- Other Agriculture
- Bare Ground
- Urban
- Water

Appendix J: Graphs from Preliminary Investigation 2
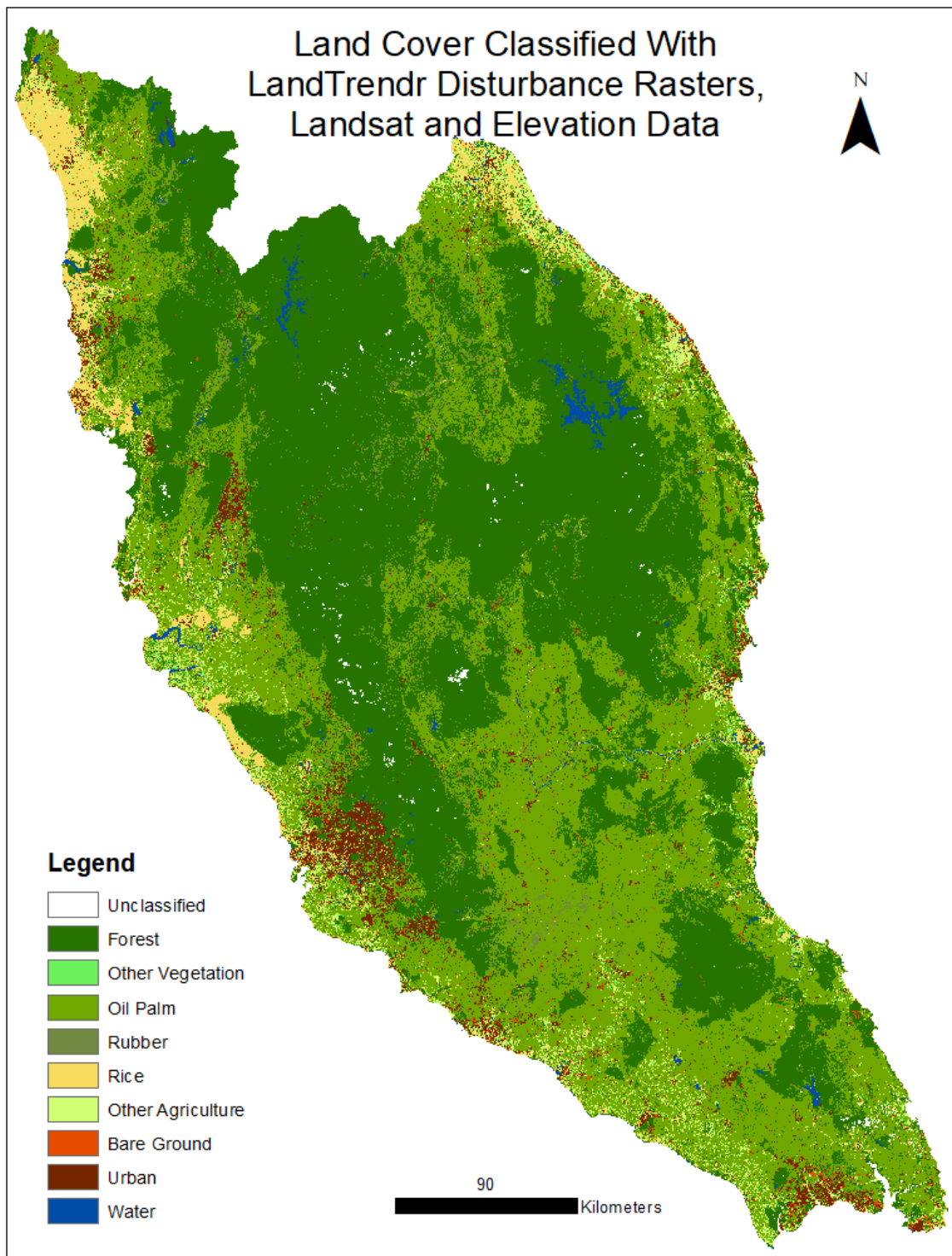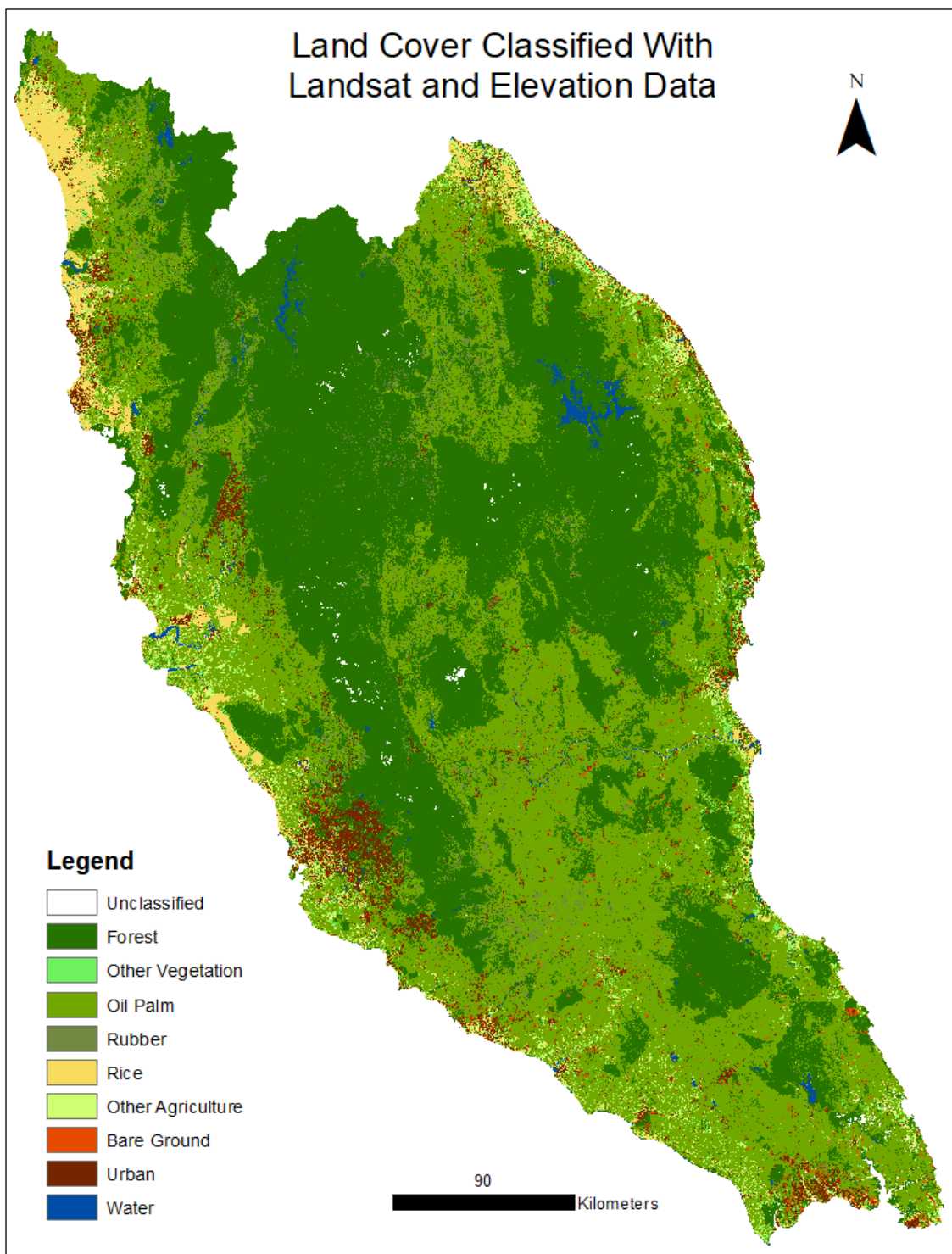
# gee−output/foresttooilpalm_selected, 2019−11−12 17:27:35

- bestModelProportion 0.75
- compositingMethod median
- endDay Dec−31
- endYear 2019
- maxSegments 6
- minObservationsNeeded 6
- preventOneYearRecovery TRUE

- pvalThreshold 0.05
- recoveryThreshold 0.25
- sampleFile foresttooilpalm_2
- spikeThreshold 0.9
- startDay 01−Jan
- startYear 1988
- vertexCountOvershoot 3

**Sample 0 (0)**
**102.31279390931334**
**2.9604640758985203**
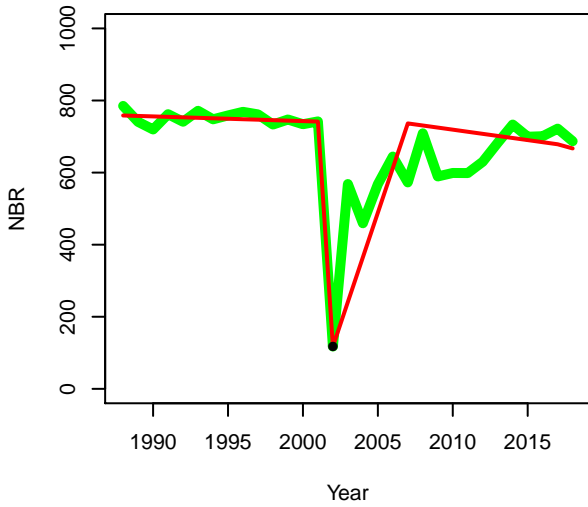


- Cleared in: 2002
- Type: forest−to−oilpalm
- Current use: oilpalm
- −

**Sample 1 (1)**
**102.32027628088102**
**2.918142747800265**
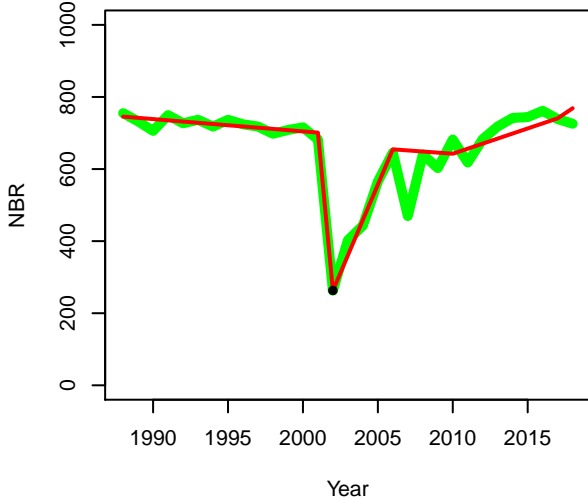


- Cleared in: 2002
- Type: forest−to−oilpalm
- Current use: oilpalm
- −

## Sample 2 (2)
## 102.32127511951698
## 2.937950074679672
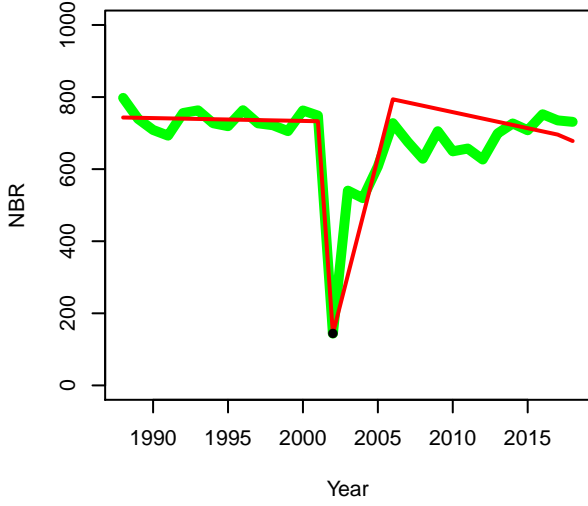


- Cleared in: 2002

- Type: forest–to–oilpalm

- Current use: oilpalm

- –

## Sample 3 (3)
## 102.32506089631136
## 2.915730374130351
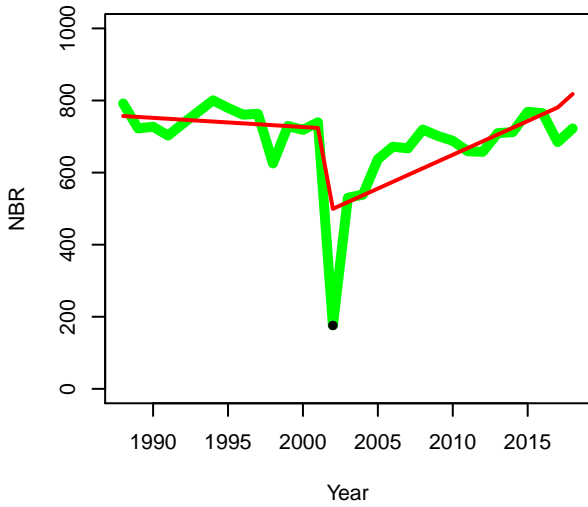


- Cleared in: 2002

- Type: forest–to–oilpalm

- Current use: oilpalm

- –

## Sample 4 (4)
## 102.32364736127742
## 2.9269717678860876
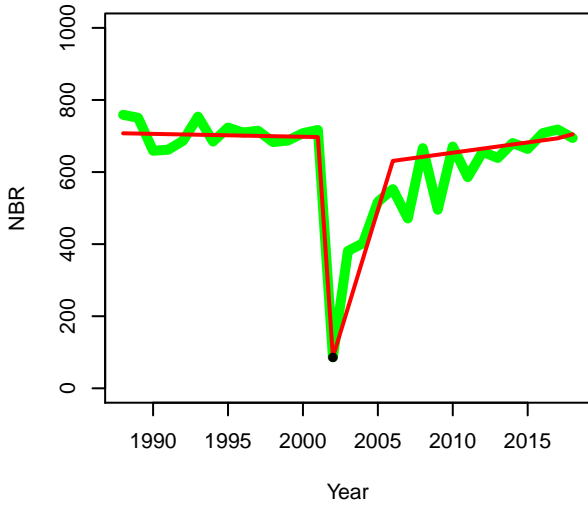


- Cleared in: 2002

- Type: forest–to–oilpalm

- Current use: oilpalm

- –

## Sample 5 (12)
## 102.9035891260865
## 2.856040847428925
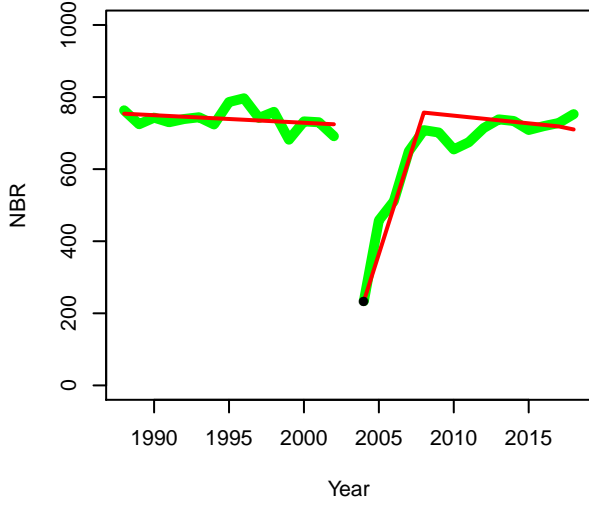


- Cleared in: 2004

- Type: forest–to–oilpalm

- Current use: oilpalm

- –

## Sample 6 (13)
## 102.9337594038141
## 2.9132288184393675
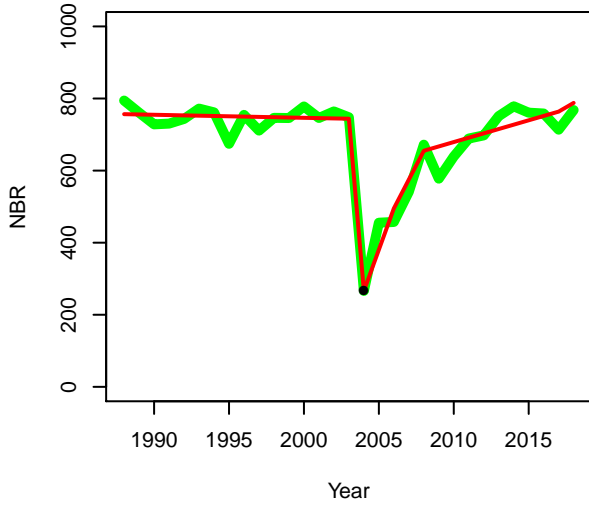


- Cleared in: 2004

- Type: forest–to–oilpalm

- Current use: oilpalm

- –

## Sample 7 (14)
## 102.90686210625972
## 2.87420276601961
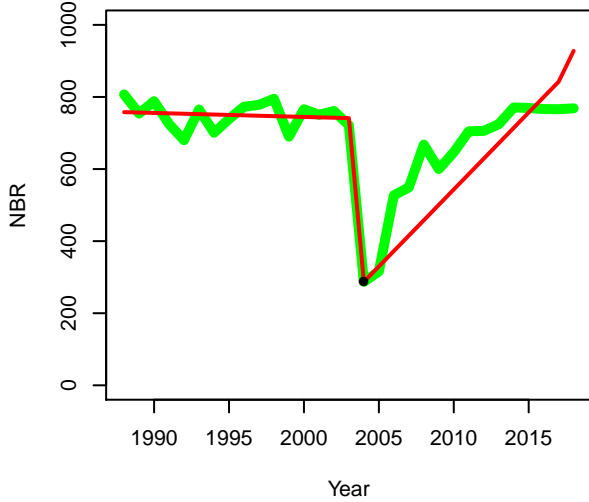


- Cleared in: 2004

- Type: forest–to–oilpalm

- Current use: oilpalm

- –

**Sample 8 (16)**
**102.91097785653204**
**2.8837630786781974**

- Cleared in: 2002
- Type: forest–to–oilpalm
- Current use: oilpalm
- may have been disturbed previously

**Sample 9 (17)**
**102.89385936758788**
**2.8722229251518794**
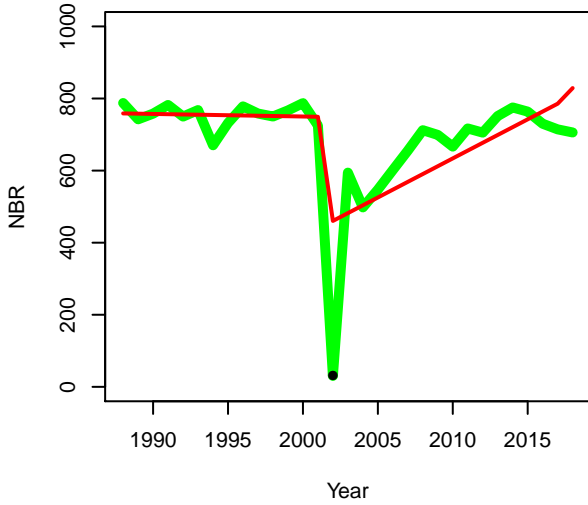
- Cleared in: 2002
- Type: forest–to–oilpalm
- Current use: oilpalm
- may have been disturbed previously

**Sample 10 (20)**
**102.9544897646116**
**2.860713985332936**
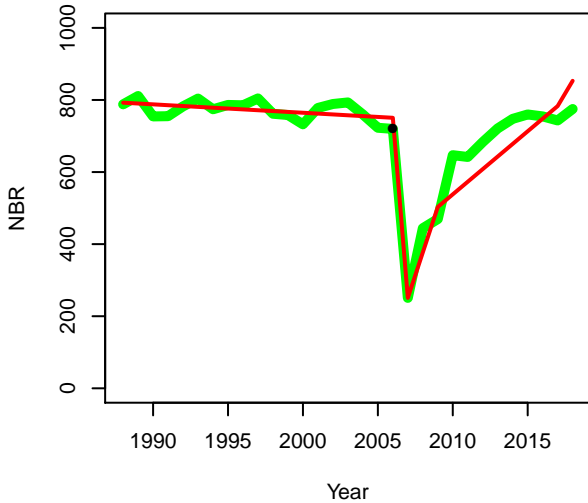
- Cleared in: 2006
- Type: forest–to–oilpalm
- Current use: oilpalm
- area has roads since 1984

**Sample 11 (21)**
**102.95366037181563**
**2.8343161070965364**
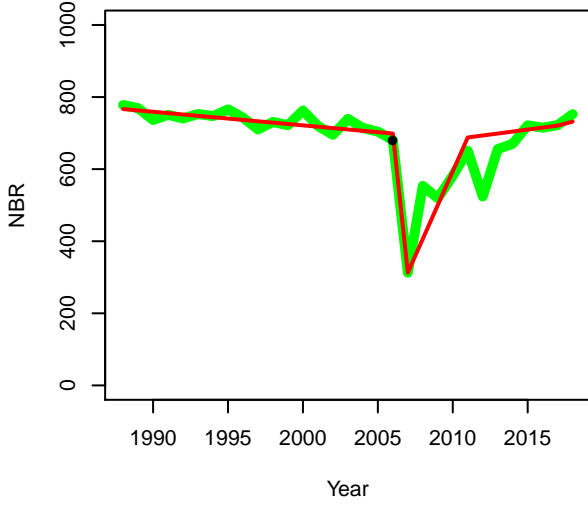
- Cleared in: 2006
- Type: forest–to–oilpalm
- Current use: oilpalm
- next to area cleared in the second half



**Sample 12 (22)**
**102.95010646827603**
**2.8259686699244857**
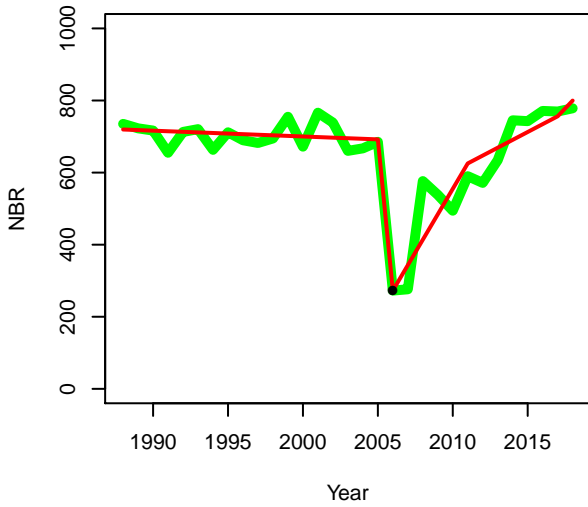
- Cleared in: 2006
- Type: forest–to–oilpalm
- Current use: oilpalm
- –



**Sample 13 (23)**
**102.97889442467708**
**2.8103083070247843**
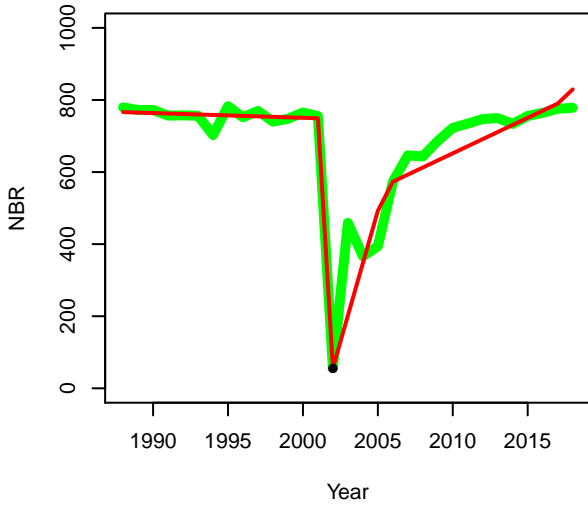
- Cleared in: 2002
- Type: forest–to–oilpalm
- Current use: oilpalm
- –

## Sample 14 (24)
## 102.95215765476064
## 2.8500433565120393
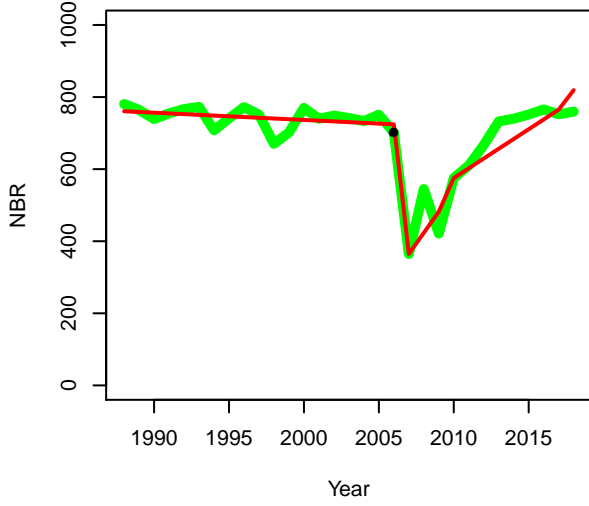


- Cleared in: 2006
- Type: forest–to–oilpalm
- Current use: oilpalm
- –

## Sample 15 (51)
## 103.54123165852715
## 2.549401845286612
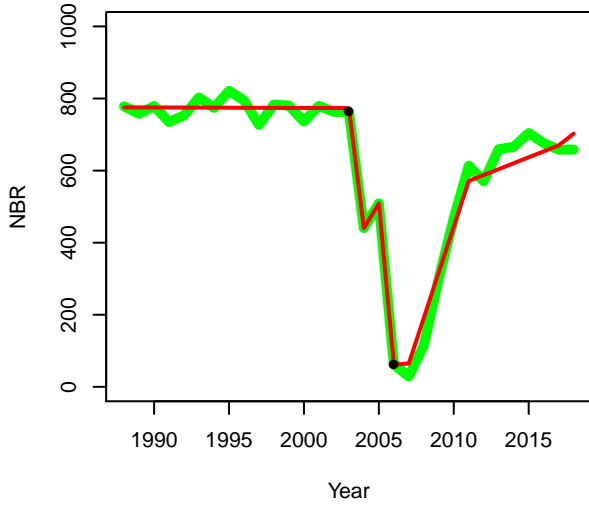


- Cleared in: 2003, 2006
- Type: forest–to–oilpalm
- Current use: oilpalm
- –

## Sample 16 (52)
## 103.54493717150257
## 2.536465993130566
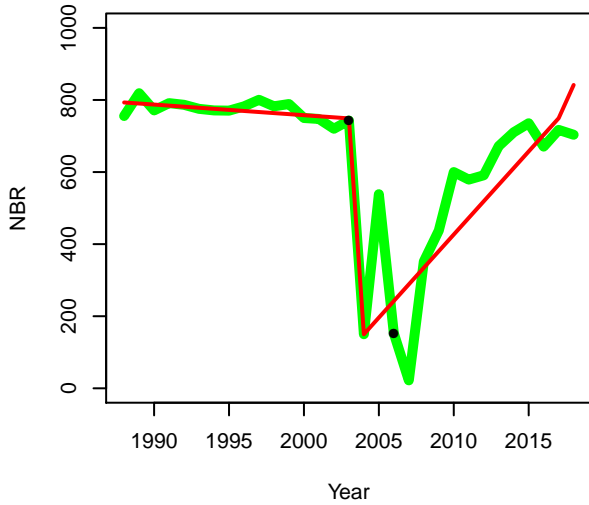


- Cleared in: 2003, 2006
- Type: forest–to–oilpalm
- Current use: oilpalm
- –

**Sample 17 (53)**
**103.54276558928953**
**2.530936707824293**

- Cleared in:  2003, 2006
- Type:  forest–to–oilpalm
- Current use:  oilpalm
- –
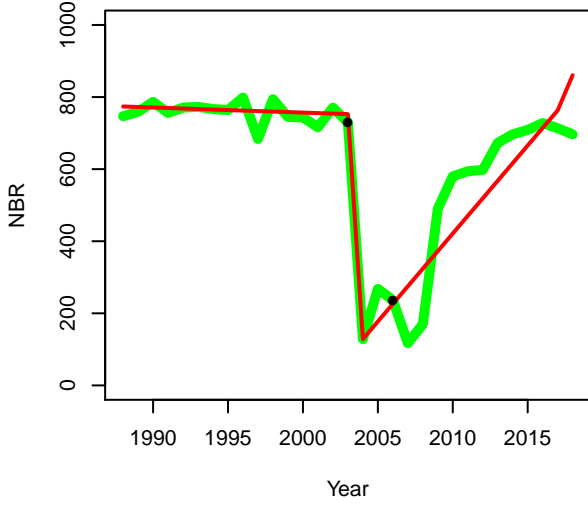


**Sample 18 (54)**
**103.57782304177171**
**2.538089105914019**

- Cleared in:  2003, 2006
- Type:  forest–to–oilpalm
- Current use:  oilpalm
- –
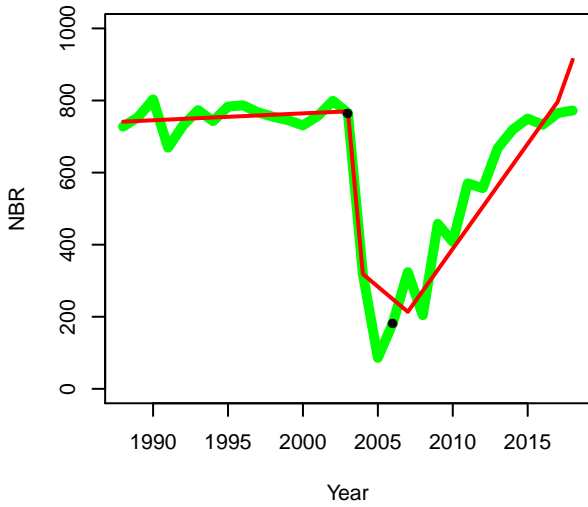


**Sample 19 (55)**
**103.52156702288144**
**2.551577886600694**

- Cleared in:  2003, 2006
- Type:  forest–to–oilpalm
- Current use:  oilpalm
- –
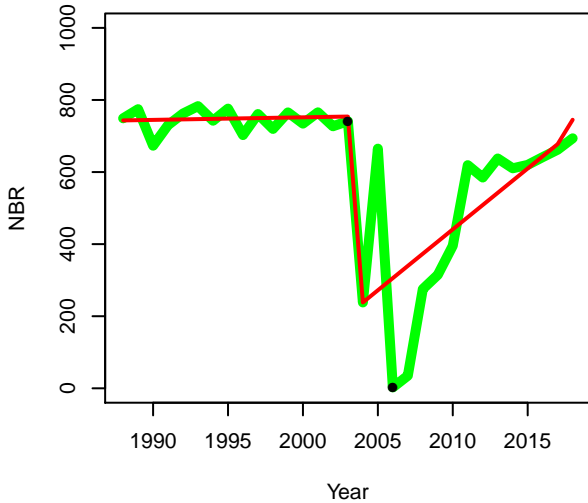
## Sample 20 (60)
## 103.48543492704538
## 2.3163335514251027
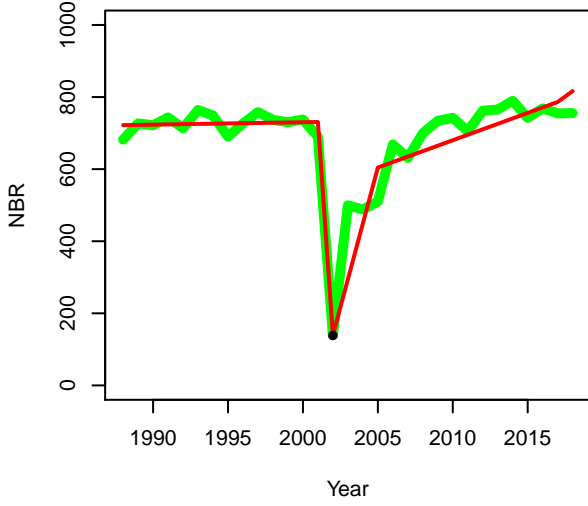


- Cleared in: 2002
- Type: forest–to–oilpalm
- Current use: oilpalm
- general area has been disturbed before

## Sample 21 (61)
## 103.48613054680973
## 2.330415392551885
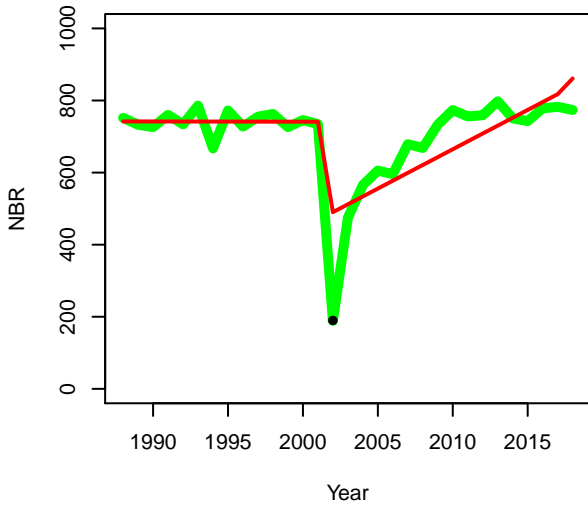


- Cleared in: 2002
- Type: forest–to–oilpalm
- Current use: oilpalm
- –

## Sample 22 (62)
## 103.49256057052877
## 2.3036206543217292
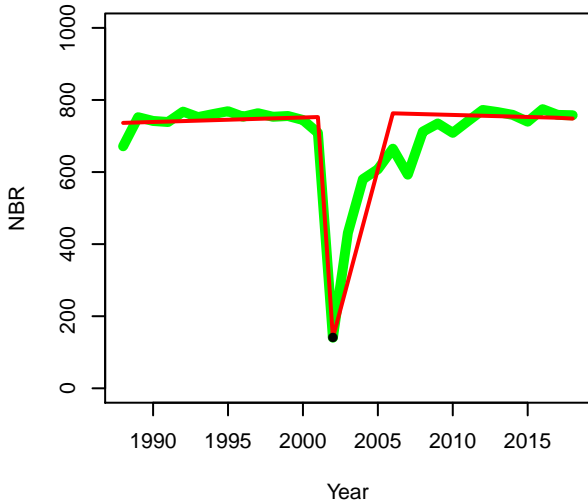


- Cleared in: 2002
- Type: forest–to–oilpalm
- Current use: oilpalm
- –

**Sample 23 (63)**
**103.51598422836253**
**2.311803104754802**
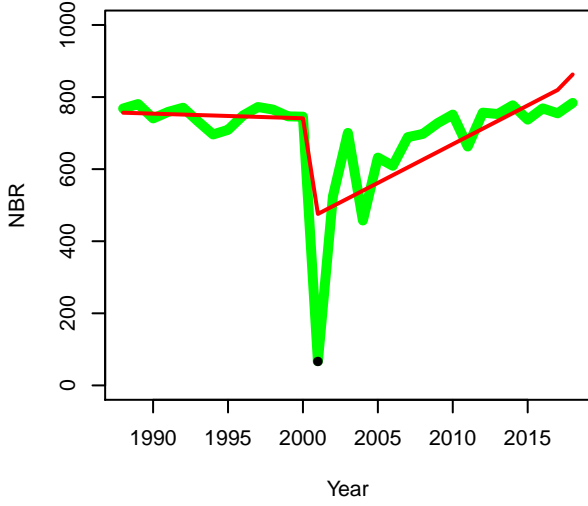
- Cleared in:  2001
- Type:  forest–to–oilpalm
- Current use:  oilpalm
- –

**Sample 24 (64)**
**103.51845011124507**
**2.313943473260456**
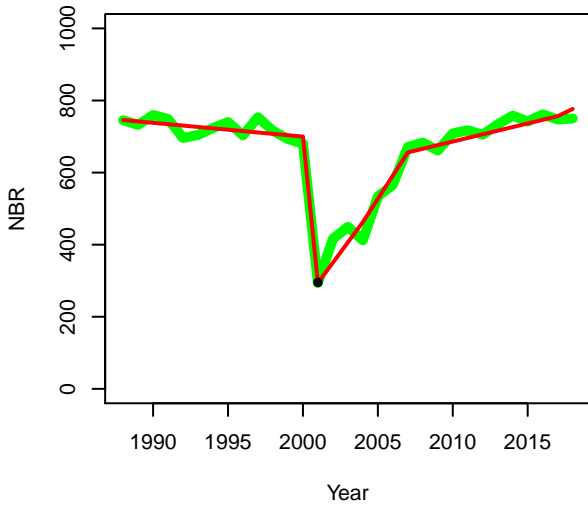
- Cleared in:  2001
- Type:  forest–to–oilpalm
- Current use:  oilpalm
- –

**Sample 25 (80)**
**103.33495364379475**
**2.181548303882595**
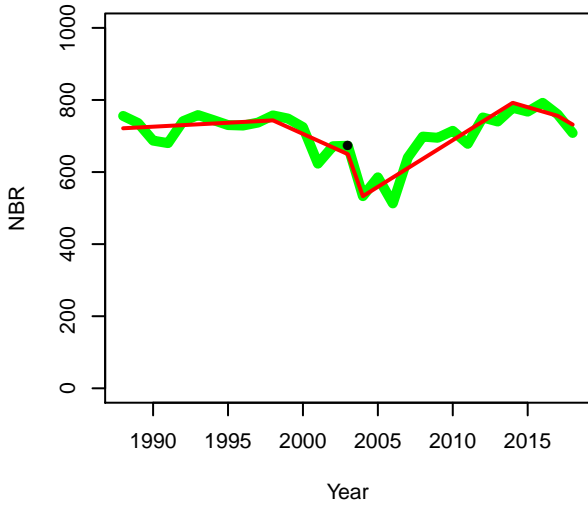
- Cleared in:  2003
- Type:  forest–to–oilpalm
- Current use:  oilpalm
- –

## Sample 26 (81)
## 103.29227112851116
## 2.1783154556188467
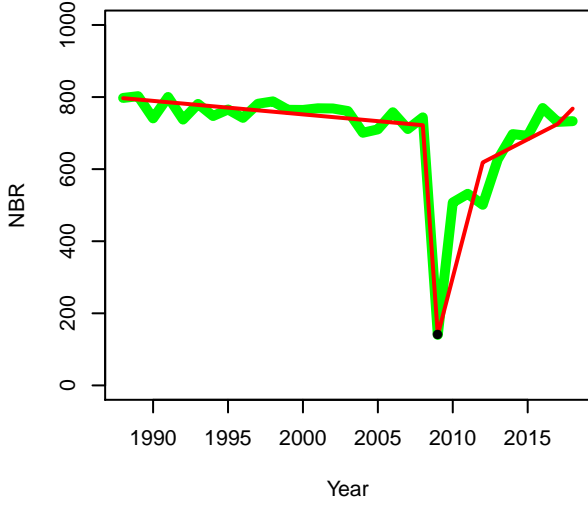


- Cleared in: 2009
- Type: forest–to–oilpalm
- Current use: oilpalm
- –

## Sample 27 (82)
## 103.31912829415607
## 2.2168777615290454
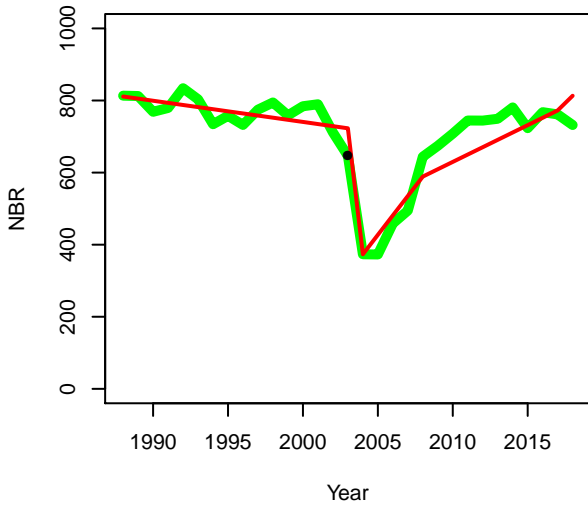


- Cleared in: 2003
- Type: forest–to–oilpalm
- Current use: oilpalm
- –

## Sample 28 (83)
## 103.3223700606219
## 2.1871221801994016
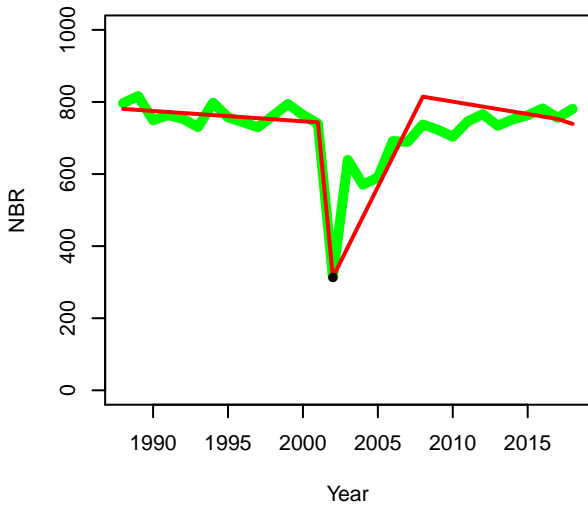


- Cleared in: 2002
- Type: forest–to–oilpalm
- Current use: oilpalm
- –

**Sample 29 (84)**
**103.34281503895198**
**2.1814502036594186**

NBR

Year
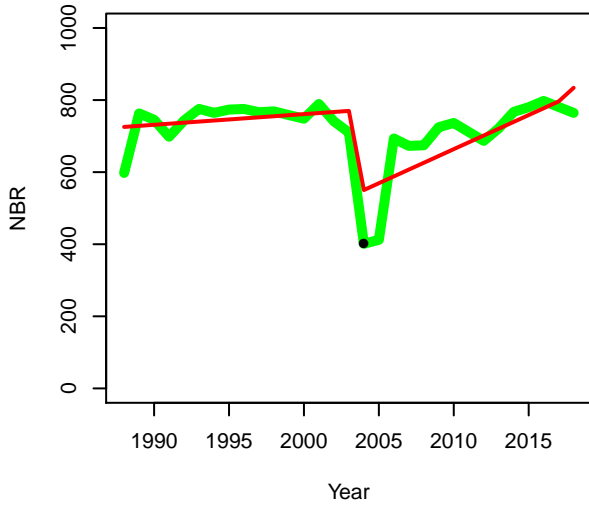
■ Cleared in: 2004

■ Type: forest–to–oilpalm

■ Current use: oilpalm

■ –

## Appendix K: Tables of Selected Accuracy Values from Parameter Optimization

Overall Accuracy of 'Forest to Oil Palm'

| Parameter ID | 1 | 2 | 3 | 4 | 5 | 6 | 7 | 8 | 9 | 10 |
|---|---|---|---|---|---|---|---|---|---|---|
| 0 | 15.34 | 18.37 | 20.45 | 20.45 | 26.70 | 20.45 | 23.13 | 18.37 | 16.70 | 18.37 |
| 100 | 15.34 | 18.37 | 20.45 | 20.45 | 26.70 | 20.45 | 23.13 | 18.37 | 16.70 | 18.37 |
| 200 | 15.34 | 18.37 | 20.45 | 20.45 | 26.70 | 20.45 | 23.13 | 18.37 | 16.70 | 18.37 |
| 300 | 15.34 | 18.37 | 20.45 | 20.45 | 26.70 | 20.45 | 23.13 | 18.37 | 16.70 | 18.37 |
| 400 | 7.71 | 10.57 | 7.71 | 7.71 | 13.07 | 10.57 | 10.57 | 8.90 | 8.90 | 10.57 |
| 500 | 10.57 | 13.07 | 10.57 | 13.07 | 25.57 | 25.57 | 17.23 | 17.23 | 10.57 | 13.07 |

(Rows labelled under "Magnitude Threshold")

| Parameter ID | 11 | 12 | 13 | 14 | 15 | 16 | 17 | 18 | 19 | 20 |
|---|---|---|---|---|---|---|---|---|---|---|
| 0 | 22.27 | 24.49 | 31.70 | 30.84 | 26.70 | 27.27 | 16.70 | 18.37 | 18.37 | 24.49 |
| 100 | 22.27 | 24.49 | 31.70 | 30.84 | 26.70 | 27.27 | 16.70 | 18.37 | 18.37 | 24.49 |
| 200 | 22.27 | 24.49 | 31.70 | 30.84 | 26.70 | 27.27 | 16.70 | 18.37 | 18.37 | 24.49 |
| 300 | 22.27 | 24.49 | 31.70 | 30.84 | 26.70 | 27.27 | 16.70 | 18.37 | 18.37 | 24.49 |
| 400 | 8.90 | 10.57 | 17.23 | 13.07 | 13.07 | 10.57 | 8.90 | 10.57 | 8.90 | 10.57 |
| 500 | 10.57 | 13.07 | 25.57 | 25.57 | 17.23 | 17.23 | 10.57 | 13.07 | 10.57 | 13.07 |

| Parameter ID | 21 | 22 | 23 | 24 | 25 | 26 | 27 | 28 | 29 | 30 |
|---|---|---|---|---|---|---|---|---|---|---|
| 0 | 25.57 | 42.27 | 17.23 | 35.61 | 16.45 | 12.27 | 71.51 | 68.92 | 74.81 | 75.14 |
| 100 | 25.57 | 42.27 | 17.23 | 35.61 | 16.45 | 12.27 | 72.73 | 70.86 | 76.84 | 77.12 |
| 200 | 25.57 | 42.27 | 17.23 | 35.61 | 12.27 | 10.04 | 70.86 | 68.92 | 75.39 | 75.62 |
| 300 | 25.57 | 42.27 | 17.23 | 35.61 | 14.77 | 12.42 | 65.98 | 63.84 | 72.29 | 72.40 |
| 400 | 25.57 | 25.57 | 17.23 | 17.23 | 5.11 | 5.57 | 53.75 | 52.75 | 63.07 | 62.13 |
| 500 | 25.57 | 25.57 | 17.23 | 17.23 | 6.82 | 7.71 | 49.13 | 46.84 | 53.98 | 52.10 |

| Parameter ID | 31 | 32 | 33 | 34 | 35 | 36 | 37 | 38 | 39 | 40 |
|---|---|---|---|---|---|---|---|---|---|---|
| 0 | 76.57 | 77.62 | 16.45 | 12.27 | 70.77 | 68.18 | 74.81 | 75.14 | 75.86 | 76.91 |
| 100 | 78.51 | 79.50 | 16.45 | 12.27 | 72.00 | 70.12 | 76.41 | 76.70 | 77.01 | 78.02 |
| 200 | 78.86 | 79.10 | 12.27 | 10.04 | 70.40 | 68.46 | 74.92 | 75.17 | 77.27 | 77.54 |
| 300 | 77.12 | 77.24 | 14.77 | 12.42 | 65.37 | 63.23 | 71.69 | 71.82 | 76.02 | 76.18 |
| 400 | 66.72 | 65.13 | 5.11 | 5.57 | 52.75 | 51.81 | 62.13 | 61.24 | 65.04 | 63.49 |
| 500 | 55.68 | 53.93 | 6.82 | 7.71 | 46.84 | 44.80 | 52.10 | 50.38 | 53.93 | 52.32 |

| Parameter ID | 41 | 42 | 43 | 44 | 45 | 46 | 47 | 48 | 49 | 50 |
|---|---|---|---|---|---|---|---|---|---|---|
| 0 | 16.45 | 12.27 | 70.77 | 68.18 | 74.43 | 74.05 | 75.86 | 76.91 | 16.45 | 12.27 |
| 100 | 16.45 | 12.27 | 72.00 | 70.12 | 76.41 | 76.00 | 77.01 | 78.02 | 16.45 | 12.27 |
| 200 | 12.27 | 10.04 | 70.40 | 68.46 | 74.92 | 74.46 | 77.27 | 77.54 | 12.27 | 10.04 |
| 300 | 14.77 | 12.42 | 65.37 | 63.23 | 71.69 | 71.82 | 76.02 | 76.18 | 14.77 | 12.42 |
| 400 | 5.11 | 5.57 | 52.75 | 51.81 | 62.13 | 61.24 | 65.04 | 63.49 | 5.11 | 5.57 |
| 500 | 6.82 | 7.71 | 46.84 | 44.80 | 52.10 | 50.38 | 53.93 | 52.32 | 6.82 | 7.71 |

Incorporation of Historical Disturbance Identified With LandTrendr Algorithm For Land Cover Mapping In Malaysia
Daniel Stephen Platt (08015557)

Page **116** of **132**

| | Parameter ID | 51 | 52 | 53 | 54 | 55 | 56 | 57 | 58 | 59 | 60 |
|---|---|---|---|---|---|---|---|---|---|---|---|
| Magnitude Threshold | 0 | 71.17 | 68.61 | 72.64 | 73.36 | 74.09 | 74.15 | 16.45 | 12.27 | 71.52 | 68.21 |
| | 100 | 71.88 | 70.03 | 74.05 | 74.77 | 75.13 | 75.49 | 16.45 | 12.27 | 72.26 | 69.67 |
| | 200 | 71.70 | 69.81 | 75.00 | 75.29 | 76.70 | 76.30 | 12.27 | 10.04 | 71.70 | 69.06 |
| | 300 | 69.98 | 67.97 | 75.33 | 75.49 | 77.56 | 77.06 | 14.77 | 12.42 | 69.98 | 67.23 |
| | 400 | 56.25 | 56.27 | 63.54 | 62.73 | 65.00 | 64.25 | 5.11 | 5.57 | 56.25 | 56.27 |
| | 500 | 50.14 | 50.14 | 54.81 | 54.81 | 54.81 | 54.81 | 6.82 | 7.71 | 50.14 | 50.14 |

| | Parameter ID | 61 | 62 | 63 | 64 | 65 | 66 | 67 | 68 | 69 | 70 |
|---|---|---|---|---|---|---|---|---|---|---|---|
| Magnitude Threshold | 0 | 72.64 | 73.36 | 73.43 | 73.52 | 16.45 | 12.27 | 71.52 | 68.95 | 72.30 | 73.36 |
| | 100 | 74.05 | 74.77 | 75.13 | 75.49 | 16.45 | 12.27 | 72.26 | 70.41 | 74.05 | 75.14 |
| | 200 | 75.00 | 75.29 | 76.70 | 76.30 | 12.27 | 10.04 | 71.70 | 69.81 | 75.00 | 75.29 |
| | 300 | 75.33 | 75.49 | 77.56 | 77.06 | 14.77 | 12.42 | 69.98 | 67.97 | 75.33 | 75.49 |
| | 400 | 63.54 | 62.73 | 65.00 | 64.25 | 5.11 | 5.57 | 56.25 | 56.27 | 63.54 | 62.73 |
| | 500 | 54.81 | 54.81 | 54.81 | 54.81 | 6.82 | 7.71 | 50.14 | 50.14 | 54.81 | 54.81 |

| | Parameter ID | 71 | 72 | 73 | 74 | 75 | 76 | 77 | 78 | 79 | 80 |
|---|---|---|---|---|---|---|---|---|---|---|---|
| Magnitude Threshold | 0 | 73.75 | 74.15 | 16.45 | 12.27 | 71.17 | 69.35 | 73.36 | 73.36 | 72.70 | 73.11 |
| | 100 | 75.13 | 75.49 | 16.45 | 12.27 | 71.88 | 70.77 | 74.77 | 74.77 | 74.41 | 74.77 |
| | 200 | 76.70 | 76.30 | 12.27 | 10.04 | 72.42 | 71.27 | 75.71 | 76.00 | 76.70 | 76.30 |
| | 300 | 77.56 | 77.06 | 14.77 | 12.42 | 70.71 | 68.71 | 77.39 | 77.56 | 78.24 | 77.74 |
| | 400 | 65.00 | 64.25 | 5.11 | 5.57 | 57.10 | 57.12 | 64.30 | 63.49 | 65.00 | 64.25 |
| | 500 | 54.81 | 54.81 | 6.82 | 7.71 | 50.14 | 50.14 | 54.81 | 54.81 | 54.81 | 54.81 |

| | Parameter ID | 81 | 82 | 83 | 84 | 85 | 86 | 87 | 88 | 89 | 90 |
|---|---|---|---|---|---|---|---|---|---|---|---|
| Magnitude Threshold | 0 | 16.45 | 12.27 | 71.52 | 69.70 | 73.36 | 73.36 | 73.03 | 73.43 | 16.45 | 12.27 |
| | 100 | 16.45 | 12.27 | 72.26 | 71.15 | 74.77 | 74.77 | 74.77 | 75.13 | 16.45 | 12.27 |
| | 200 | 12.27 | 10.04 | 72.42 | 71.27 | 75.71 | 76.00 | 76.70 | 76.30 | 12.27 | 10.04 |
| | 300 | 14.77 | 12.42 | 70.71 | 68.71 | 77.39 | 77.56 | 78.24 | 77.74 | 14.77 | 12.42 |
| | 400 | 5.11 | 5.57 | 57.10 | 57.12 | 64.30 | 63.49 | 65.00 | 64.25 | 5.11 | 5.57 |
| | 500 | 6.82 | 7.71 | 50.14 | 50.14 | 54.81 | 54.81 | 54.81 | 54.81 | 6.82 | 7.71 |

| | Parameter ID | 91 | 92 | 93 | 94 | 95 | 96 | 97 | 98 | 99 | 100 |
|---|---|---|---|---|---|---|---|---|---|---|---|
| Magnitude Threshold | 0 | 71.52 | 69.70 | 73.03 | 73.03 | 73.36 | 73.75 | 16.45 | 12.27 | 71.17 | 69.35 |
| | 100 | 72.26 | 71.15 | 74.77 | 74.77 | 74.77 | 75.13 | 16.45 | 12.27 | 71.88 | 70.77 |
| | 200 | 72.42 | 71.27 | 75.71 | 76.00 | 76.70 | 76.30 | 12.27 | 10.04 | 72.42 | 71.27 |
| | 300 | 70.71 | 68.71 | 77.39 | 77.56 | 78.24 | 77.74 | 14.77 | 12.42 | 70.71 | 68.71 |
| | 400 | 57.10 | 57.12 | 64.30 | 63.49 | 65.00 | 64.25 | 5.11 | 5.57 | 57.10 | 57.12 |
| | 500 | 50.14 | 50.14 | 54.81 | 54.81 | 54.81 | 54.81 | 6.82 | 7.71 | 50.14 | 50.14 |

| Parameter ID | 101 | 102 | 103 | 104 | 105 | 106 | 107 | 108 | 109 | 110 |
|---|---|---|---|---|---|---|---|---|---|---|
| 0 | 73.03 | 72.64 | 73.03 | 73.11 | 16.45 | 12.27 | 71.52 | 69.70 | 73.36 | 73.36 |
| 100 | 74.41 | 74.05 | 74.41 | 74.77 | 16.45 | 12.27 | 72.26 | 71.15 | 74.77 | 74.77 |
| 200 | 75.29 | 75.29 | 76.70 | 76.30 | 12.27 | 10.04 | 72.42 | 71.27 | 75.71 | 76.00 |
| 300 | 76.87 | 76.87 | 78.24 | 77.74 | 14.77 | 12.42 | 70.71 | 68.71 | 77.39 | 77.56 |
| 400 | 63.49 | 63.49 | 65.00 | 64.25 | 5.11 | 5.57 | 57.10 | 57.12 | 64.30 | 63.49 |
| 500 | 54.81 | 54.81 | 54.81 | 54.81 | 6.82 | 7.71 | 50.14 | 50.14 | 54.81 | 54.81 |

*Magnitude Threshold (rows above)*

| Parameter ID | 111 | 112 | 113 | 114 | 115 | 116 | 117 | 118 | 119 | 120 |
|---|---|---|---|---|---|---|---|---|---|---|
| 0 | 73.36 | 73.43 | 16.45 | 12.27 | 71.52 | 69.70 | 73.03 | 72.70 | 73.70 | 74.09 |
| 100 | 74.77 | 75.13 | 16.45 | 12.27 | 72.26 | 71.15 | 74.77 | 74.41 | 74.77 | 75.13 |
| 200 | 76.70 | 76.30 | 12.27 | 10.04 | 72.42 | 71.27 | 75.71 | 75.59 | 76.70 | 76.30 |
| 300 | 78.24 | 77.74 | 14.77 | 12.42 | 70.71 | 68.71 | 77.39 | 77.06 | 78.24 | 77.74 |
| 400 | 65.00 | 64.25 | 5.11 | 5.57 | 57.10 | 57.12 | 64.30 | 62.72 | 65.00 | 64.25 |
| 500 | 54.81 | 54.81 | 6.82 | 7.71 | 50.14 | 50.14 | 54.81 | 54.81 | 54.81 | 54.81 |

*Magnitude Threshold (rows above)*

Overall Accuracy of 'Oil Palm to Oil Palm' (replanting)

| Parameter ID | 1 | 2 | 3 | 4 | 5 | 6 | 7 | 8 | 9 | 10 |
|---|---|---|---|---|---|---|---|---|---|---|
| 0 | 0.00 | NA | 50.16 | 50.16 | 50.16 | 50.16 | 50.16 | 50.16 | 0.00 | NA |
| 100 | 0.00 | NA | 50.16 | 50.16 | 50.16 | 50.16 | 50.16 | 50.16 | 0.00 | NA |
| 200 | NA | NA | 50.16 | 50.16 | 50.16 | 50.16 | 50.16 | 50.16 | NA | NA |
| 300 | NA | NA | NA | NA | NA | NA | NA | NA | NA | NA |
| 400 | NA | NA | NA | NA | NA | NA | NA | NA | NA | NA |
| 500 | NA | NA | NA | NA | NA | NA | NA | NA | NA | NA |

*Magnitude Threshold (rows above)*

| Parameter ID | 11 | 12 | 13 | 14 | 15 | 16 | 17 | 18 | 19 | 20 |
|---|---|---|---|---|---|---|---|---|---|---|
| 0 | 50.16 | NA | 50.16 | 50.16 | 50.16 | 50.16 | 0.00 | NA | NA | NA |
| 100 | 50.16 | NA | 50.16 | 50.16 | 50.16 | 50.16 | 0.00 | NA | NA | NA |
| 200 | 50.16 | NA | 50.16 | 50.16 | 50.16 | 50.16 | NA | NA | NA | NA |
| 300 | NA | NA | NA | NA | NA | NA | NA | NA | NA | NA |
| 400 | NA | NA | NA | NA | NA | NA | NA | NA | NA | NA |
| 500 | NA | NA | NA | NA | NA | NA | NA | NA | NA | NA |

*Magnitude Threshold (rows above)*

| Parameter ID | 21 | 22 | 23 | 24 | 25 | 26 | 27 | 28 | 29 | 30 |
|---|---|---|---|---|---|---|---|---|---|---|
| 0 | NA | NA | NA | NA | 47.07 | 51.45 | 83.15 | 83.60 | 85.62 | 85.54 |
| 100 | NA | NA | NA | NA | 47.07 | 51.45 | 83.15 | 83.60 | 85.62 | 85.54 |
| 200 | NA | NA | NA | NA | 51.29 | 51.13 | 79.20 | 79.45 | 82.65 | 82.37 |
| 300 | NA | NA | NA | NA | 50.97 | 50.97 | 68.26 | 68.26 | 73.10 | 72.75 |
| 400 | NA | NA | NA | NA | 50.32 | 50.32 | 60.26 | 60.26 | 64.46 | 64.29 |
| 500 | NA | NA | NA | NA | NA | NA | 56.45 | 56.29 | 59.19 | 59.03 |

*Magnitude Threshold (rows above)*

| | Parameter ID | 31 | 32 | 33 | 34 | 35 | 36 | 37 | 38 | 39 | 40 |
|---|---|---|---|---|---|---|---|---|---|---|---|
| Magnitude Threshold | 0 | 86.86 | 87.40 | 47.07 | 51.45 | 83.15 | 83.10 | 85.28 | 85.54 | 86.36 | 86.90 |
| | 100 | 86.86 | 87.40 | 47.07 | 51.45 | 83.15 | 83.10 | 85.28 | 85.54 | 86.36 | 86.90 |
| | 200 | 84.37 | 84.76 | 51.29 | 51.13 | 80.03 | 79.78 | 83.15 | 83.04 | 84.54 | 84.92 |
| | 300 | 75.09 | 75.26 | 50.97 | 50.97 | 69.48 | 68.96 | 74.12 | 73.95 | 75.43 | 75.60 |
| | 400 | 66.80 | 66.80 | 50.32 | 50.32 | 61.15 | 61.15 | 65.83 | 65.83 | 67.46 | 67.46 |
| | 500 | 60.16 | 60.00 | NA | NA | 57.10 | 57.10 | 60.32 | 60.32 | 60.81 | 60.65 |

| | Parameter ID | 41 | 42 | 43 | 44 | 45 | 46 | 47 | 48 | 49 | 50 |
|---|---|---|---|---|---|---|---|---|---|---|---|
| Magnitude Threshold | 0 | 47.07 | 51.45 | 83.32 | 83.21 | 85.79 | 85.66 | 86.86 | 87.03 | 47.07 | 51.45 |
| | 100 | 47.07 | 51.45 | 83.32 | 83.21 | 85.79 | 85.66 | 86.86 | 87.03 | 47.07 | 51.45 |
| | 200 | 51.29 | 51.13 | 80.20 | 79.87 | 83.65 | 83.32 | 84.54 | 84.71 | 51.29 | 51.13 |
| | 300 | 50.97 | 50.97 | 69.82 | 69.48 | 74.80 | 74.63 | 75.60 | 75.77 | 50.97 | 50.97 |
| | 400 | 50.32 | 50.32 | 61.51 | 61.51 | 66.34 | 66.34 | 67.62 | 67.62 | 50.32 | 50.32 |
| | 500 | NA | NA | 57.42 | 57.42 | 60.65 | 60.65 | 60.97 | 60.81 | NA | NA |

| | Parameter ID | 51 | 52 | 53 | 54 | 55 | 56 | 57 | 58 | 59 | 60 |
|---|---|---|---|---|---|---|---|---|---|---|---|
| Magnitude Threshold | 0 | 83.32 | 83.15 | 86.49 | 86.33 | 87.52 | 87.82 | 47.07 | 51.45 | 83.49 | 83.15 |
| | 100 | 83.32 | 83.15 | 86.49 | 86.33 | 87.52 | 87.82 | 47.07 | 51.45 | 83.49 | 83.15 |
| | 200 | 81.54 | 81.14 | 84.87 | 84.32 | 85.58 | 85.54 | 51.29 | 51.13 | 81.87 | 81.31 |
| | 300 | 73.74 | 73.44 | 76.27 | 75.99 | 78.05 | 77.95 | 50.97 | 50.97 | 74.42 | 73.95 |
| | 400 | 66.17 | 65.89 | 67.36 | 66.93 | 68.55 | 68.28 | 50.32 | 50.32 | 66.68 | 66.41 |
| | 500 | 60.32 | 60.16 | 60.81 | 60.81 | 60.81 | 60.65 | NA | NA | 60.48 | 60.48 |

| | Parameter ID | 61 | 62 | 63 | 64 | 65 | 66 | 67 | 68 | 69 | 70 |
|---|---|---|---|---|---|---|---|---|---|---|---|
| Magnitude Threshold | 0 | 86.33 | 86.49 | 88.02 | 87.99 | 47.07 | 51.45 | 83.49 | 82.98 | 86.66 | 86.49 |
| | 100 | 86.33 | 86.49 | 88.02 | 87.99 | 47.07 | 51.45 | 83.49 | 82.98 | 86.66 | 86.49 |
| | 200 | 85.04 | 84.66 | 85.75 | 85.54 | 51.29 | 51.13 | 81.87 | 81.14 | 85.20 | 84.66 |
| | 300 | 76.27 | 76.16 | 78.21 | 78.11 | 50.97 | 50.97 | 74.59 | 73.95 | 76.61 | 76.33 |
| | 400 | 67.53 | 67.28 | 68.87 | 68.61 | 50.32 | 50.32 | 66.85 | 66.59 | 67.86 | 67.45 |
| | 500 | 61.13 | 61.13 | 61.13 | 60.97 | NA | NA | 60.65 | 60.65 | 61.29 | 61.13 |

| | Parameter ID | 71 | 72 | 73 | 74 | 75 | 76 | 77 | 78 | 79 | 80 |
|---|---|---|---|---|---|---|---|---|---|---|---|
| Magnitude Threshold | 0 | 88.02 | 87.99 | 47.07 | 51.45 | 83.87 | 83.49 | 86.86 | 86.49 | 88.38 | 88.15 |
| | 100 | 88.02 | 87.99 | 47.07 | 51.45 | 83.87 | 83.49 | 86.86 | 86.49 | 88.38 | 88.15 |
| | 200 | 85.75 | 85.70 | 51.29 | 51.13 | 82.44 | 81.81 | 85.91 | 85.16 | 86.62 | 86.36 |
| | 300 | 78.21 | 78.11 | 50.97 | 50.97 | 74.76 | 74.46 | 76.77 | 76.50 | 78.38 | 78.45 |
| | 400 | 68.87 | 68.61 | 50.32 | 50.32 | 66.85 | 66.59 | 67.53 | 67.28 | 69.03 | 68.78 |
| | 500 | 61.13 | 60.97 | NA | NA | 60.81 | 60.65 | 61.13 | 61.13 | 61.29 | 60.97 |

| | Parameter ID | 81 | 82 | 83 | 84 | 85 | 86 | 87 | 88 | 89 | 90 |
|---|---|---|---|---|---|---|---|---|---|---|---|

| Magnitude Threshold | | | | | | | | | | |
|---|---|---|---|---|---|---|---|---|---|---|
| 0 | 47.07 | 51.45 | 83.87 | 83.32 | 86.86 | 86.49 | 88.55 | 87.99 | 47.07 | 51.45 |
| 100 | 47.07 | 51.45 | 83.87 | 83.32 | 86.86 | 86.49 | 88.55 | 87.99 | 47.07 | 51.45 |
| 200 | 51.29 | 51.13 | 82.60 | 81.81 | 85.91 | 85.16 | 86.62 | 86.20 | 51.29 | 51.13 |
| 300 | 50.97 | 50.97 | 75.26 | 74.80 | 76.77 | 76.50 | 78.38 | 78.45 | 50.97 | 50.97 |
| 400 | 50.32 | 50.32 | 67.19 | 66.93 | 67.53 | 67.28 | 69.03 | 68.78 | 50.32 | 50.32 |
| 500 | NA | NA | 60.97 | 60.97 | 61.13 | 61.13 | 61.29 | 60.97 | NA | NA |

| Parameter ID | 91 | 92 | 93 | 94 | 95 | 96 | 97 | 98 | 99 | 100 |
|---|---|---|---|---|---|---|---|---|---|---|
| 0 | 83.65 | 83.15 | 86.66 | 86.33 | 88.35 | 88.15 | 47.07 | 51.45 | 83.87 | 83.49 |
| 100 | 83.65 | 83.15 | 86.66 | 86.33 | 88.35 | 88.15 | 47.07 | 51.45 | 83.87 | 83.49 |
| 200 | 82.37 | 81.64 | 85.70 | 84.99 | 86.41 | 86.36 | 51.29 | 51.13 | 82.44 | 81.81 |
| 300 | 75.43 | 74.80 | 76.94 | 76.50 | 78.38 | 78.45 | 50.97 | 50.97 | 74.76 | 74.46 |
| 400 | 67.36 | 66.93 | 67.69 | 67.45 | 69.03 | 68.78 | 50.32 | 50.32 | 66.85 | 66.59 |
| 500 | 60.97 | 60.81 | 61.13 | 61.13 | 61.29 | 60.97 | NA | NA | 60.81 | 60.65 |

| Parameter ID | 101 | 102 | 103 | 104 | 105 | 106 | 107 | 108 | 109 | 110 |
|---|---|---|---|---|---|---|---|---|---|---|
| 0 | 86.86 | 86.49 | 88.38 | 87.99 | 47.07 | 51.45 | 83.87 | 83.32 | 86.86 | 86.49 |
| 100 | 86.86 | 86.49 | 88.38 | 87.99 | 47.07 | 51.45 | 83.87 | 83.32 | 86.86 | 86.49 |
| 200 | 85.91 | 85.16 | 86.62 | 86.20 | 51.29 | 51.13 | 82.60 | 81.81 | 85.91 | 85.16 |
| 300 | 76.77 | 76.50 | 78.38 | 78.28 | 50.97 | 50.97 | 75.26 | 74.80 | 76.77 | 76.50 |
| 400 | 67.53 | 67.28 | 69.03 | 68.78 | 50.32 | 50.32 | 67.19 | 66.93 | 67.53 | 67.28 |
| 500 | 61.13 | 61.13 | 61.29 | 60.97 | NA | NA | 60.97 | 60.97 | 61.13 | 61.13 |

| Parameter ID | 111 | 112 | 113 | 114 | 115 | 116 | 117 | 118 | 119 | 120 |
|---|---|---|---|---|---|---|---|---|---|---|
| 0 | 88.55 | 88.15 | 47.07 | 51.45 | 83.65 | 83.32 | 86.86 | 86.33 | 88.35 | 88.15 |
| 100 | 88.55 | 88.15 | 47.07 | 51.45 | 83.65 | 83.32 | 86.86 | 86.33 | 88.35 | 88.15 |
| 200 | 86.62 | 86.36 | 51.29 | 51.13 | 82.37 | 81.81 | 85.91 | 84.99 | 86.41 | 86.36 |
| 300 | 78.38 | 78.45 | 50.97 | 50.97 | 75.43 | 74.97 | 76.94 | 76.50 | 78.38 | 78.45 |
| 400 | 69.03 | 68.78 | 50.32 | 50.32 | 67.36 | 67.11 | 67.69 | 67.28 | 69.03 | 68.78 |
| 500 | 61.29 | 60.97 | NA | NA | 60.97 | 60.97 | 61.13 | 60.97 | 61.29 | 60.97 |

Overall Accuracy of 'Forest to Urban and Other Brown'

| Parameter ID | 1 | 2 | 3 | 4 | 5 | 6 | 7 | 8 | 9 | 10 |
|---|---|---|---|---|---|---|---|---|---|---|
| 0 | 7.64 | 9.23 | 8.33 | 8.33 | 14.58 | 0.00 | 12.08 | 0.00 | 8.33 | 9.23 |
| 100 | 7.64 | 9.23 | 8.33 | 8.33 | 14.58 | 0.00 | 12.08 | 0.00 | 8.33 | 9.23 |
| 200 | 0.00 | 0.00 | 0.00 | 8.33 | 0.00 | 0.00 | 0.00 | 0.00 | 0.00 | 0.00 |
| 300 | 0.00 | 0.00 | 0.00 | 8.33 | 0.00 | 0.00 | 0.00 | 0.00 | 0.00 | 0.00 |
| 400 | 0.00 | 0.00 | 0.00 | 9.23 | 0.00 | 0.00 | 0.00 | 0.00 | 0.00 | 0.00 |
| 500 | 0.00 | 0.00 | 0.00 | 0.00 | 0.00 | 0.00 | 0.00 | 0.00 | 0.00 | 0.00 |

| Parameter ID | 11 | 12 | 13 | 14 | 15 | 16 | 17 | 18 | 19 | 20 |
|---|---|---|---|---|---|---|---|---|---|---|

| Magnitude Threshold | | | | | | | | | | |
|---|---|---|---|---|---|---|---|---|---|---|
| 0 | 9.23 | 0.00 | 0.00 | 0.00 | 0.00 | 0.00 | 8.33 | 9.23 | 0.00 | 0.00 |
| 100 | 9.23 | 0.00 | 0.00 | 0.00 | 0.00 | 0.00 | 8.33 | 9.23 | 0.00 | 0.00 |
| 200 | 0.00 | 0.00 | 0.00 | 0.00 | 0.00 | 0.00 | 0.00 | 0.00 | 0.00 | 0.00 |
| 300 | 0.00 | 0.00 | 0.00 | 0.00 | 0.00 | 0.00 | 0.00 | 0.00 | 0.00 | 0.00 |
| 400 | 0.00 | 0.00 | 0.00 | 0.00 | 0.00 | 0.00 | 0.00 | 0.00 | 0.00 | 0.00 |
| 500 | 0.00 | 0.00 | 0.00 | 0.00 | 0.00 | 0.00 | 0.00 | 0.00 | 0.00 | 0.00 |

| Parameter ID | 21 | 22 | 23 | 24 | 25 | 26 | 27 | 28 | 29 | 30 |
|---|---|---|---|---|---|---|---|---|---|---|
| **Magnitude Threshold** | | | | | | | | | | |
| 0 | 0.00 | 0.00 | 0.00 | 0.00 | 9.43 | 9.72 | 39.63 | 36.33 | 43.75 | 40.38 |
| 100 | 0.00 | 0.00 | 0.00 | 0.00 | 9.43 | 9.72 | 41.67 | 38.19 | 46.20 | 42.65 |
| 200 | 0.00 | 0.00 | 0.00 | 0.00 | 5.02 | 5.21 | 40.66 | 40.10 | 45.00 | 44.35 |
| 300 | 0.00 | 0.00 | 0.00 | 0.00 | 5.93 | 6.25 | 44.92 | 44.07 | 46.83 | 45.83 |
| 400 | 0.00 | 0.00 | 0.00 | 0.00 | 6.63 | 7.08 | 43.75 | 42.43 | 43.33 | 41.67 |
| 500 | 0.00 | 0.00 | 0.00 | 0.00 | 8.33 | 9.23 | 36.90 | 33.33 | 36.90 | 33.33 |

| Parameter ID | 31 | 32 | 33 | 34 | 35 | 36 | 37 | 38 | 39 | 40 |
|---|---|---|---|---|---|---|---|---|---|---|
| **Magnitude Threshold** | | | | | | | | | | |
| 0 | 43.33 | 40.00 | 9.43 | 9.72 | 39.63 | 36.33 | 43.75 | 40.38 | 43.33 | 40.00 |
| 100 | 45.65 | 42.14 | 9.43 | 9.72 | 41.67 | 38.19 | 45.65 | 42.14 | 44.65 | 41.22 |
| 200 | 45.00 | 44.35 | 5.02 | 5.21 | 40.10 | 39.58 | 44.35 | 43.75 | 43.75 | 43.18 |
| 300 | 46.83 | 45.83 | 5.93 | 6.25 | 44.07 | 43.29 | 45.83 | 44.92 | 44.92 | 44.07 |
| 400 | 43.33 | 41.67 | 6.63 | 7.08 | 42.43 | 41.25 | 41.67 | 40.20 | 40.20 | 38.89 |
| 500 | 31.25 | 27.68 | 8.33 | 9.23 | 33.33 | 30.56 | 33.33 | 30.56 | 27.68 | 25.00 |

| Parameter ID | 41 | 42 | 43 | 44 | 45 | 46 | 47 | 48 | 49 | 50 |
|---|---|---|---|---|---|---|---|---|---|---|
| **Magnitude Threshold** | | | | | | | | | | |
| 0 | 9.43 | 9.72 | 39.63 | 36.33 | 43.33 | 40.00 | 43.33 | 40.00 | 9.43 | 9.72 |
| 100 | 9.43 | 9.72 | 41.67 | 38.19 | 45.65 | 42.14 | 44.65 | 41.22 | 9.43 | 9.72 |
| 200 | 5.02 | 5.21 | 40.10 | 39.58 | 44.35 | 43.75 | 43.75 | 43.18 | 5.02 | 5.21 |
| 300 | 5.93 | 6.25 | 44.07 | 43.29 | 45.83 | 44.92 | 44.92 | 44.07 | 5.93 | 6.25 |
| 400 | 6.63 | 7.08 | 42.43 | 41.25 | 41.67 | 40.20 | 40.20 | 38.89 | 6.63 | 7.08 |
| 500 | 8.33 | 9.23 | 33.33 | 30.56 | 33.33 | 30.56 | 27.68 | 25.00 | 8.33 | 9.23 |

| Parameter ID | 51 | 52 | 53 | 54 | 55 | 56 | 57 | 58 | 59 | 60 |
|---|---|---|---|---|---|---|---|---|---|---|
| **Magnitude Threshold** | | | | | | | | | | |
| 0 | 38.64 | 38.33 | 41.53 | 41.53 | 41.53 | 40.91 | 9.43 | 9.72 | 38.95 | 38.64 |
| 100 | 40.00 | 39.63 | 42.94 | 42.94 | 42.56 | 42.20 | 9.43 | 9.72 | 40.38 | 40.00 |
| 200 | 39.09 | 41.67 | 42.65 | 45.14 | 42.14 | 44.65 | 5.02 | 5.21 | 39.09 | 41.67 |
| 300 | 43.29 | 42.56 | 44.92 | 44.07 | 47.22 | 46.43 | 5.93 | 6.25 | 43.29 | 42.56 |
| 400 | 41.25 | 40.18 | 40.20 | 38.89 | 42.43 | 41.25 | 6.63 | 7.08 | 41.25 | 40.18 |
| 500 | 33.33 | 33.33 | 33.33 | 33.33 | 33.33 | 33.33 | 8.33 | 9.23 | 33.33 | 33.33 |

| Parameter ID | 61 | 62 | 63 | 64 | 65 | 66 | 67 | 68 | 69 | 70 |
|---|---|---|---|---|---|---|---|---|---|---|

| Magnitude Threshold | | | | | | | | | | |
|---|---|---|---|---|---|---|---|---|---|---|
| 0 | 41.53 | 41.53 | 40.91 | 40.35 | 9.43 | 9.72 | 38.95 | 38.64 | 41.21 | 41.53 |
| 100 | 42.94 | 42.94 | 42.56 | 42.20 | 9.43 | 9.72 | 40.38 | 40.00 | 42.94 | 43.33 |
| 200 | 42.65 | 45.14 | 42.14 | 44.65 | 5.02 | 5.21 | 39.09 | 41.67 | 42.65 | 45.14 |
| 300 | 44.92 | 44.07 | 47.22 | 46.43 | 5.93 | 6.25 | 43.29 | 42.56 | 44.92 | 44.07 |
| 400 | 40.20 | 38.89 | 42.43 | 41.25 | 6.63 | 7.08 | 41.25 | 40.18 | 40.20 | 38.89 |
| 500 | 33.33 | 33.33 | 33.33 | 33.33 | 8.33 | 9.23 | 33.33 | 33.33 | 33.33 | 33.33 |

| Parameter ID | 71 | 72 | 73 | 74 | 75 | 76 | 77 | 78 | 79 | 80 |
|---|---|---|---|---|---|---|---|---|---|---|
| Magnitude Threshold 0 | 41.21 | 40.91 | 9.43 | 9.72 | 38.64 | 38.33 | 41.53 | 41.53 | 40.91 | 40.63 |
| 100 | 42.56 | 42.20 | 9.43 | 9.72 | 40.00 | 39.63 | 42.94 | 42.94 | 42.56 | 42.20 |
| 200 | 42.14 | 44.65 | 5.02 | 5.21 | 39.09 | 41.67 | 42.65 | 45.14 | 42.14 | 44.65 |
| 300 | 47.22 | 46.43 | 5.93 | 6.25 | 43.29 | 42.56 | 44.92 | 44.07 | 47.22 | 46.43 |
| 400 | 42.43 | 41.25 | 6.63 | 7.08 | 41.25 | 40.18 | 40.20 | 38.89 | 42.43 | 41.25 |
| 500 | 33.33 | 33.33 | 8.33 | 9.23 | 33.33 | 33.33 | 33.33 | 33.33 | 33.33 | 33.33 |

| Parameter ID | 81 | 82 | 83 | 84 | 85 | 86 | 87 | 88 | 89 | 90 |
|---|---|---|---|---|---|---|---|---|---|---|
| Magnitude Threshold 0 | 9.43 | 9.72 | 38.95 | 38.64 | 41.53 | 41.53 | 41.21 | 40.91 | 9.43 | 9.72 |
| 100 | 9.43 | 9.72 | 40.38 | 40.00 | 42.94 | 42.94 | 42.94 | 42.56 | 9.43 | 9.72 |
| 200 | 5.02 | 5.21 | 39.09 | 41.67 | 42.65 | 45.14 | 42.14 | 44.65 | 5.02 | 5.21 |
| 300 | 5.93 | 6.25 | 43.29 | 42.56 | 44.92 | 44.07 | 47.22 | 46.43 | 5.93 | 6.25 |
| 400 | 6.63 | 7.08 | 41.25 | 40.18 | 40.20 | 38.89 | 42.43 | 41.25 | 6.63 | 7.08 |
| 500 | 8.33 | 9.23 | 33.33 | 33.33 | 33.33 | 33.33 | 33.33 | 33.33 | 8.33 | 9.23 |

| Parameter ID | 91 | 92 | 93 | 94 | 95 | 96 | 97 | 98 | 99 | 100 |
|---|---|---|---|---|---|---|---|---|---|---|
| Magnitude Threshold 0 | 38.95 | 38.64 | 41.21 | 41.21 | 41.53 | 41.21 | 9.43 | 9.72 | 38.64 | 38.33 |
| 100 | 40.38 | 40.00 | 42.94 | 42.94 | 42.94 | 42.56 | 9.43 | 9.72 | 40.00 | 39.63 |
| 200 | 39.09 | 41.67 | 42.65 | 45.14 | 42.14 | 44.65 | 5.02 | 5.21 | 39.09 | 41.67 |
| 300 | 43.29 | 42.56 | 44.92 | 44.07 | 47.22 | 46.43 | 5.93 | 6.25 | 43.29 | 42.56 |
| 400 | 41.25 | 40.18 | 40.20 | 38.89 | 42.43 | 41.25 | 6.63 | 7.08 | 41.25 | 40.18 |
| 500 | 33.33 | 33.33 | 33.33 | 33.33 | 33.33 | 33.33 | 8.33 | 9.23 | 33.33 | 33.33 |

| Parameter ID | 101 | 102 | 103 | 104 | 105 | 106 | 107 | 108 | 109 | 110 |
|---|---|---|---|---|---|---|---|---|---|---|
| Magnitude Threshold 0 | 41.21 | 41.53 | 41.21 | 40.63 | 9.43 | 9.72 | 38.95 | 38.64 | 41.53 | 41.53 |
| 100 | 42.56 | 42.94 | 42.56 | 42.20 | 9.43 | 9.72 | 40.38 | 40.00 | 42.94 | 42.94 |
| 200 | 42.14 | 45.14 | 42.14 | 44.65 | 5.02 | 5.21 | 39.09 | 41.67 | 42.65 | 45.14 |
| 300 | 44.07 | 44.07 | 47.22 | 46.43 | 5.93 | 6.25 | 43.29 | 42.56 | 44.92 | 44.07 |
| 400 | 38.89 | 38.89 | 42.43 | 41.25 | 6.63 | 7.08 | 41.25 | 40.18 | 40.20 | 38.89 |
| 500 | 33.33 | 33.33 | 33.33 | 33.33 | 8.33 | 9.23 | 33.33 | 33.33 | 33.33 | 33.33 |

| Parameter ID | 111 | 112 | 113 | 114 | 115 | 116 | 117 | 118 | 119 | 120 |
|---|---|---|---|---|---|---|---|---|---|---|
| Magnitude Threshold 0 | 41.53 | 40.91 | 9.43 | 9.72 | 38.95 | 38.64 | 41.21 | 40.91 | 41.86 | 41.53 |
| 100 | 42.94 | 42.56 | 9.43 | 9.72 | 40.38 | 40.00 | 42.94 | 42.56 | 42.94 | 42.56 |

| | 200 | 42.14 | 44.65 | 5.02 | 5.21 | 39.09 | 41.67 | 42.65 | 44.65 | 42.14 | 44.65 |
| | 300 | 47.22 | 46.43 | 5.93 | 6.25 | 43.29 | 42.56 | 44.92 | 43.29 | 47.22 | 46.43 |
| | 400 | 42.43 | 41.25 | 6.63 | 7.08 | 41.25 | 40.18 | 40.20 | 37.72 | 42.43 | 41.25 |
| | 500 | 33.33 | 33.33 | 8.33 | 9.23 | 33.33 | 33.33 | 33.33 | 33.33 | 33.33 | 33.33 |

## Overall Accuracy of 'Forest to Other Green'

| | Parameter ID | 1 | 2 | 3 | 4 | 5 | 6 | 7 | 8 | 9 | 10 |
|---|---|---|---|---|---|---|---|---|---|---|---|
| Magnitude Threshold | 0 | 29.81 | 33.40 | 25.46 | 25.46 | 27.78 | 21.53 | 28.70 | 23.70 | 25.46 | 27.36 |
| | 100 | 29.81 | 33.40 | 25.46 | 25.46 | 27.78 | 21.53 | 28.70 | 23.70 | 25.46 | 27.36 |
| | 200 | 26.98 | 30.56 | 25.46 | 25.46 | 27.78 | 21.53 | 24.21 | 19.44 | 25.46 | 27.36 |
| | 300 | 20.37 | 23.70 | 21.89 | 21.89 | 21.85 | 16.14 | 18.52 | 14.35 | 17.78 | 19.44 |
| | 400 | 19.44 | 24.21 | 14.35 | 14.35 | 21.85 | 18.52 | 18.52 | 16.14 | 16.14 | 18.52 |
| | 500 | 18.52 | 21.85 | 18.52 | 21.85 | 35.19 | 35.19 | 26.85 | 26.85 | 10.93 | 13.43 |

| | Parameter ID | 11 | 12 | 13 | 14 | 15 | 16 | 17 | 18 | 19 | 20 |
|---|---|---|---|---|---|---|---|---|---|---|---|
| Magnitude Threshold | 0 | 23.70 | 29.63 | 26.85 | 21.85 | 21.85 | 18.52 | 25.46 | 27.36 | 23.70 | 29.63 |
| | 100 | 23.70 | 29.63 | 26.85 | 21.85 | 21.85 | 18.52 | 25.46 | 27.36 | 23.70 | 29.63 |
| | 200 | 23.70 | 29.63 | 26.85 | 21.85 | 21.85 | 18.52 | 25.46 | 27.36 | 23.70 | 29.63 |
| | 300 | 19.44 | 21.53 | 17.59 | 13.43 | 13.43 | 10.93 | 17.78 | 19.44 | 19.44 | 21.53 |
| | 400 | 9.26 | 10.93 | 17.59 | 13.43 | 13.43 | 10.93 | 16.14 | 18.52 | 9.26 | 10.93 |
| | 500 | 10.93 | 13.43 | 25.93 | 25.93 | 17.59 | 17.59 | 10.93 | 13.43 | 10.93 | 13.43 |

| | Parameter ID | 21 | 22 | 23 | 24 | 25 | 26 | 27 | 28 | 29 | 30 |
|---|---|---|---|---|---|---|---|---|---|---|---|
| Magnitude Threshold | 0 | 35.19 | 35.19 | 26.85 | 26.85 | 25.64 | 24.07 | 55.86 | 55.44 | 64.87 | 64.42 |
| | 100 | 35.19 | 35.19 | 26.85 | 26.85 | 25.64 | 24.07 | 58.20 | 57.70 | 67.39 | 66.85 |
| | 200 | 35.19 | 35.19 | 26.85 | 26.85 | 26.33 | 24.80 | 56.44 | 55.85 | 65.43 | 64.81 |
| | 300 | 25.93 | 25.93 | 17.59 | 17.59 | 16.20 | 17.04 | 55.20 | 54.40 | 64.75 | 63.93 |
| | 400 | 25.93 | 25.93 | 17.59 | 17.59 | 14.32 | 15.28 | 43.40 | 43.89 | 49.60 | 48.15 |
| | 500 | 25.93 | 25.93 | 17.59 | 17.59 | 12.96 | 14.35 | 43.77 | 42.95 | 47.72 | 44.97 |

| | Parameter ID | 31 | 32 | 33 | 34 | 35 | 36 | 37 | 38 | 39 | 40 |
|---|---|---|---|---|---|---|---|---|---|---|---|
| Magnitude Threshold | 0 | 63.17 | 63.97 | 25.64 | 24.07 | 55.86 | 58.04 | 64.87 | 63.17 | 64.42 | 63.97 |
| | 100 | 65.62 | 66.33 | 25.64 | 24.07 | 58.20 | 60.30 | 66.85 | 65.09 | 65.83 | 65.34 |
| | 200 | 64.17 | 64.81 | 26.33 | 24.80 | 57.19 | 57.95 | 64.81 | 64.23 | 64.23 | 63.66 |
| | 300 | 64.75 | 65.19 | 16.20 | 17.04 | 55.78 | 55.03 | 63.93 | 63.15 | 64.41 | 63.67 |
| | 400 | 54.13 | 54.23 | 14.32 | 15.28 | 42.13 | 42.74 | 46.50 | 45.14 | 51.52 | 51.85 |
| | 500 | 51.11 | 50.27 | 12.96 | 14.35 | 42.95 | 42.59 | 44.97 | 42.59 | 48.61 | 48.15 |

| | Parameter ID | 41 | 42 | 43 | 44 | 45 | 46 | 47 | 48 | 49 | 50 |
|---|---|---|---|---|---|---|---|---|---|---|---|
| Magnitude Threshold | 0 | 25.64 | 24.07 | 54.54 | 56.75 | 63.17 | 61.46 | 63.17 | 62.72 | 25.64 | 24.07 |
| | 100 | 25.64 | 24.07 | 56.89 | 59.00 | 65.62 | 63.84 | 64.59 | 64.10 | 25.64 | 24.07 |

| | | | | | | | | | | |
|---|---|---|---|---|---|---|---|---|---|---|
| 200 | 26.33 | 24.80 | 55.85 | 56.62 | 63.56 | 62.96 | 62.96 | 62.39 | 26.33 | 24.80 |
| 300 | 19.34 | 20.25 | 54.40 | 53.64 | 62.66 | 61.87 | 63.15 | 62.40 | 16.20 | 17.04 |
| 400 | 14.32 | 15.28 | 42.13 | 40.96 | 48.15 | 46.81 | 51.52 | 50.35 | 14.32 | 15.28 |
| 500 | 12.96 | 14.35 | 42.95 | 40.48 | 44.97 | 42.59 | 48.61 | 46.41 | 12.96 | 14.35 |

| Parameter ID | 51 | 52 | 53 | 54 | 55 | 56 | 57 | 58 | 59 | 60 |
|---|---|---|---|---|---|---|---|---|---|---|
| Magnitude Threshold 0 | 54.63 | 55.56 | 62.33 | 63.58 | 63.58 | 64.06 | 25.64 | 24.07 | 55.03 | 57.24 |
| 100 | 56.30 | 57.17 | 63.97 | 65.22 | 64.79 | 65.61 | 25.64 | 24.07 | 56.75 | 58.90 |
| 200 | 56.08 | 55.56 | 64.37 | 65.09 | 63.84 | 64.59 | 26.33 | 24.80 | 57.41 | 58.20 |
| 300 | 56.40 | 55.68 | 64.41 | 63.67 | 63.67 | 62.96 | 16.20 | 17.04 | 57.74 | 57.04 |
| 400 | 44.44 | 45.05 | 50.00 | 48.81 | 53.32 | 52.26 | 14.32 | 15.28 | 44.44 | 45.05 |
| 500 | 42.95 | 44.97 | 48.61 | 48.61 | 51.85 | 51.85 | 12.96 | 14.35 | 44.97 | 46.85 |

| Parameter ID | 61 | 62 | 63 | 64 | 65 | 66 | 67 | 68 | 69 | 70 |
|---|---|---|---|---|---|---|---|---|---|---|
| Magnitude Threshold 0 | 61.07 | 61.07 | 62.82 | 63.35 | 25.64 | 24.07 | 53.70 | 57.24 | 60.69 | 61.07 |
| 100 | 62.72 | 62.72 | 64.79 | 65.61 | 25.64 | 24.07 | 55.43 | 58.90 | 62.72 | 63.17 |
| 200 | 63.11 | 62.58 | 63.84 | 64.59 | 26.33 | 24.80 | 56.08 | 58.20 | 63.11 | 62.58 |
| 300 | 63.15 | 62.40 | 63.67 | 62.96 | 19.34 | 20.25 | 56.40 | 57.04 | 63.15 | 62.40 |
| 400 | 48.43 | 47.22 | 53.32 | 52.26 | 14.32 | 15.28 | 44.44 | 45.05 | 48.43 | 47.22 |
| 500 | 48.61 | 48.61 | 51.85 | 51.85 | 12.96 | 14.35 | 44.97 | 46.85 | 48.61 | 48.61 |

| Parameter ID | 71 | 72 | 73 | 74 | 75 | 76 | 77 | 78 | 79 | 80 |
|---|---|---|---|---|---|---|---|---|---|---|
| Magnitude Threshold 0 | 63.19 | 64.06 | 25.64 | 24.07 | 57.24 | 58.14 | 62.33 | 63.58 | 61.57 | 62.46 |
| 100 | 64.79 | 65.61 | 25.64 | 24.07 | 58.90 | 59.75 | 63.97 | 65.22 | 63.54 | 64.37 |
| 200 | 63.84 | 64.59 | 26.33 | 24.80 | 60.02 | 59.50 | 64.37 | 65.09 | 63.84 | 64.59 |
| 300 | 63.67 | 62.96 | 16.20 | 17.04 | 57.74 | 57.04 | 65.66 | 64.93 | 64.93 | 64.23 |
| 400 | 53.32 | 52.26 | 14.32 | 15.28 | 44.44 | 45.05 | 50.00 | 48.81 | 53.32 | 52.26 |
| 500 | 51.85 | 51.85 | 12.96 | 14.35 | 42.95 | 44.97 | 48.61 | 48.61 | 51.85 | 51.85 |

| Parameter ID | 81 | 82 | 83 | 84 | 85 | 86 | 87 | 88 | 89 | 90 |
|---|---|---|---|---|---|---|---|---|---|---|
| Magnitude Threshold 0 | 25.64 | 24.07 | 57.64 | 58.53 | 61.07 | 62.33 | 61.95 | 62.82 | 25.64 | 24.07 |
| 100 | 25.64 | 24.07 | 59.35 | 60.19 | 62.72 | 63.97 | 63.97 | 64.79 | 25.64 | 24.07 |
| 200 | 26.33 | 24.80 | 60.02 | 59.50 | 63.11 | 63.84 | 63.84 | 64.59 | 26.33 | 24.80 |
| 300 | 16.20 | 17.04 | 57.74 | 57.04 | 64.41 | 63.67 | 64.93 | 64.23 | 19.34 | 20.25 |
| 400 | 14.32 | 15.28 | 44.44 | 45.05 | 48.43 | 47.22 | 53.32 | 52.26 | 14.32 | 15.28 |
| 500 | 12.96 | 14.35 | 44.97 | 46.85 | 48.61 | 48.61 | 51.85 | 51.85 | 12.96 | 14.35 |

| Parameter ID | 91 | 92 | 93 | 94 | 95 | 96 | 97 | 98 | 99 | 100 |
|---|---|---|---|---|---|---|---|---|---|---|
| 0 | 56.34 | 58.53 | 60.69 | 61.95 | 62.33 | 63.19 | 25.64 | 24.07 | 55.94 | 58.14 |
| 100 | 58.06 | 60.19 | 62.72 | 63.97 | 63.97 | 64.79 | 25.64 | 24.07 | 57.60 | 59.75 |
| 200 | 58.72 | 59.50 | 63.11 | 63.84 | 63.84 | 64.59 | 26.33 | 24.80 | 58.72 | 59.50 |
| 300 | 56.40 | 57.04 | 64.41 | 63.67 | 64.93 | 64.23 | 16.20 | 17.04 | 56.40 | 57.04 |
| 400 | 44.44 | 45.05 | 48.43 | 47.22 | 53.32 | 52.26 | 14.32 | 15.28 | 44.44 | 45.05 |
| 500 | 44.97 | 46.85 | 48.61 | 48.61 | 51.85 | 51.85 | 12.96 | 14.35 | 42.95 | 44.97 |

Magnitude Threshold (rows 0–500)

| Parameter ID | 101 | 102 | 103 | 104 | 105 | 106 | 107 | 108 | 109 | 110 |
|---|---|---|---|---|---|---|---|---|---|---|
| 0 | 61.95 | 62.33 | 61.95 | 62.46 | 25.64 | 24.07 | 57.64 | 58.53 | 61.07 | 62.33 |
| 100 | 63.54 | 63.97 | 63.54 | 64.37 | 25.64 | 24.07 | 59.35 | 60.19 | 62.72 | 63.97 |
| 200 | 63.84 | 63.84 | 63.84 | 64.59 | 26.33 | 24.80 | 60.02 | 59.50 | 63.11 | 63.84 |
| 300 | 64.93 | 63.67 | 64.93 | 64.23 | 16.20 | 17.04 | 57.74 | 57.04 | 64.41 | 63.67 |
| 400 | 48.81 | 48.81 | 53.32 | 52.26 | 14.32 | 15.28 | 44.44 | 45.05 | 48.43 | 47.22 |
| 500 | 48.61 | 48.61 | 51.85 | 51.85 | 12.96 | 14.35 | 44.97 | 46.85 | 48.61 | 48.61 |

Magnitude Threshold (rows 0–500)

| Parameter ID | 111 | 112 | 113 | 114 | 115 | 116 | 117 | 118 | 119 | 120 |
|---|---|---|---|---|---|---|---|---|---|---|
| 0 | 62.33 | 62.82 | 25.64 | 24.07 | 56.34 | 58.53 | 60.69 | 61.57 | 62.72 | 63.58 |
| 100 | 63.97 | 64.79 | 25.64 | 24.07 | 58.06 | 60.19 | 62.72 | 63.54 | 63.97 | 64.79 |
| 200 | 63.84 | 64.59 | 26.33 | 24.80 | 58.72 | 59.50 | 63.11 | 63.33 | 63.84 | 64.59 |
| 300 | 64.93 | 64.23 | 19.34 | 20.25 | 56.40 | 57.04 | 64.41 | 62.96 | 64.93 | 64.23 |
| 400 | 53.32 | 52.26 | 14.32 | 15.28 | 44.44 | 45.05 | 48.43 | 46.10 | 53.32 | 52.26 |
| 500 | 51.85 | 51.85 | 12.96 | 14.35 | 44.97 | 46.85 | 48.61 | 48.61 | 51.85 | 51.85 |

Magnitude Threshold (rows 0–500)

Overall Accuracy of 'Other Green to Oil Palm'

| Parameter ID | 1 | 2 | 3 | 4 | 5 | 6 | 7 | 8 | 9 | 10 |
|---|---|---|---|---|---|---|---|---|---|---|
| 0 | NA | NA | 27.00 | 27.00 | 52.00 | 52.00 | 52.00 | 52.00 | NA | NA |
| 100 | NA | NA | 27.00 | 27.00 | 52.00 | 52.00 | 52.00 | 52.00 | NA | NA |
| 200 | NA | NA | 27.00 | 27.00 | 52.00 | 52.00 | 52.00 | 52.00 | NA | NA |
| 300 | NA | NA | 27.00 | 27.00 | 52.00 | 52.00 | 52.00 | 52.00 | NA | NA |
| 400 | NA | NA | 0.00 | 0.00 | NA | NA | NA | NA | NA | NA |
| 500 | NA | NA | 0.00 | 0.00 | NA | NA | NA | NA | NA | NA |

Magnitude Threshold (rows 0–500)

| Parameter ID | 11 | 12 | 13 | 14 | 15 | 16 | 17 | 18 | 19 | 20 |
|---|---|---|---|---|---|---|---|---|---|---|
| 0 | 0.00 | 0.00 | NA | NA | NA | NA | NA | NA | 0.00 | 0.00 |
| 100 | 0.00 | 0.00 | NA | NA | NA | NA | NA | NA | 0.00 | 0.00 |
| 200 | 0.00 | 0.00 | NA | NA | NA | NA | NA | NA | 0.00 | 0.00 |
| 300 | 0.00 | 0.00 | NA | NA | NA | NA | NA | NA | 0.00 | 0.00 |
| 400 | 0.00 | 0.00 | NA | NA | NA | NA | NA | NA | 0.00 | 0.00 |
| 500 | 0.00 | 0.00 | NA | NA | NA | NA | NA | NA | 0.00 | 0.00 |

Magnitude Threshold (rows 0–500)

| | Parameter ID | 21 | 22 | 23 | 24 | 25 | 26 | 27 | 28 | 29 | 30 |
|---|---|---|---|---|---|---|---|---|---|---|---|
| Magnitude Threshold | 0 | NA | NA | NA | NA | 0.00 | 0.00 | 51.25 | 53.33 | 70.10 | 70.10 |
| | 100 | NA | NA | NA | NA | 0.00 | 0.00 | 51.25 | 53.33 | 70.10 | 70.10 |
| | 200 | NA | NA | NA | NA | 0.00 | 0.00 | 45.82 | 49.00 | 66.89 | 66.89 |
| | 300 | NA | NA | NA | NA | 0.00 | 0.00 | 41.25 | 41.25 | 61.50 | 61.50 |
| | 400 | NA | NA | NA | NA | NA | NA | 48.00 | 48.00 | 49.00 | 49.00 |
| | 500 | NA | NA | NA | NA | NA | NA | 52.00 | 52.00 | 54.00 | 54.00 |

| | Parameter ID | 31 | 32 | 33 | 34 | 35 | 36 | 37 | 38 | 39 | 40 |
|---|---|---|---|---|---|---|---|---|---|---|---|
| Magnitude Threshold | 0 | 64.84 | 64.84 | 0.00 | 0.00 | 51.25 | 53.33 | 67.50 | 67.50 | 62.11 | 62.11 |
| | 100 | 64.84 | 64.84 | 0.00 | 0.00 | 51.25 | 53.33 | 67.50 | 67.50 | 62.11 | 62.11 |
| | 200 | 61.50 | 61.50 | 0.00 | 0.00 | 45.82 | 49.00 | 66.89 | 66.89 | 61.50 | 61.50 |
| | 300 | 55.71 | 55.71 | 0.00 | 0.00 | 41.25 | 41.25 | 58.67 | 58.67 | 52.62 | 52.62 |
| | 400 | 37.78 | 37.78 | NA | NA | 48.00 | 48.00 | 49.00 | 49.00 | 37.78 | 37.78 |
| | 500 | 54.00 | 54.00 | NA | NA | 52.00 | 52.00 | 54.00 | 54.00 | 54.00 | 54.00 |

| | Parameter ID | 41 | 42 | 43 | 44 | 45 | 46 | 47 | 48 | 49 | 50 |
|---|---|---|---|---|---|---|---|---|---|---|---|
| Magnitude Threshold | 0 | 0.00 | 0.00 | 53.33 | 55.71 | 66.89 | 66.89 | 64.24 | 64.24 | 0.00 | 0.00 |
| | 100 | 0.00 | 0.00 | 53.33 | 55.71 | 66.89 | 66.89 | 64.24 | 64.24 | 0.00 | 0.00 |
| | 200 | 0.00 | 0.00 | 49.00 | 52.89 | 66.63 | 66.63 | 66.63 | 66.63 | 0.00 | 0.00 |
| | 300 | 0.00 | 0.00 | 41.25 | 45.71 | 58.46 | 58.46 | 58.46 | 58.46 | 0.00 | 0.00 |
| | 400 | NA | NA | 41.33 | 48.00 | 52.89 | 52.89 | 45.33 | 45.33 | NA | NA |
| | 500 | NA | NA | 52.00 | 52.00 | 54.00 | 54.00 | 54.00 | 54.00 | NA | NA |

| | Parameter ID | 51 | 52 | 53 | 54 | 55 | 56 | 57 | 58 | 59 | 60 |
|---|---|---|---|---|---|---|---|---|---|---|---|
| Magnitude Threshold | 0 | 54.35 | 56.38 | 68.36 | 68.36 | 67.50 | 67.50 | 0.00 | 0.00 | 56.38 | 56.38 |
| | 100 | 54.35 | 56.38 | 68.36 | 68.36 | 67.50 | 67.50 | 0.00 | 0.00 | 56.38 | 56.38 |
| | 200 | 46.77 | 49.33 | 66.89 | 66.89 | 59.29 | 59.29 | 0.00 | 0.00 | 46.77 | 49.33 |
| | 300 | 43.17 | 45.82 | 61.50 | 61.50 | 53.33 | 53.33 | 0.00 | 0.00 | 43.17 | 45.82 |
| | 400 | 45.71 | 51.67 | 45.33 | 45.33 | 30.22 | 30.22 | NA | NA | 45.71 | 51.67 |
| | 500 | 52.00 | 52.00 | 43.50 | 43.50 | 18.67 | 18.67 | NA | NA | 52.00 | 52.00 |

| | Parameter ID | 61 | 62 | 63 | 64 | 65 | 66 | 67 | 68 | 69 | 70 |
|---|---|---|---|---|---|---|---|---|---|---|---|
| Magnitude Threshold | 0 | 67.50 | 65.71 | 64.84 | 64.84 | 0.00 | 0.00 | 56.38 | 55.71 | 65.71 | 65.71 |
| | 100 | 67.50 | 65.71 | 64.84 | 64.84 | 0.00 | 0.00 | 56.38 | 55.71 | 65.71 | 65.71 |
| | 200 | 64.24 | 64.24 | 59.29 | 59.29 | 0.00 | 0.00 | 49.33 | 49.00 | 64.24 | 64.24 |
| | 300 | 58.67 | 58.67 | 53.33 | 53.33 | 0.00 | 0.00 | 45.82 | 45.33 | 58.67 | 58.67 |
| | 400 | 41.25 | 41.25 | 30.22 | 30.22 | NA | NA | 45.71 | 51.67 | 41.25 | 41.25 |
| | 500 | 37.33 | 37.33 | 18.67 | 18.67 | NA | NA | 52.00 | 52.00 | 37.33 | 37.33 |

| | Parameter ID | 71 | 72 | 73 | 74 | 75 | 76 | 77 | 78 | 79 | 80 |
|---|---|---|---|---|---|---|---|---|---|---|---|
| Magnitude Threshold | 0 | 67.50 | 67.50 | 0.00 | 0.00 | 54.35 | 56.38 | 68.36 | 68.36 | 68.36 | 68.36 |
| | 100 | 67.50 | 67.50 | 0.00 | 0.00 | 54.35 | 56.38 | 68.36 | 68.36 | 68.36 | 68.36 |
| | 200 | 64.84 | 64.84 | 0.00 | 0.00 | 44.57 | 46.77 | 65.71 | 65.71 | 63.00 | 63.00 |
| | 300 | 56.38 | 56.38 | 0.00 | 0.00 | 40.92 | 43.17 | 60.21 | 60.21 | 57.33 | 57.33 |
| | 400 | 35.00 | 35.00 | NA | NA | 41.25 | 45.71 | 39.27 | 39.27 | 32.73 | 32.73 |
| | 500 | 18.67 | 18.67 | NA | NA | 52.00 | 52.00 | 43.50 | 43.50 | 29.00 | 29.00 |

| | Parameter ID | 81 | 82 | 83 | 84 | 85 | 86 | 87 | 88 | 89 | 90 |
|---|---|---|---|---|---|---|---|---|---|---|---|
| Magnitude Threshold | 0 | 0.00 | 0.00 | 54.35 | 56.38 | 65.71 | 65.71 | 65.71 | 65.71 | 0.00 | 0.00 |
| | 100 | 0.00 | 0.00 | 54.35 | 56.38 | 65.71 | 65.71 | 65.71 | 65.71 | 0.00 | 0.00 |
| | 200 | 0.00 | 0.00 | 44.57 | 46.77 | 63.00 | 63.00 | 63.00 | 63.00 | 0.00 | 0.00 |
| | 300 | 0.00 | 0.00 | 40.92 | 43.17 | 57.33 | 57.33 | 57.33 | 57.33 | 0.00 | 0.00 |
| | 400 | NA | NA | 41.25 | 45.71 | 35.00 | 35.00 | 32.73 | 32.73 | NA | NA |
| | 500 | NA | NA | 52.00 | 52.00 | 37.33 | 37.33 | 29.00 | 29.00 | NA | NA |

| | Parameter ID | 91 | 92 | 93 | 94 | 95 | 96 | 97 | 98 | 99 | 100 |
|---|---|---|---|---|---|---|---|---|---|---|---|
| Magnitude Threshold | 0 | 53.33 | 55.71 | 65.71 | 65.71 | 68.36 | 68.36 | 0.00 | 0.00 | 54.35 | 56.38 |
| | 100 | 53.33 | 55.71 | 65.71 | 65.71 | 68.36 | 68.36 | 0.00 | 0.00 | 54.35 | 56.38 |
| | 200 | 43.17 | 45.82 | 63.00 | 63.00 | 65.71 | 65.71 | 0.00 | 0.00 | 44.57 | 46.77 |
| | 300 | 39.27 | 42.00 | 57.33 | 57.33 | 57.33 | 57.33 | 0.00 | 0.00 | 40.92 | 43.17 |
| | 400 | 41.25 | 45.71 | 35.00 | 35.00 | 37.00 | 37.00 | NA | NA | 41.25 | 45.71 |
| | 500 | 52.00 | 52.00 | 37.33 | 37.33 | 29.00 | 29.00 | NA | NA | 52.00 | 52.00 |

| | Parameter ID | 101 | 102 | 103 | 104 | 105 | 106 | 107 | 108 | 109 | 110 |
|---|---|---|---|---|---|---|---|---|---|---|---|
| Magnitude Threshold | 0 | 68.36 | 68.36 | 68.36 | 68.36 | 0.00 | 0.00 | 54.35 | 56.38 | 65.71 | 65.71 |
| | 100 | 68.36 | 68.36 | 68.36 | 68.36 | 0.00 | 0.00 | 54.35 | 56.38 | 65.71 | 65.71 |
| | 200 | 65.71 | 65.71 | 63.00 | 63.00 | 0.00 | 0.00 | 44.57 | 46.77 | 63.00 | 63.00 |
| | 300 | 60.21 | 60.21 | 57.33 | 57.33 | 0.00 | 0.00 | 40.92 | 43.17 | 57.33 | 57.33 |
| | 400 | 39.27 | 39.27 | 32.73 | 32.73 | NA | NA | 41.25 | 45.71 | 35.00 | 35.00 |
| | 500 | 43.50 | 43.50 | 29.00 | 29.00 | NA | NA | 52.00 | 52.00 | 37.33 | 37.33 |

| | Parameter ID | 111 | 112 | 113 | 114 | 115 | 116 | 117 | 118 | 119 | 120 |
|---|---|---|---|---|---|---|---|---|---|---|---|
| Magnitude Threshold | 0 | 65.71 | 65.71 | 0.00 | 0.00 | 53.33 | 55.71 | 65.71 | 65.71 | 68.36 | 68.36 |
| | 100 | 65.71 | 65.71 | 0.00 | 0.00 | 53.33 | 55.71 | 65.71 | 65.71 | 68.36 | 68.36 |
| | 200 | 63.00 | 63.00 | 0.00 | 0.00 | 43.17 | 45.82 | 63.00 | 63.00 | 65.71 | 65.71 |
| | 300 | 57.33 | 57.33 | 0.00 | 0.00 | 39.27 | 42.00 | 57.33 | 57.33 | 57.33 | 57.33 |
| | 400 | 32.73 | 32.73 | NA | NA | 41.25 | 45.71 | 35.00 | 35.00 | 37.00 | 37.00 |
| | 500 | 29.00 | 29.00 | NA | NA | 52.00 | 52.00 | 37.33 | 37.33 | 29.00 | 29.00 |

Appendix L: Graphs from Preliminary Investigation 1

# NDVI
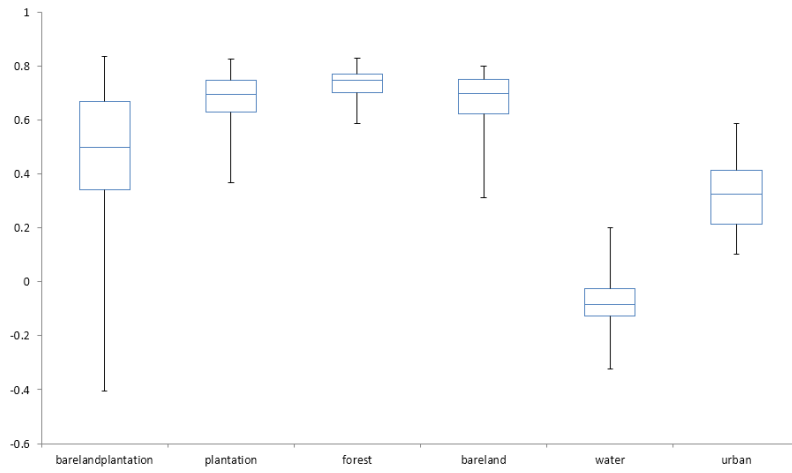


# NBR (NIR-SWIR/NIR+SWIR)
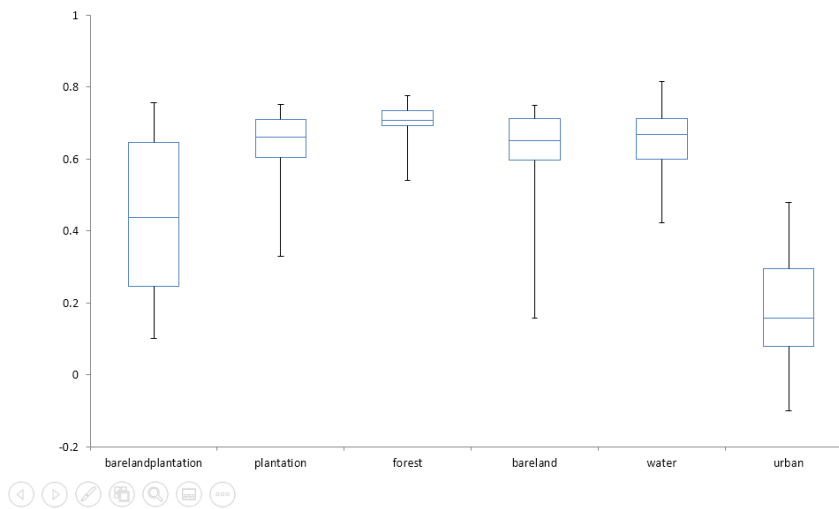
## Appendix M: Cloud Cover Mapper

```
// Select year and boundary.

var year = 2005;

var roi = ee.FeatureCollection("users/danplatt1010/Peninsular");


// Creates RGB map of 4-month periods for a single year.

// Shows: count of cloudy-free pixels (ie availability of spectral data)

//       percentage of pixels that are cloudy (ie spatial and seasonal distribution of cloud cover)

//       total number of available pixels (scaled between 10-20 to show seasonal distribution)


// Colour-Scheme:

//   Red: Jan-Apr

//   Green: May-Aug

//   Blue: Sep-Dec

// Cloudfree Pixels - white indicates high coverage all year, black indicates zero coverage

// Percentage Cloudy Pixels - whiter/brighter colour equals more cloud, black equals no cloud or no available pixels.


// Troubleshoot

//   If 'Cloudfree Pixels' is over- or under-exposed, try adjusting the maximum value in the visualization parameters.

//   The range of values in the console are summarized from the region 'geometry'.

//   The tile covering part of Johor near Mersing is missing data. This is a problem with the GEE dataset.


var L7_SR = ee.ImageCollection("LANDSAT/LE07/C01/T1_SR"),

    L5_SR = ee.ImageCollection("LANDSAT/LT05/C01/T1_SR"),

    L57_SR = L5_SR.merge(L7_SR),

    L8_SR = ee.ImageCollection("LANDSAT/LC08/C01/T1_SR");

Map.centerObject(roi,7);


var empty = ee.Image().byte();
```

```
var outline = empty.paint({

  featureCollection: roi,

  color: 1,

  width: 3});

// Layer added at on top of all other layers (see below).


var maskL57sr = function(image) {

  var qa = image.select('pixel_qa');

  var cloud = qa.bitwiseAnd(1 << 5)

          .and(qa.bitwiseAnd(1 << 7))

          .or(qa.bitwiseAnd(1 << 3));

  var mask2 = image.mask().reduce(ee.Reducer.min());

  return image.updateMask(cloud.not()).updateMask(mask2);

};


var maskL8sr = function (image) {

  var cloudShadowBitMask = (1 << 3);

  var cloudsBitMask = (1 << 5);

  var qa = image.select('pixel_qa');

  var mask = qa.bitwiseAnd(cloudShadowBitMask).eq(0)

          .and(qa.bitwiseAnd(cloudsBitMask).eq(0));

  return image.updateMask(mask);};


var blank = ee.Image.constant(0).clip(roi);

Map.addLayer(blank, {palette: ['white']}, 'background');


var cloudFunction = function(start,end) {

  var WcloudsL57 = L57_SR.filterDate(start,end).filterBounds(roi),

    WcloudsL8 = L8_SR.filterDate(start,end).filterBounds(roi),

    Wclouds = WcloudsL57.merge(WcloudsL8);

  var WOcloudsL57 = WcloudsL57.map(maskL57sr),
```

```
    WOcloudsL8 = WcloudsL8.map(maskL8sr),

    WOclouds = WOcloudsL57.merge(WOcloudsL8);



  var countPixels = function(imageCollection) {

    return imageCollection.select('B1').count().rename("px_count");

  };



  var Wclouds_n = countPixels(Wclouds),

      wBlank = Wclouds_n.addBands(blank).unmask(),

      isData = wBlank.bandNames().length(),

      Wclouds_n = ee.Image(ee.Algorithms.If(isData.eq(2),Wclouds_n,blank)).unmask();

  var WOclouds_n = countPixels(WOclouds).unmask(),

      WOclouds_n = ee.Image(ee.Algorithms.If(isData.eq(2),WOclouds_n,blank));



  var cloudy_n = Wclouds_n.subtract(WOclouds_n);

  var cloudy_pc = cloudy_n.divide(Wclouds_n).multiply(100);

  var cloud_image =
Wclouds_n.rename('Total').addBands(WOclouds_n.rename('NonCloudy')).addBands(cloudy_n.rename('Cloudy')).addBands(cloudy_pc.rename('PercentageCloudy'));

  var mask = Wclouds_n.not().not();

  var cloud_index = cloud_image.normalizedDifference(['NonCloudy', 'Cloudy']).mask(mask);

  var cloud_image = cloud_image.addBands(cloud_index.rename('CloudIndex')).clip(roi);



return cloud_image;

};



var rgbmap = function(year,metric) {
```

```
  var year1 = ee.Number(year)

  var year2 = ee.String(year1),

     year3 = ee.String(year1.add(1));

  var d1 = ee.Date(year2.cat('-01-01')),

     d2 = ee.Date(year2.cat('-05-01')),

     d3 = ee.Date(year2.cat('-09-01')),

     d4 = ee.Date(year3.cat('-01-01'));

  var third1 = cloudFunction(d1, d2).select(metric).rename('Jan-Apr'),

     third2 = cloudFunction(d2, d3).select(metric).rename('May-Aug'),

     third3 = cloudFunction(d3, d4).select(metric).rename('Sep-Dec');

  var map = third1.addBands(third2).addBands(third3);

return map;

};




//Available bands: 'Total', 'NonCloudy', 'Cloudy', 'PercentageCloudy' and 'CloudIndex'.

var cloudfreeCount = rgbmap(year, 'NonCloudy');

  var minmax = cloudfreeCount.reduceRegion(ee.Reducer.minMax(), geometry, 30);

  print('Cloudfree Pixels', minmax);


var cloudpc = rgbmap(year, 'PercentageCloudy');

  var minmax = cloudpc.reduceRegion(ee.Reducer.minMax(), geometry, 30);

  print('Percentage Cloudy Pixels', minmax);


var totalCount = rgbmap(year, 'Total');

  var minmax = totalCount.reduceRegion(ee.Reducer.minMax(), geometry, 30);

  print('Total Pixels', minmax);


Map.addLayer(cloudfreeCount, {min:0, max:5}, 'Cloudfree Pixels');

Map.addLayer(cloudpc, {min:0, max:100}, 'Percentage Cloudy Pixels', false);

Map.addLayer(totalCount, {min:10, max:20}, 'Total Pixels', false);
```

```
Map.addLayer(outline, {palette: 'FF0000'}, 'Boundary');
```